The Human Recognition Mechanism of Thin Foil: an FEM and Psychophysical Investigation
(FEM と心理物理学を用いたヒトの薄膜認識機構の調査)

MAT JUSOH Mohammad Azzeim Bin

Abstract

A major focus in the human tactile sensation field is the study of the human delicate tactile sensing processes. A significant challenge is how to adapt this concept effectively to robotics. Although differentiating the properties of two extremely thin foils is a commonplace task for most people when using their fingertips, it is an extremely difficult task for robots equipped with tactile sensors. A dexterous mechanical hand that would be capable of such sensitivity could be beneficial to many people as it would be better able to perform daily tasks such as housework and nursing. In order to create a device capable of performing such tasks, one effective approach is to study the complexity of the human tactile mechanism. In this research, our main focus is to study the human capacity to discern membrane thickness via touch. Through this research, we will be able to improve and optimize the performance of tactile sensing for use in intelligent robotics. A future goal for this research is to apply any increased understanding of the human tactile mechanism to a human-machine interface, such as virtual reality enhanced by a haptic device.

In research projects such as ours, one extremely difficult challenge is directly monitoring the physical behavior inside our skin during contact. As a solution, we adopt psychophysics and finite element analysis (FEA) in our experiment. The specific focus of this research is the Slowly Adaptive Type I (SA-I) mechanoreceptor unit, which plays a role in recognizing uneven surface patterns through the skin. Therefore, this psychophysics experiment aims to elucidate the mechanism by which SA-I tactile sensation facilitates discrimination of ultra-thin foils' thickness.

Two previous psychophysics experiments in the literature pertain directly to human discrimination of material thickness. One is John, et al. (1989), which found that human subjects were capable of discriminating the thickness of thin materials using specimens from t = 200 ~ 500 μm within 75 μm range. The second is Miyaoka and Ohka (2001, 2002), which found that human beings are able to discriminate even thinner material from t = 8 ~ 50 μm. Two key findings from Miyaoka's paper inform our research. First, we presume that the human evaluation of material with less than 70 μm thicknesses is made using the SA-I mechanoreceptor that exists inside the structured layer of the human skin. Second, we also presume human evaluation of material with a thickness of more than 350 μm employs a different, separate system through the angular sensory organ.

From our psychophysics experiment, we were able to verify the influence that gripping angle has on increasing the detection rate between different material types and different thicknesses. We also examined the human tactile mechanism's evaluation of extremely thin foils in the gap between the functional sensing range of SA-I and angular sensory organ, in particular those below 150-μm thicknesses. We found that the psychometric function increases as the thickness of the foils being compared increases. Simply put, test subjects could more accurately distinguish between foils as the foils increased in thickness.

We conducted our FEA analysis using a 3D model of an index finger, a thumb, and a metal circular sheet. By optimizing the mesh size of the 3D model we managed to both maintain the convergence rate of the simulation and also to keep the numerical error below 4%. In this series of simulations, we compared the differences between the von Mises (VM) stress generated in the skin under different loading states when both Cu and

SUS foils were grasped. This approach was adopted because previous studies showed that activation of SA-I coincided with VM stress. Our hypothesis is that the ability to differentiate two extremely thin materials comes from the comparison process between the vertical loading state (which is the datum) versus the angled loading state (pinch or twitch motion). We therefore designed our experiment to monitor the performance of the VM stress value inside the epidermis section, and were successful in collecting data showing that tangential load does indeed play an assisting role in distinguishing between foil thicknesses. We believe this finding will help further illuminate the complicated human delicate tactile function.

These findings based on human subject experiments were reinforced by the following robotic experiments. Using a three-axis tactile sensor to distinguish the number of 1,000-yen bills in a pile, evaluations were conducted using both a direct pinch motion (normal load) and also a sliding motion (tangential load). We found that it was difficult for the robotic hand to distinguish the numbers of sheets using only normal load. However, by including tangential load the sensor could more effectively distinguish differences in piles of bills even with a low numbers of sheets. Although different materials were used in the three-axis tactile sensor experiment compared to the psychophysical experiment and FEA simulation, the finding was consistent that tangential force is essential for evaluation processes in both human and robotic tactile sensing.

In conclusion, our research contributes to previous findings by refining the experimentally confirmed sensitivity of human's ability to distinguish between very thin foils. Previous studies found that for foils with thicknesses in the range between 70-μm to 350-μm human subjects could not effectively discriminate differences in

thickness. Our experiments were able to shrink this range to foils with a thickness between 150-μm to 350-μm. A further significant finding was that our data support our initial hypothesis that while SA-I mechanoreceptors are the primary means by which human distinguish between foils, tangential force plays an important role in successfully verifying minute differences.

Acknowledgement

At first, I would like to express my gratitude to the examiner of this thesis, Prof Hideyuki Azegami and Prof Eisuke Kita, for their time and effort to examine this thesis. Thank you for the positive feedbacks and constructive advices during the review process.

I would like to express my deepest gratitude to my supervisor, Prof Masahiro Ohka. Thank you for your kindness and patience in guiding me to become a better researcher and apprentice during this long internship period. Thank you for continuously reminding and keeping me in track; also for all the great ideas, support and encouragement, which pushes me forward to pursue this research work. I would also like to express my gratitude to Prof. Tetsu Miyaoka for the strong effort and wonderful ideas; which helps us greatly throughout this research process. Also, to all of my colleagues in Ohka Lab during my period of stay in Nagoya University. It's a privilege to know you all. Next, thank you to all the Malaysian students and families in Nagoya. A big thank you to the FKM dean Prof Salmiah, for the concern and understanding plus continuous support. Not forgetting all my colleagues in UiTM Shah Alam. It's a wonderful blessing for me to work and pursue knowledge in the education field.

I would like to dedicate my special love and thanks to my wife, Suhaibah Bte Ja'affar for the patience and understanding during this long PhD duration. Also to my kids, Muhammad Fahim, Muhammad Ilman and Muhammad Amin; may you all grow up to be the best muslim. The highest appreciatiation to my beloved mother, Hjh. Nik Zah Bte Nik Yusoff; thank you for giving birth to me, for the support and patience, and for

always believing in me. Also, to my late father, Hj. Mat Jusoh Bin Mat for the struggle and endless sacrifice; to ensure all his kids to have the best education and life. You shall be in our heart, always. Thank you to my mother and father in law, Ustazah Jamilah and Hj. Ja'affar; not forgetting all my siblings and family members.

Finally, I would like to conclude my gratitude to the Universiti Teknologi MARA (UiTM), Kementerian Pendidikan Malaysia (KPM), the Malaysian Government and the people of Malaysia for supporting my doctorate study. Alhamdulillah and thank you Allah SWT, for this great opportunity. Amin.

Table of Contents

List of Figures

List of Tables

Chapter 1

INTRODUCTION

1.1 Overview

The human body is a fascinating thing. Consider the abilities to detect subtle differences, such as the abilities to sense a slight change of room temperature, to differentiate the roughness of a paper, or to accurately estimate the size and weight of an object. For normal people, performing the above-mentioned activities seems normal, even though such tasks require a tremendous amount of complex work by the human sensory system. With extensive training and practice, professionals are able to combine many of these sensory mechanisms to complete critical tasks such as transplanting human organs. Robots are currently unable to duplicate such tasks requiring minute sensory perception combined with judgement and object manipulation. There has been significant progress in this area however, as there is no doubt that robots can be of great assistance to such delicate and crucial tasks. Thus exploring and refining robot sensory perception is an important and expanding field.

A major focus in the tactile sensing field is the study of the delicate human tactile sensing process. A significant challenge is how to adapt this concept effectively to robotics. For example, although differentiating the properties of two extremely thin foils is natural for most people when using their fingertips, it is an extremely difficult task for robots equipped with tactile sensors. Even though there are products on the market capable of conducting a similar task, such as an automatic page turning device or a bank note counter, the vast majority of such devices are non-versatile and limited to their specific task and function.

For this reason, the development of a dexterous mechanical hand capable of handling delicate functions is needed, especially for common daily tasks. To create a device capable of performing such tasks, a good option is to study the complexity of the human tactile mechanism. For the research detailed in this paper, the main focus is

to study human tactile sensing of membrane thickness. Through this study, we aspire to improve and optimize the performance of tactile sensors, especially those used in robotics. At the same time, a more long-term goal is to elucidate the human mechanism of tactile recognition.

1.2 Tactile sensing in robotics

The study of tactile sensors started in the 1970's, developed slowly during the 1980's, and has subsequently matured over the past 30 years (Harmon, 1982; Nicholls and Lee, 1989; Najarian et al, 2009; Dahiya et al., 2012). Although initial designs were more focused on industrial use, researchers slowly ventured into other fields such as developing a new generation of intelligent robots. One of the current trends in the tactile sensing research environment is the development of robots with soft touch or compliant actuation function (Guizzo and Deyle, 2013). One specific aim of this branch of research is to increase the number of rehabilitation products related to human-robotic interaction, such as a machine capable of interacting delicately with humans through improving compliant actuation and tactile sensing technologies.

By definition, a tactile sensor is a device capable of acquiring tactile information through physical contact. The majority of such sensors are transducer based, including such varieties as capacitive, piezo-resistive, optoelectric, and piezoelectric sensors (Tiwana, 2012; Hernandez, 2015). The application of robotic tactile sensors has spread into diverse fields, a few of which are human-robotic interaction, biomedical tasks, rehabilitation, and prosthetic limbs. Among them, notable trends are the development of tactile sensing with flexible and stretchable features, multi-functional tactile sensors, and nano-structured devices (Dahiya and Valle, 2013; Tawil, 2015).

One of the most recent examples is the design of flexible and wearable liquid-based microfluidic tactile sensors, which currently are being developed for biomechanical applications (NUS, 2015). Another recent example relevant to the research conducted for this paper are the advancements in the medical field such as MIS (Minimal Invasive Surgery), palpation characterization, and tactile sensors for prosthesis (Tiwana, 2012).

Research in applying humanoid robotic function towards the daily human environment is ongoing. Most common tactile sensors need to be produced for

specifically targeted tasks and sensation types such as contact position, contact force, slippage, or texture. In the Ohka Lab, we use a three-axis tactile sensor designed by Ohka et al. (2004) that is able to measure variables related to contact and touch, shape, normal and shear forces, and slippage. The three basic criteria employed in our research for assessing a robot's performance at a task are touch sensing in manipulation, exploration and sensing reaction force.

It is fascinating that our human body is capable of simultaneously performing the functions specified in the previous paragraph. By studying human function, such extraordinary skill can hopefully someday be replicated by tactile sensing robots. This is one of the long-term objectives with which this thesis is concerned.

In conclusion, current technologies continue to diversify and be refined in the development of tactile sensors. One promising path towards related improvement is to benefit from possible insights gained by researching how to reproduce human tactile sensing via mechanical robotic sensors. In the following section, we will therefore consider and discuss one aspect of this research area, which is some of the means by which humans differentiate load directions. In particular we will examine their ability to more accurately and consistently distinguish different material thicknesses by employing tangential forces via their fingertips.

1.3 Human tactile sensing

The human body fills with endless source of knowledge not only related to natural design, but also in mechanism, structure, functionality, reliability, resistance, accuracy, and more. This is the main motivation for this study. Inspired by nature, we able to carve new path towards a better design concept.

The human attributes can be categorized into two types, which are the physical attributes (for example, defining shape, structure, mechanism, etc.) and performance attributes (for example, functionality, reliability, resistance, accuracy, etc.). The basic function or sense of human can be divided into five categories, which are sight, hearing/sound, sense of touch, scent/smell and sense of taste. Taking a closer look at the sense of touch, which consist of physical sensation such as texture (surface roughness/finish), hardness/strength, shape and sizes, weight/mass, vibration, temperature, pain, and more.

Next is to identify the distinctive behavior of human tactile function. In developing new technology, one of the important aspects is to understand the basic function of the human skin. Our skin provides physical protection, at the same time having good sensing ability with other tremendous skills. The human tactile sensation also has good characteristics in terms of high sensitive detection capability, for example discriminating the thickness between a single sheet of paper versus multiple ones. Other than that, the robust ability of human being in terms of manipulating surrounding object effectively is also a great skill.

In general, the human skin provides physical protection combined with delicate tactile sensations. One tremendous characteristic of tactile sensations is the ability to distinguish foil thickness until several 10-μms of thicknesses when such ultra-thin thickness cannot be monitored through joint sensory organs. Since tactile sensations play a major role in this thickness discrimination process of ultra-thin foils, elucidating this mechanism is the main focus of our study. During contact, at first the skin will deform and adapt to the basic shape of the object. Next, the stress-strain properties 'produced' by the skin shall deliver mechanical stimulation to the mechanoreceptors. Finally, the mechanoreceptors shall transform the mechanical stimulation into neural pulses, which then carry the stimulation information to the brain for the next processing phase.

Our human skin consists of various sensory receptors with the basic functions, which aid us in exploring and defining our environment by responding to mechanical stimuli. Each sensory end organ inside the skin are responsible in detecting different type of stimuli. For example, the mechanoreceptor detects mechanical deformation, thermoreceptor perceives temperature change and the nociceptor respond to potential injury stimuli (Moss-Salentijn, 1992).

The mechanoreceptor is a sensory receptor that provides information about mechanical changes in the environment to the organism and further responds to physical stimuli such as touch, pressure, motion, and others. There are about 17,000 mechanoreceptor units within the glabrous skin of a human hand and each behaves according to their own basic function (Vallbo and Johansson, 1984).

The human mechanoreceptor consists of four main components, which are the Meissner's Corpuscles (FA-I), the Pacinian Corpuscles (FA-II), the Merkel's Discs (SA-I) and the Ruffini's End organs (SA-II) (Johansson and Vallbo, 1979, 1984; Darian-Smith, 1984; Bolanowski et. al. 1988). Basically, the FA-I system provides a

neural image of motion signal from the whole hand. The FA-II system provides a neural image of rapid vibration transmitted to the hand (from object contacting the hand), around 200~300 Hz. As for the SA-I, it detects sustained touch and pressure by providing a high quality neural image of the spatial structure of objects and surfaces. Finally, the SA-II, which exists in the deep skin, detects skin tension, by providing a neural image of skin stretch over the whole hand (Kandel et al., 2000; Johnson, 2000; Johanness, 2010). Details regarding the human body shall be briefed in Chapter 2.

In this research, we are focusing on the SA-I unit, which plays the main role towards defining the sensitive sensation from the skin. The touch sensitivity is a function of the rate at which the skin is deformed. The SA-I constitutes about 25% of the 17,000 tactile units in the glabrous skin area of one hand. It is sensitive to static force and most easily excited by the low-frequency dynamic skin deformations below 5 Hz (Johansson and Flanagan, 2009), and responds to sustained deformations. Vallbo and Johansson (1984) studied the properties of the SA-I mechanoreceptor unit such as the size of receptive fields and the density of units.

Next is to review regarding one of the most important organ inside our body, which is the brain. Professor William James from Harvard stated that the average men develop only 10% of his latent mental ability during the 1890's (Boyd, 2008). Some neurologist describes this myth as false by adding that human being virtually every part of the brain and that most of the brain is active almost all of the time (Beyerstein, 1999). The human brain fills with unlimited potential that may link to all mentioned phenomena. However, in this research, we shall focus more towards the physical aspect of human tactile function.

Finally, one of the important question is what can we learn from our human body and how to adapt such information to improve the performance of other devices, such as the robotic system. During rehabilitation process for example, people with serious sensory problem requires a more delicate interaction with the operating machines. Thus, by understanding how the human body works, proper adaptation on operating process could be applied. This idea does not always need to be novel. A combination of multiple ideas is also one good step towards producing one final solution.

1.4 Research background and motivation

The objective of this research is to study the mechanism of delicate tactile sensations for future research & development of a new robotic sensor and a human-machine interface. One extremely difficult challenge is directly monitoring the physical behavior inside our skin during contact. Although past researchers used primates as test subjects, current experimentation on live animals becomes much stricter because of the increased awareness of animal rights. Based on the above situation, we used an indirect method and performed finite element analysis (FEA) on a human finger model during contact with extremely thin foils made of copper (Cu) and stainless steel (SUS) materials.

Previously, microneurography is one of the methods used by inserting electrodes through the skin and nerves. Other than humans, primates were also a part of the test subject. This is based from research by Knibelstol (1973, 1975), who showed that the mechanoreceptor of human was similar to one of monkey. Other research related to tactile sensation also used primates as showed by LaMotte and Srinivasan (1987), Srinivasan and Dandekar (1996), Dandekar, Balasundar and Srinivasan (2003), and also others. However, finding a voluntary human subject is extremely difficult and tedious. This also includes experimentation on live animals as mentioned previously. Although other methods such as in-vivo are also available, they require strict protocols. As a solution, we have chosen psychophysics and FEA in our experiment.

As mentioned previously, the main focus of this research is towards the Slowly Adaptive Type I (SA-I) mechanoreceptor unit, which plays the role of defining the sensitive sensation from the skin. The application of FEA for the behavior study of mechanoreceptors under loading was proposed by Srinivasan and Dandenkar in 1996, Maeno, Kobayashi and Yamazaki (1998), Wu et al. (2006), Gerling and Thomas (2008), and others. Other research by Dandekar, Raju and Srinivasan (2003) and Sripati, Bensmaia and Johnson (2006) provided a good fit between the rate of the spikes fired by the SA-I afferent and the Strain Energy Density (SED). Lesniak and Gerling (2009) focused more on the response of a single SA-I receptor by comparing the result with the psychophysics data of Johnson and Philips (1981). While Maeno et al (1998), focused on Von Mises (VM) stress, as it is proportional with SED. By conducting analytical measurement in three different layers of fingertips, he was able to calculate

the deformation of fingertips with respect to shear force. The stress distribution analysis on his FEA result shows that the structure of epidermal ridge and the geometry of papillae influence tactile sensation on Merkel Disc (SA-I).

In our research, we are focusing our analysis on von Mises stress values by assuming that the SA-I mechanoreceptor is as natural stress sensors capable of detecting sustained touch and pressure. As mentioned by Gerling et al (2014), even though SED is one possible measure of stress and strain by the SA-I end organ, other theoretical concept could also be used in relation, such as maximum compressive stress, maximum compressive strain, von Mises stress, and others.

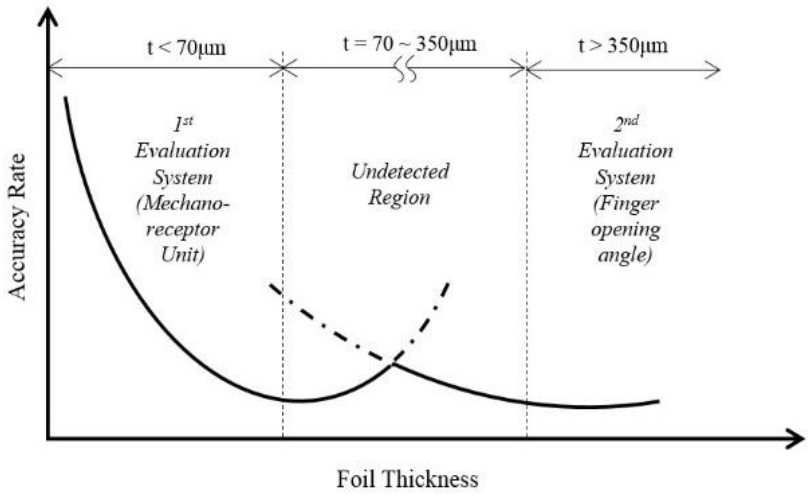

Fig. 1 The hypothesis for material thickness detecting rate.

Next is to brief regarding psychophysics. It can be defined as the study of the relationship between the physical properties of a stimulus and perception ability. One of the most significant researchers in this field is G.T. Fechner, who is also known as the father of psychophysics. His greatest contribution is regarding the importance of measuring how human perceive sensation, even though physically it is difficult to measure the magnitude of sensation. He discovered that it is near impossible to measure such mental event and we could only monitor it through sensitivity. It all begins during the early 1800s, E. H. Weber questioned the differences between stimulus and perception; he suggested that it could be possible to judge and measure human perception even though it may not equal actual physical measurement. Later, Fechner analyzed this concept and proposed what is known as Weber's Law or the

Weber fraction (Gescheider, 1997; Maning and Rosenstock, 1968; Stevens, 1975). Theoretically, the Weber fraction shows the ability of a subject to detect distortion of stimuli and discriminate stimuli from the amount of distortion.

Next is to focus on psychophysics experimentation related to our study. Based from previous psychophysics literature in discriminating material thickness; John, et al. (1989) found that human was capable in discriminating the thickness between thin material using specimens from $t = 200 \sim 500$ μm within 75 μm range and highlighted the importance of gripping angle between fingers, which is controlled throughout the experimentation. Whereas, Miyaoka and Ohka (2001, 2002) proposed that human being is able to discriminate even thinner material from $t = 8 \sim 50$ μm. Normally, such delicate capability cannot be detected by the angular sensory organs of the human finger.

From here, one of the hypotheses that could be made is that the evaluation for material with less than 70 μm thicknesses shall be made using the SA-I (Slowly Adaptive Type I) mechanoreceptor unit that exists inside the structured layer of the human skin. As for material with thickness more than 350 μm, the evaluation shall be made by another system. Hypothetically, the graphical interpretation of this concept can be viewed from Fig. 1, showing an undetected region between mechanoreceptor unit‘s evaluation versus other system.

This finding is also consistent compared to result by Ho and Srinivasan (1997). Using sample of plastic/plexiglass plates between 250 ~ 10,000-μm thickness and steel plates between 50 ~ 500-μm thickness. From Just Noticeable Difference (JND) evaluation, it is concluded that when the plate was thinner than critical thickness, the deformation caused by applied force became large enough to be detected through tactile function. Whereas, when the plate was effectively unbendable, the kinesthetic function was the only hint for discriminating thickness. For evaluation other than metal materials, Summers and Irwin (2005) performed experiments to differentiate between 10 types of plain papers with human test subjects using Multi-Dimensional Scaling (MDS) method. However, the observation was more towards the roughness/smoothness properties rather than hardness/softness or spring constant, which is the focus of our experiment. Other experiment or evaluation using robotic hands, which was related to our research objective, was not available.

It is astonishing how the cutaneous function of human tactile sensation is capable of distinguishing ultra-thin foil thicknesses up to several 10 μms, which is unable to be

monitored by kinesthetic or joint sensory organs. This motivates us to further study treating this mechanism with a goal towards robotics application. Since tactile sensations play a major role in the thickness discrimination of ultra-thin foils, elucidating this mechanism is the aim of this psychophysical experiment.

For humans, the process of thickness discrimination is influenced by two major sensing systems: the cutaneous function related to delicate contact or touch and the kinesthetic function, which is influenced by muscle joint motion (Jones and Lederman, 2006; Bossomaier, 2012). One hypothesis is that both systems are functioning simultaneously and the transition state occurs somewhere within this region. For the cutaneous function, such critical skill could be activated by mechanoreceptors that are sensitive to constant pressure, constant velocity, or acceleration-type information acquired by SA-I, SA-II, FA-I, and FA-II. As discriminating extremely thin materials, it could be possible that plastic deformation may also influence the result.

We have conducted psychophysical experimentations using SUS and Cu foils with variety of thickness. Based on the psychophysics theory by Fechner (1860), the Weber Fraction and Tactile Ratio shall be used as the main references in order to summarize the behavior between experimental, theoretical and FEA results. Details shall be discussed in Chapters 3 and 4.

From the tactile ratio result, it could be possible that SA-I or FA-I is responsible in detecting the distortion during extremely thin thickness. Burgess et al. (1982) also states that compression signaled by cutaneous mechanoreceptor particularly the slow adapting class. However, research by Srinivasan and La Motte (1995) states that the tactile information alone is sufficient to discriminate the softness perception of an object, and that kinesthetic information has no effect in discriminating even between the hardness and softness. Goodwin (1998) also reports that SA-I responds the best to static stimuli when encoding object with curvature, while only 50% of FA-I responds and none for FA-II. From here, we could summarize that SA-I is the primary source for tactile discrimination.

For current simulation, even though majority of the effort is focused towards controlling the detection feeling through static load, it is quite impossible for the test subject to perform and response throughout the whole experiment without involving dynamic motion. As the thickness increases from around 50 ~ 90 μm, the detection could have been made by another mechanoreceptor unit such as the FA-II. The basis on such hypothesis was made referring to the findings by Bolanowski et al. (1988). Details

shall be summarized and discussed in Chapter 5. Finally, we can relate all ideas to sensor fusion technique in order to enhance the performance of available sensors.

1.5 Research objective and methodology

In this research, we are focusing on the decisive factor of human being in differentiating the thickness properties between two basic materials, which are the stainless steel (SUS) and copper (Cu). The objective is to study the behavior of the human tactile mechanism during the evaluation of extremely thin foils and to close the gap of the undetected regions, especially below 150-μm thicknesses. Analysis and simulation shall be made towards the reception of SA-I mechanoreceptor unit in differentiating variety of thickness using these two types of materials.

Below are the general summary of the research objective:

- To understand the behavior of human tactile function in interpreting subjective matters such as thickness discrimination, tactile illusions, and others.
- To understand how human mind operates during critical task, especially on human tactile sensation during psychophysics experimentation (either conscious and subconsciously).
- To verify possibility of simulating the environment using FEA as base. Also, to validate the accuracy of the output.
- To consider towards future application on robotic environment (through tactile sensor environment etc.). Also, the possibility to replicate such extraordinary skill into tactile environment from the study of human function.
- To study the possibility in reflecting the final outcome towards new concept, system or product (such as towards Kansei Engineering field).

Psychophysics remains the most suitable method for describing the relationship between a person's physical sensations and psychological judgement (Gescheider, 1997). In order to achieve the objective, we will validate and compare the Weber fraction between the current and previous psychophysics experiments. We will monitor

this phenomenon during the current psychophysics experiment using a group of extremely thin stainless steel (SUS) foils.

The evaluation process is more detailed with a higher thickness test ratio (by focusing on a single thickness group with seven samples) as compared to previous experiments (Miyaoka and Ohka, 2002) that conducted piecewise examination using four groups of material thicknesses, but with fewer samples. The number of thickness samples was increased to monitor the detection, especially between the cutaneous function and the undetected region. Details shall be discussed in Chapter 3.

Next, we used the FEA method instead of microneurography (which directly obtains neuron activity through a micro needle that penetrates a specific nerve fiber) due to technical limitation. We have conducted a series of simulations using CATIA V5 with a 3D elastic model of the index finger and thumb (consisting of the epidermis, dermis, bones, and nails) while grasping the Cu or SUS foil with thicknesses.

The main focus for this analysis identifies the specific nodal points, which represent the contact areas and the location of the SA-I mechanoreceptor unit on the fingers. An OCTREE tetrahedron mesh was applied with a revised element type from linear to quadratic to reduce the aspect ratio, especially on the foil part. Considering that a metal foil is the most critical part (due to the high aspect ratio), the verification process uses a simple model of a clamped circular foil with the concentrated load applied to the center.

In a series of simulations, we compare the differences between the von Mises stresses generated in the skin under different loading states when the Cu and SUS foils are grasped. Since von Mises stress is equivalent to SED, we can estimate the tactile sensations from von Mises stress variations.

We also studied the possible behavior of both the index finger and the thumb during the evaluation process of foil thickness by handling the foils. In thickness discrimination, our hypothesis is that the ability to differentiate two extremely thin materials comes from the comparison process between the vertical loading state (which is the datum) versus the angled loading state (pinch or twitch motion). Details shall be discussed in Chapter 4.

Below are the general summary of the experimentation process:

- To conduct comprehensive literature review based on tactile sensing environment. At the same time, to enhance experimentation and technical skills in psychophysics experiment procedure and also three-dimensional FEA simulation.
- To re-generate previous psychophysical experimentation and FEA simulation (based on the function of human mechanoreceptor unit). Also to prepare for new psychophysics experiment and FEA simulation.
- To gather and perform data analysis (qualitative and quantitative result) based from psychophysics experiment and FEA simulation result.
- To analyze both psychophysics and FEA result; and consider the application towards tactile sensing environment.
- To summarize research findings and preparation for future research work.

1.6 Significance of research

The sensitivity of human in detecting such a small changes in its surrounding requires tremendous amount of process and operating system. For example, the ability of a blind person to identify each braille letters or sign is an amazing process. Even for an average person, the ability to do mundane yet critical task such as holding an egg without breaking it requires tremendous amount of concentration. We need to be delicate at the same time able to provide strong grip, yet the whole process could be performed naturally. Imagine if such task was to be conducted independently by one single robots, the programmer and designer must really have a hard time.

The possible outcome from this research is the application towards human-machine interface in rehabilitation process especially related to the human hand function recovery. One idea is towards the bionic hands performance, which functions through the detection of muscular motion. Instead of using a one-way function, the product could be upgraded by including feedback system in order to give input to user.

In general, human thinks and acts in a very complex manner. The decision made by each person differs in relative to emotions, surroundings, experience, and other factors. By slowly understanding the common behavior and closing in the gap between peoples,

we can slowly work towards producing something, which is much more practical and closer to the human heart. In future, it could be possible that the human emotions can be 'captured' and conveyed through the product design with the aid of computers and machine for example through Kansei engineering study.

Through the study of delicate behavior mechanism, it may generate more ideas towards the development of an ultra-sensitive sensor and also other human-machine interface devices. We need to be reminded that no matter how good a prosthetic part is being made, it could never ever replace the original God given parts. But as human, we must bring hope especially for those in needs, especially people with physical handicapped.

1.7 Thesis overview

The contents of this thesis has been arranged accordingly as follows:

- Chapter 2 introduces on human tactile system, which is related to this research. Details information regarding the human tactile sensing, the sense of touch and psychophysics behavior of human shall be briefed and discussed here.
- Chapter 3 explains regarding psychophysics contents, including experimentation process and overall result. Basically, the stainless steel material (SUS) and copper (Cu) shall be used as the main material. Also, comparison shall be made by referring to previous experimentation results.
- Chapter 4 elaborates on the usage of FEA in order to achieve specified objective. From here we shall discuss on the level of design process involved, (which consist of initial, preliminary and final stage). Simulation result shall be analyzed and discussed for each stage.
- Chapter 5 shall review on current research and development of three-axis tactile study, especially those related to differentiating between thicknesses. Finally, discuss and suggestion on future tactile sensing study shall be made.
- Finally, in Chapter 6, the overall conclusions shall be made from the thesis contents.

Chapter 2

THE HUMAN TACTILE SYSTEM AND ITS MECHANISM

2.1 Introduction

In general, the hierarchical organization of the human body consist of four basic levels. The most basic component is a cell, which is the simplest unit of function. A group of cells (with similar appearance and function) shall merge to become sets of tissues. Tissues can be categorised into epithelial, connective, muscle and nervous type tissues. Next, the organ (for example the heart) is consisted of different types of tissue function together for a specific purpose.

The highest level is the organ system (as shown in Fig. 2) is the level where several organs working together to perform a systematic function. For example, the nervous system oversees body coordination, and works for detection and response to stimuli. It consists of a brain, spinal cords, nerves, sensory organs, and others. Another example of an organ system is the integumentary system (Fig. 3) which consists of skin and its derivatives, with the main function to protect our body from external damages such as physical injury, infection, loss of water or abrasion and more.

These are the fundamental aspect which runs the human body. Throughout this chapter, we shall introduce on the basic human function, especially the tactile system and its mechanism.

2.2 The nervous system and its function

In tactile sensation, the nervous system plays a main role especially towards defining physical sensation. It is most suitable for directing immediate and rapid responses to the environment. Basically, the human nervous system can be divided into two parts, which are the central nervous system (CNS) consists of a brain and spinal cords, and peripheral nervous system (PNS) consists of cranial nerves and spinal nerves (including ganglia). In definition, nerves are group of axons, while ganglia are a collections of cell bodies of neurons.

The sensory nerve functions by conveying sensory information towards the CNS, and the process starts from first contact. The signal process begins from nerve cells such as neurons, which are capable of transmitting nerve impulses between receptors and effectors. Neurons are divided into three categories, which are the sensory (afferent) neurons, motor (efferent) neurons and interneurons. As in our tactile study, the function of the afferent neuron is important for transmitting impulses from sensory receptors towards the CNS. From Fig. 4, we can see dendrons, which are a number of long and thin fibres extending out of the cell body, which is further divided into subform called dendrites. The longest part of the fibre is called axons, with purpose of conducting nerve impulses away from the cell body. The end of an axon branch goes out to contact other neuron or cells through synapse. Normally, only four types of cells receive nerve impulses, which consist of muscle cells, endocrine cells, extocrine cells, and other neurons.

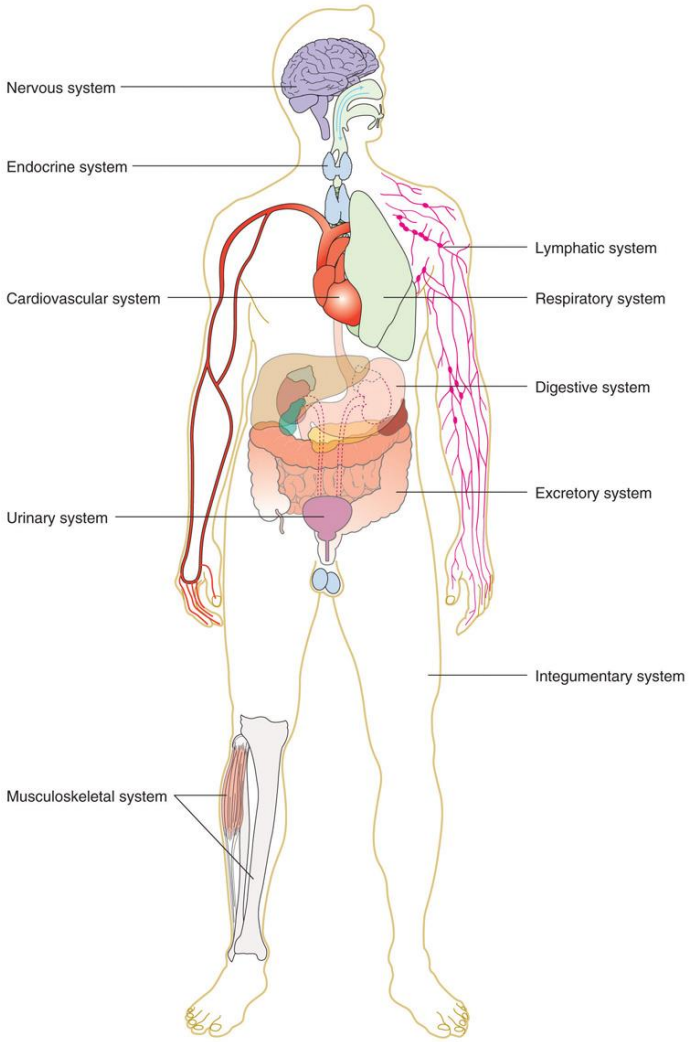

Fig. 2 The organ systems in the human body (Zimmerman & Snow, 2012).

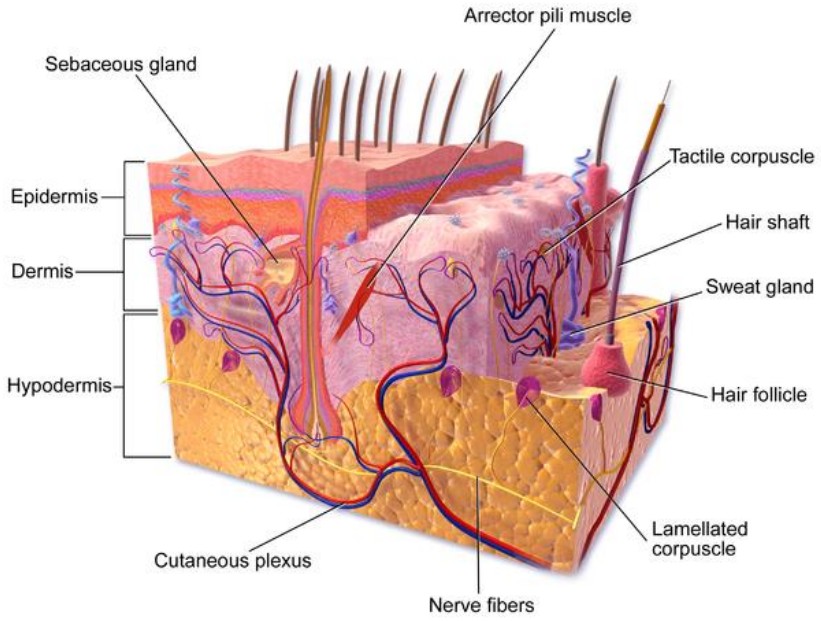

Fig. 3 The components of integumentary system (Blausen gallery).

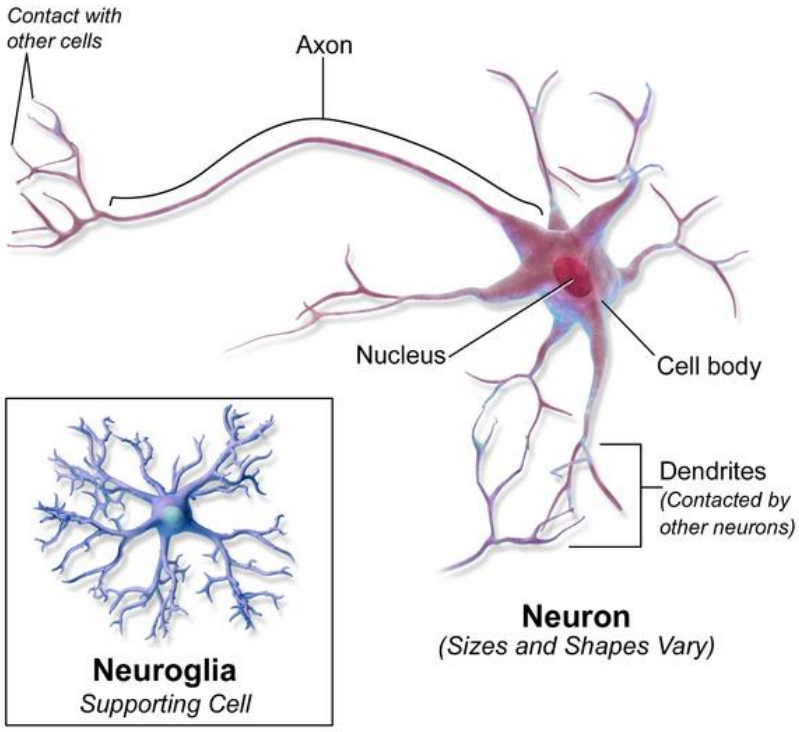

Fig. 4 Neural tissue (Adapted from Blausen gallery).

The nerve impulse is transmitted through out the nervous system in the form of electrical signal through action potentials with response to stimulus such as touch. Normally, the action potential occurs as all-or-none-event. Stronger stimuli shall produce greater frequency of action potentials (but without increasing the amplitude). The traveling speed of action potentials is influenced by the diameter of the axon and

myelination properties. Results from intracellular recording measurement show that myelinated neurons are able to carry impulses much faster compared to nonmyelinated one due to proper insulation. From other example, the four types of mechanoreceptor in our fingertips are also myelinated type, which possesses the high sensitivity and accuracy level compared to other part of the human body.

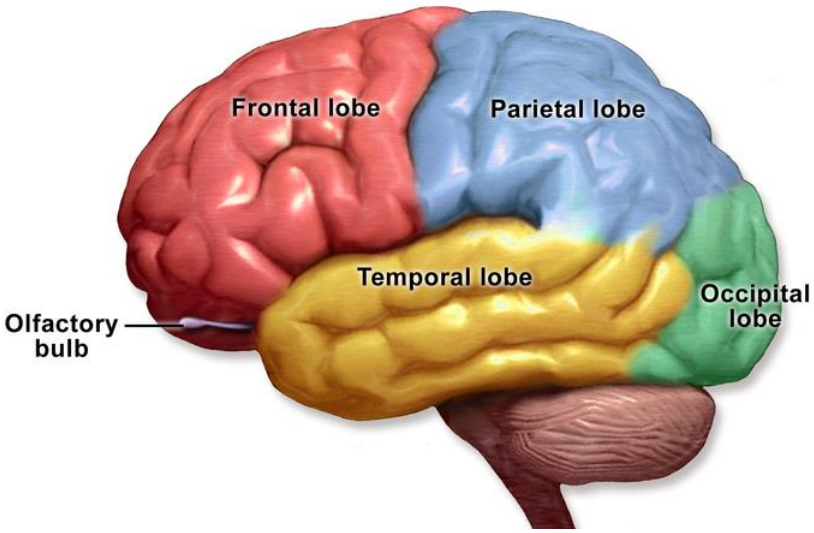

Fig. 5 The four major lobes of the cerebral cortex (Adapted from Blausen gallery).

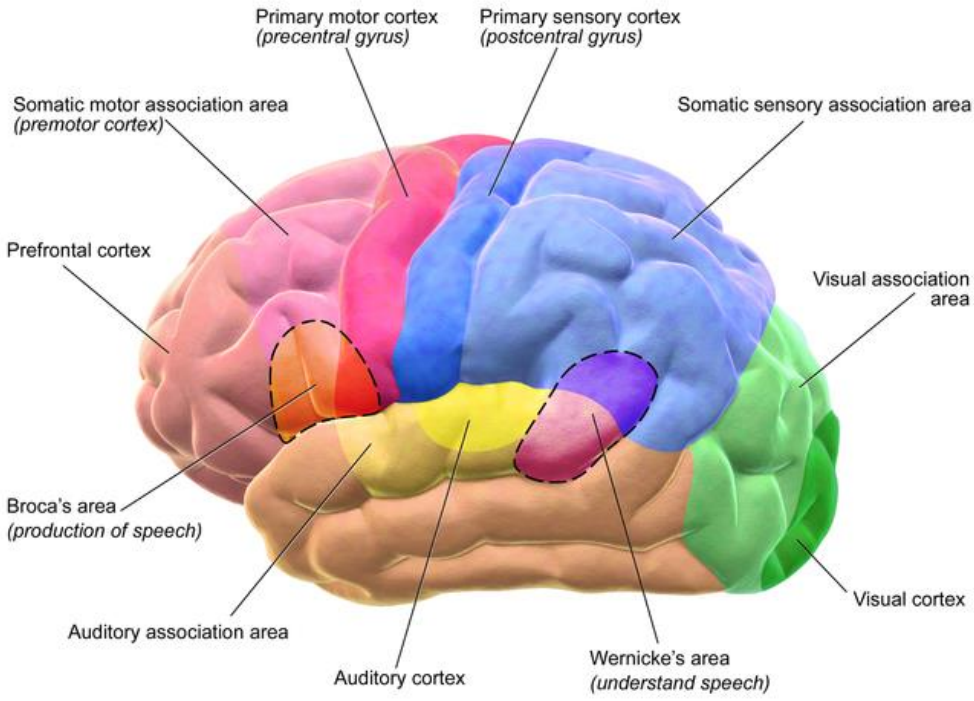

Fig. 6 Motor and Sensory regions of the Cerebral Cortex
(Adapted from Blausen gallery).

Next, we shall review on one of the most important organs inside our body, which is the human brain. In general, the brain can be divided into four main regions which is the cerebrum, cerebellum, dienchepalon (consist of hypothalamus, thalamus and epithalamus) and the brainstem (consist of medulla oblongata, midbrain and pons). The cerebrum is the largest, visible part of the brain, which is the center of information processing. Next, we have the cerebellum, which is in charge of coordination, movement and balance. While the dienchepalon, which is positioned within the inner central part, acts as a relay station to convey information flow from the body to the cerebrum region and vice versa. Finally, the brainstem or the lower brain section, is in charge of conducting information between PNS and the midbrain and forebrain section. It also functions during homeostasis (regulation of body temperature) and also important during coordination of movement.

Next, we shall review on the cerebral cortex. The cerebral cortex is the terms used to define the outermost layer of the cerebrum, which is very important in cognitive process. Referring to Figs. 5 and 6, at first we could see the frontal lobe section, that controls the speech process (from the frontal association area), which also consist of motor cortex. Next is the parietal lobe section consisting of somatosensory cortex, which is closely positioned beside the motor cortex. The somatosensory association area is important also for speech, taste and cognitive process such as reading. Next is the occipital lobe, which is positioned on the rear end, is the section which process visual. Finally, we have the temporal lobe at the lower side, which plays the main role during hearing, smelling and auditory process. By using the functional magnetic resonance imaging (fMRI) scanning technology, observation could be made on the image, to monitor parts of the brain (especially the cerebral cortex region) that is active during each particular activities or process.

The somatosensory cortex is a region of cerebral cortex (on parietal lobe section), which processes information on touch, pain, pressure, temperature, and position of muscle and limbs. Neurons are distributed in an orderly manner according to part of the body that generates the sensory input. The human brain itself contains over one hundred billion neurons, including over one trillion cells. Fig. 7 represents the cortical surface area devoted to each body part and the magnitude of sensation has been displayed in relative to size of the figure. For example, by referring to the middle section of the cross section, we can see that the human finger is one of the most sensitive part of the human body.

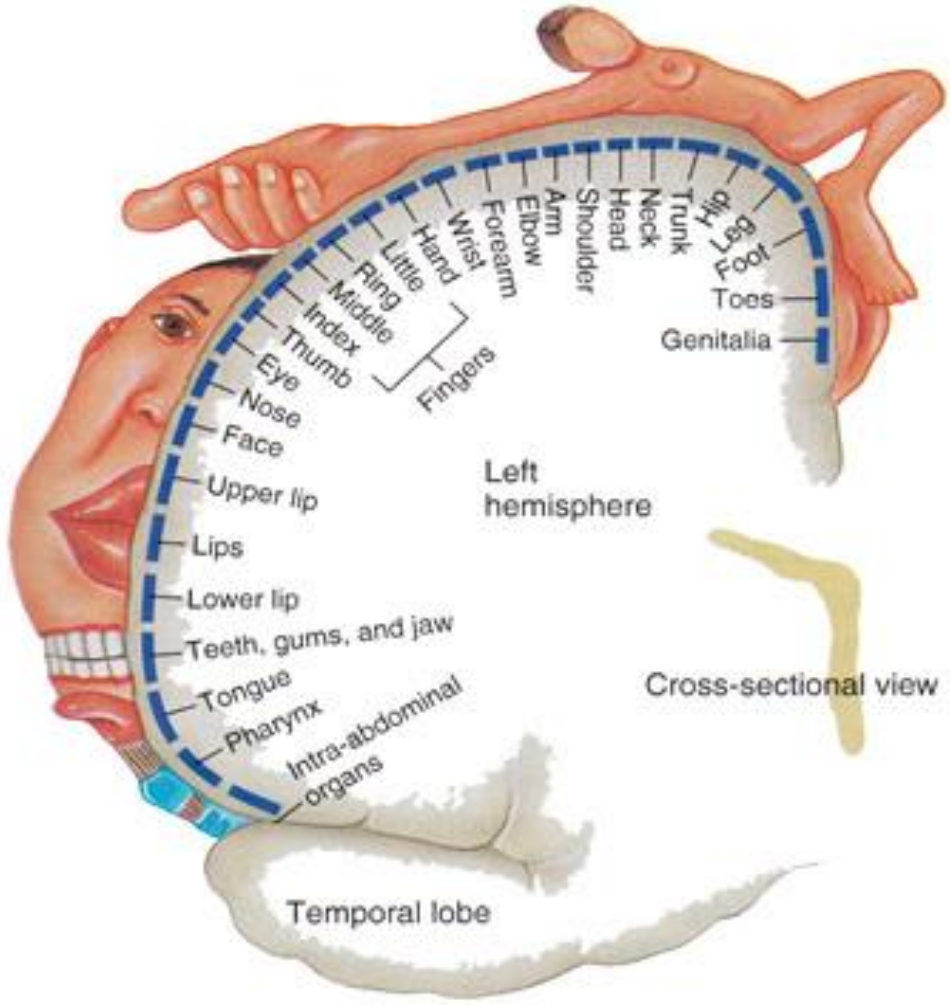

Fig. 7 The sensory homunculus (Penfield & Rasmussen, 1950).

2.3 Skin properties and mechanoreceptor

Our human skin consists of various sensory receptors with multiple purpose and functions. The mechanoreceptor detects mechanical deformation, the thermoreceptor perceives temperature change and the nociceptor respond to potential injury stimuli. In this section, we shall focus on the role of the mechanoreceptors especially during tactile process.

The human skin is the largest organ in human body, weight around 3 to 4.5 kg for an average adult, with surface area around two-meter square. Positioned on the most external layer we have the epidermis, which is an epithelium composed of multiple tiers of cell (stratified squamous epithelium) with around 0.1 mm mean thickness. It is composed mostly of dead epithelial cells that continuously falls off, and are replaced with each new cells continuously growing and pushing from the bottom layer.

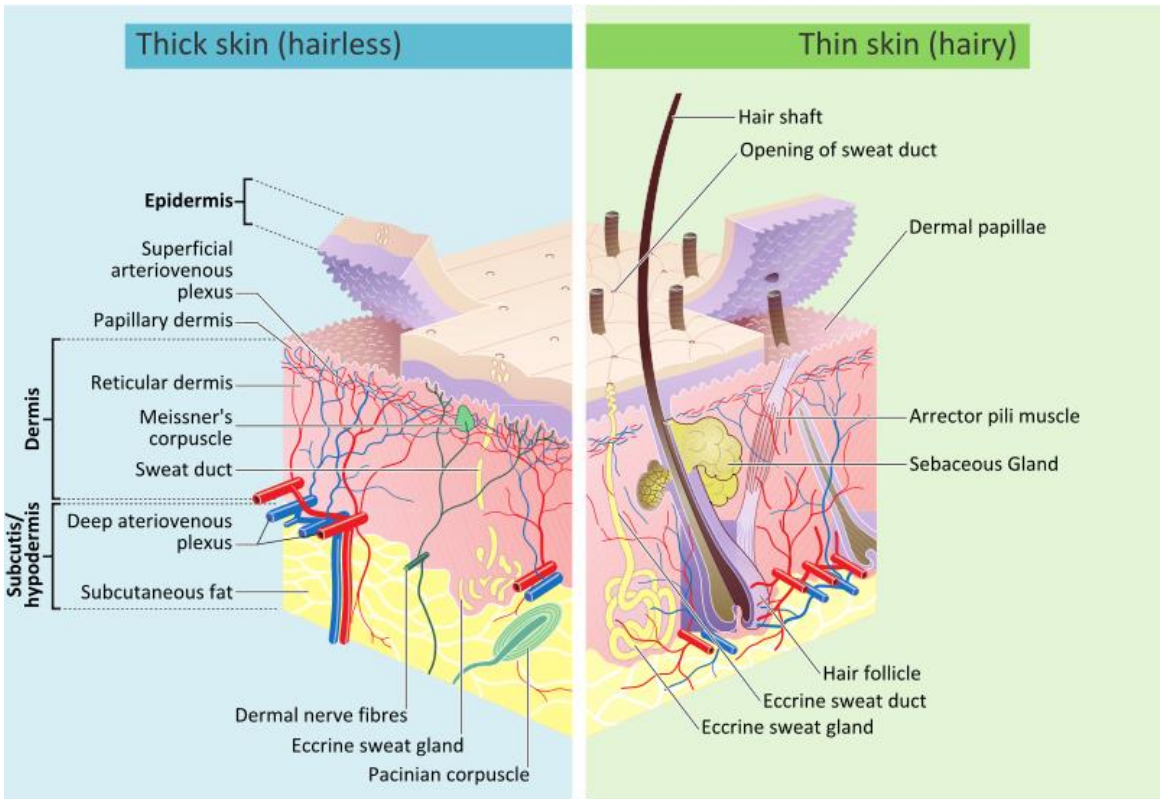

Fig. 8 Glabrous (hairless) and hairy skin (Adapted from wikilibrary).

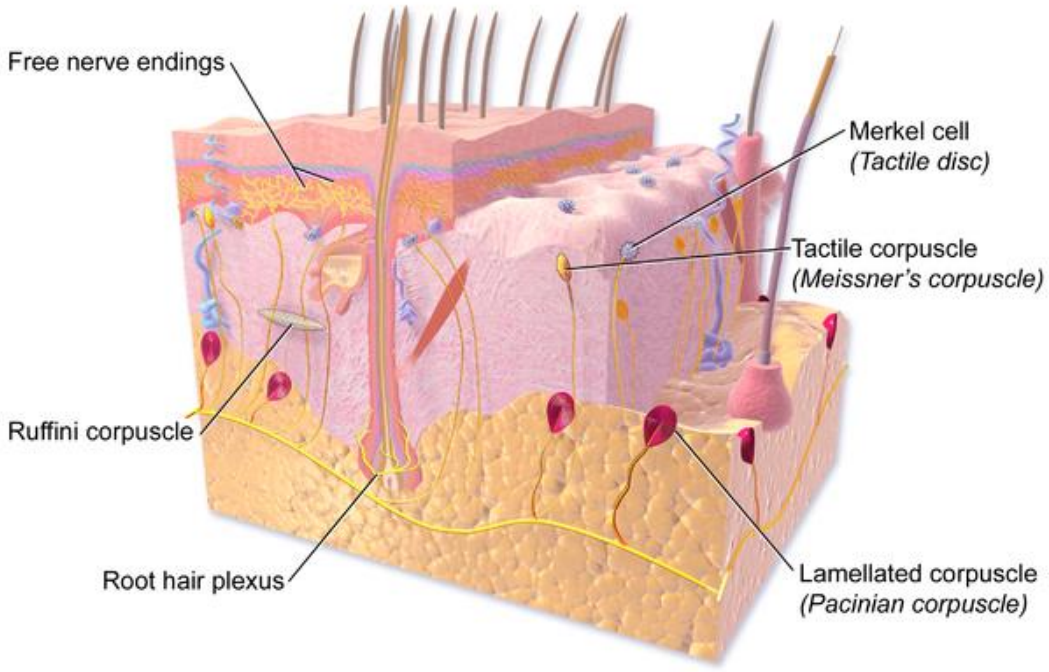

Fig. 9 Tactile receptors in the skin (Adapted from Blausen gallery).

Next, we explain the dermis, which is positioned underneath the epidermis section, with mean thickness about 1.0 mm, and consists of two layers. One of the layer is a thick and densely packed stretch resistant collagen fiber that runs parallel with the skin surface, with smaller population of elastic fibers. The other one consists of papillary layer, much thinner and located between epidermises. It also contains hair follicles, oil and sweat glands, muscles, nerves, and blood vessels (refer Fig. 8). Finally, we explain the hypodermis section, which consists of loose connective tissue layer, containing blood vessels, nerves and fat cells. Sometimes, the hypodermis is not categorized as a part of the skin.

The mechanoreceptor is a sensory receptor which provides information about mechanical changes in the environment to the organism or human, with responds to physical stimuli such as touch, pressure, motion and others. There are about 17,000 tactile efferent in the glabrous skin area of one hand (Johansson et al. 1979) with specific behavior and functions. One of the remarkable feature about the mechanoreceptor is the extreme sensitivity to detect the smallest possible unit of stimulus.

Referring to Figs. 8 and 9, the human mechanoreceptor consists of four main components which is the Meissner's Corpuscles (Fast Adaptive mecanoreceptive type I unit; FA-I), the Pacinian Corpuscles (Fast Adaptive mecanoreceptive type II unit; FA-II), the Merkel's Discs (Slowly Adaptive mecanoreceptive type I unit; SA-I) and the Ruffini' s End organs (Slowly Adaptive mecanoreceptive type II unit; SA-II) (Johansson and Vallbo, 1979, 1984; Darian-Smith, 1984; Bolanowski et. al. 1988). Fast Adapting (FA) receptor produces impulses that rapidly return to zero or threshold value, when the intensity does not vary. The next impulse discharge shall be produced only in respond to a changing stimulus (either increase or decrease). Whereas the Slow Adapting (SA) receptor responds to stimulus by producing impulses according to the duration of the stimulus. Any increase on the intensity of the stimulus shall also increase the receptive output.

The FA-I is sensitive towards skin indentation, capable of detecting changes in terms of normal vibration (around 50 Hz) and adapt rapidly regardless the stimulus size. The FA-II detects rapid vibrations (around 200~300 Hz) according to stimulus size. As for SA-I, it detects sustained touch and pressure, and having high sustained sensitivity especially to static force. Finally, the SA-II is sensitive to low dynamic sensation and able to detect tension deep within the skin regardless the stimulus size

(Johansson, 1991, 2009; Kandel, 2000; Johanness, 2010). In general, the performance of the receptor depends on the physical properties of the receptor such as receptor size and shape, quantity of receptive field and also the location within the skin.

During physical contact such as fine touch, vibration, etc., the skin shall experience changes and these shall activate the mechanoreceptors. Even the slightest input of the mechanical energy shall be transduced into receptor potentials, which then transmitted across the CNS to the somatosensory region of the cerebral cortex for processing. This is known as the posterior column–medial lemniscus (PCML) pathway, also known as the dorsal column–medial lemniscus pathway, in relative to the mechanoreceptor function (Refer Fig. 10). It deals not only with skin related sensation (ex: fine touch, during two-point discrimination, etc.), but also joints; for example, proprioception (position sense), bending properties and more. The Pacinian type endings and Ruffini type endings, also exist in muscle and joint receptors. This could explain regarding the role of kinaesthetic function during finger opening angle.

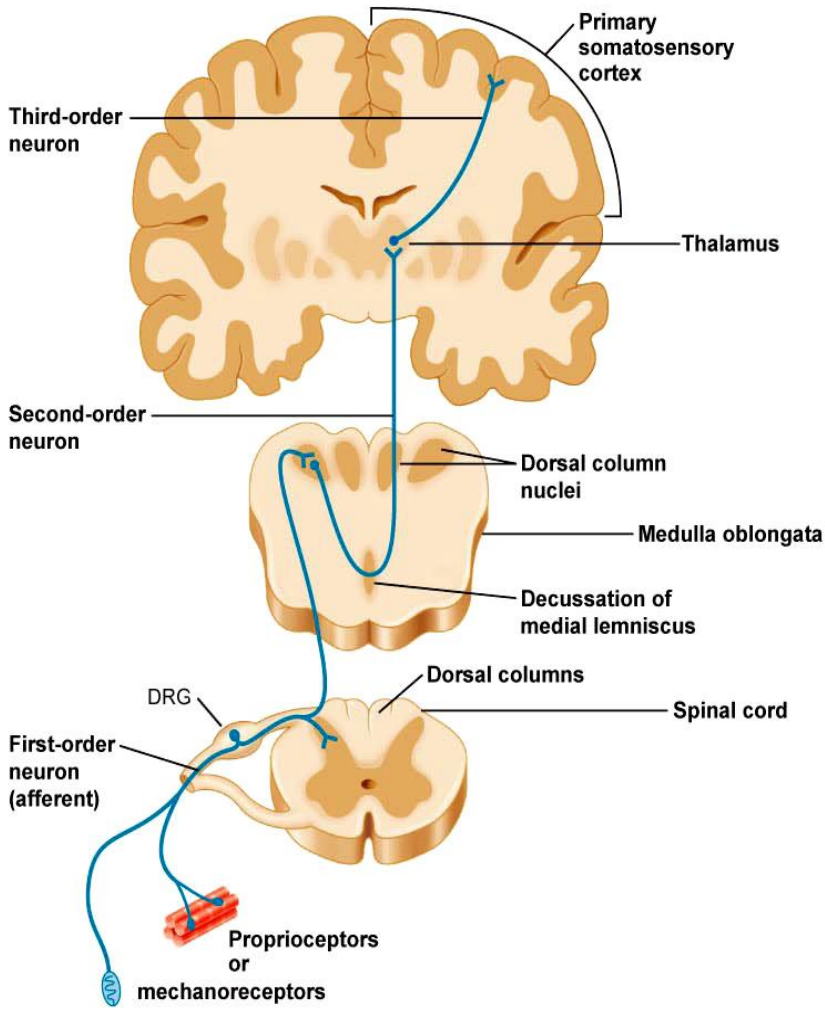

Fig. 10 The Lemniscal pathway (Gardner, 2000)

Among the method that could be used to monitor the performance of the mechanoreceptor is microneurographic (refer Figs. 11 & 12), where a fine tungsten needle is used to penetrate specific nerve fiber in order to obtain direct feedback of neuron activity. From Fig. 13, the morphology in recording feedback from a receptor can be viewed. The generator potential shall be recorded at location (B) and the action potential at (C). During contact (whether in terms of mechanical pressure or load), skin displacement shall occur at point (A), at the same time response shall be taken from each (B) and (C) location. The output shall give a hint whether the receptor behaves in a fast-adaptive manner or slow-adaptive type (Fig. 14).

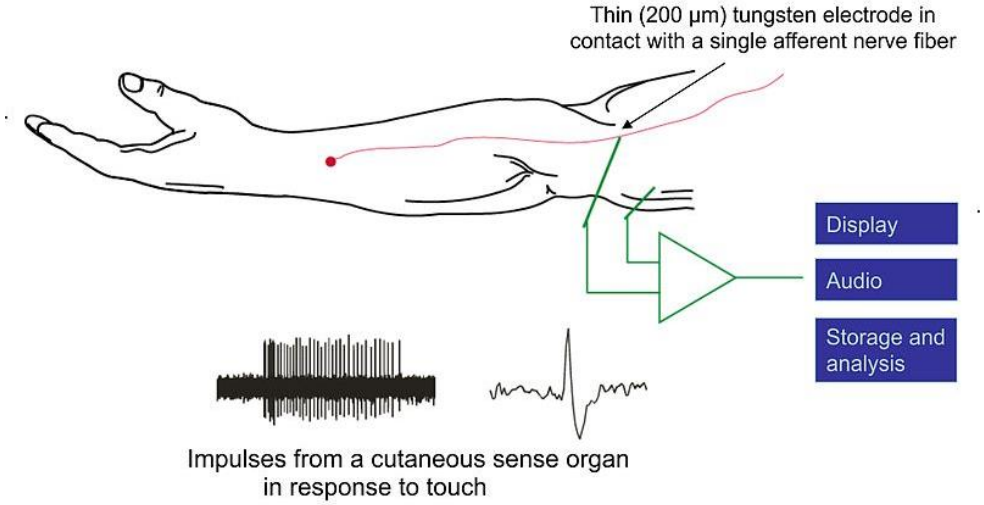

Fig. 11 The microneurographic technique (Adapted from wikilibrary).

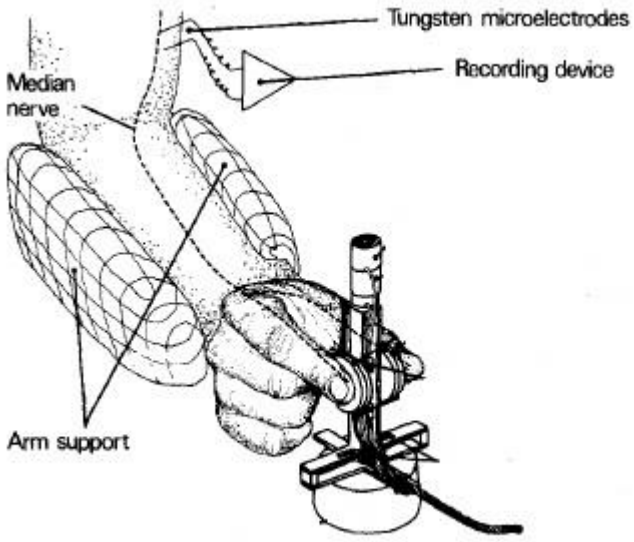

Fig. 12 Example of microneurographic application in experiment (Westling and Johansson, 1997).

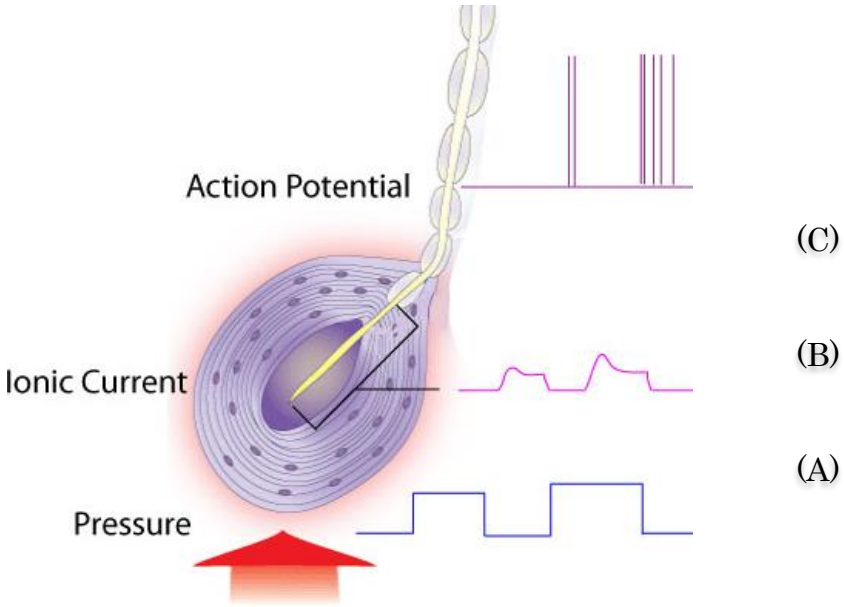

Fig. 13 Morphology for recording electrodes from receptor (Adapted from Biobook).

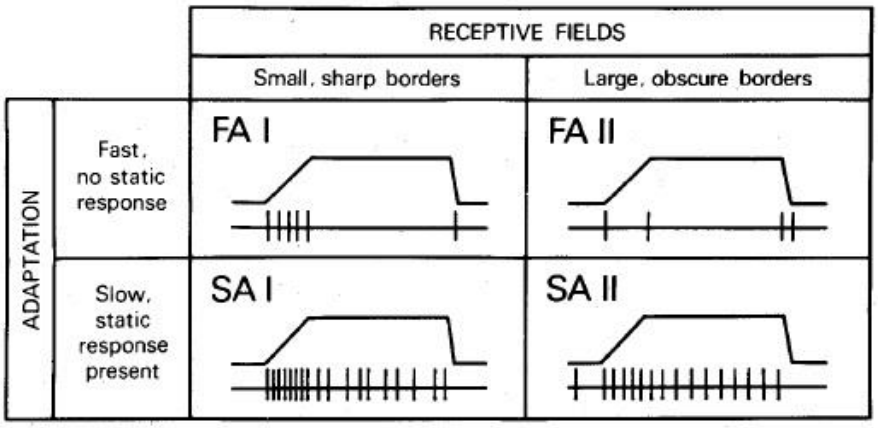

Fig. 14 Types of tactile afferent units in the glabrous skin of the human hand (Johansson and Vallbo, 1983).

The touch sensitivity is a function of the rate at which the skin is deformed. In general, the skin responds to separate touches up to a frequency of about 20 Hz, at which point it changes to a feeling of vibration. The maximum vibration sensitivity is about 250 Hz, and the differences between this vibration frequency can be determined physically.

The tactile resolution, also known as the receptive field size, varies for different areas of the body surface. For example, the fingertip is much more sensitive compared to our palm. The receptive field size (RF) determines spatial resolution or the number of points that can be detected in a given skin area. The larger the RF size, the lower the resolution shall be, and vice versa. Experimental result from Johansson (2000, 2009) is able to give general perspective on the receptive field and density of different mechanoreceptor at human hand (Fig. 15).

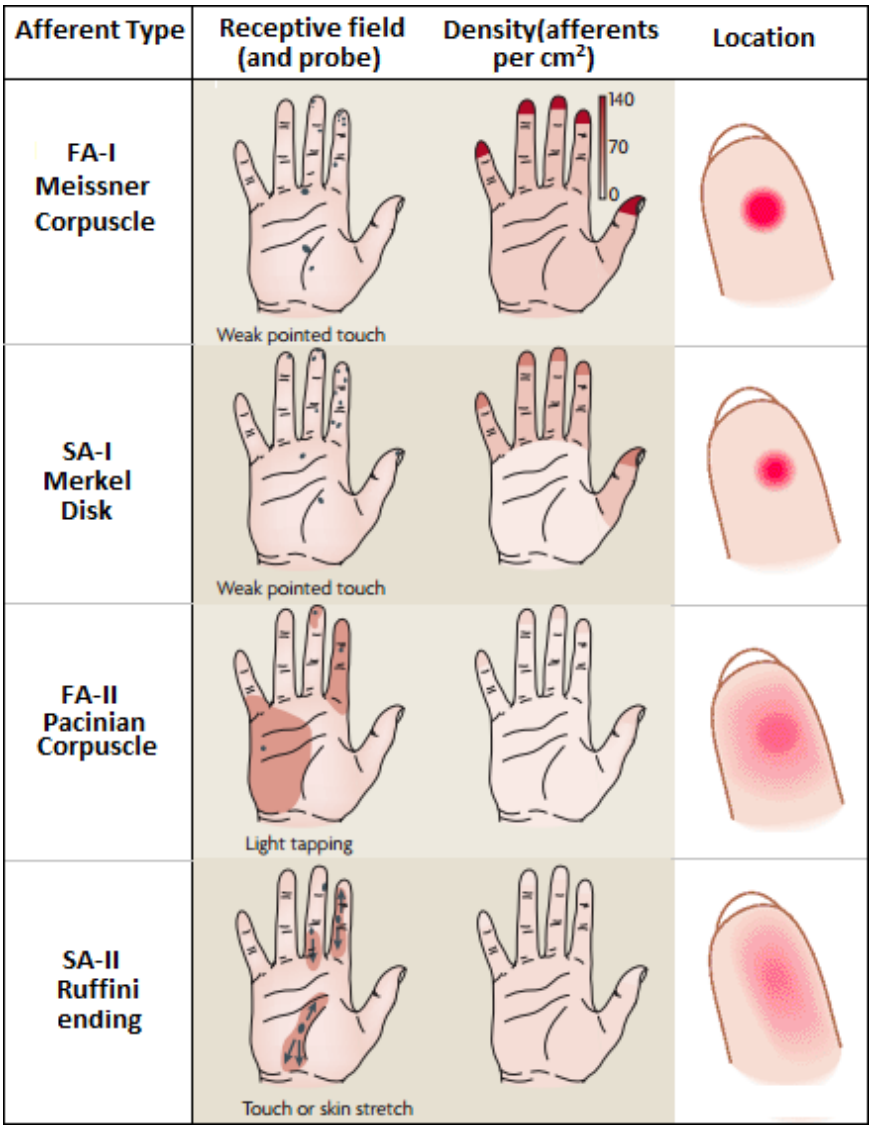

Fig. 15 Tactile sensory innervations of the human hand (Johansson, 2000 & 2009).

2.4 Conclusion

The main focus of this research towards the SA-I mechanoreceptor unit, which plays the role of defining the sensitive sensation from the skin. Research regarding mechanoreceptor already began during the 20th century, and escalated after the discovery of the microneurography technique by Vallbo and Johansson in 1965. The research by Dandekar, Raju and Srinivasan (1996), and Sripati, Bensmaia and Johnson (2006) able to provide a good fit between the rate of the spikes fired by the Slowly Adaptive Type I (SA-I) afferent and the Strain Energy Density (SED). Lesniak and Gerling (2009) focused more on the response of a single SA-I receptor by comparing the result with the psychophysics data of Phillips and Johnson (1981).

Information gained from mentioned experiment and simulation able to provide some basic guideline, which is the significance in observing the von Mises stress value to evaluate the performance of the SA-I mechanoreceptor during contact. In our research, we shall be focusing on non-invasive technique such as psychophysics experiment and FEA method instead of invasive one such as microneurography. Details regarding each process shall be explained further in Chapters 3 and 4.

Chapter 3

PSYCHOPHYSICAL EXPERIMENT

3.1 Introduction

A major focus in the tactile sensing field is the study of the delicate human detection process. A significant challenge is how to adapt this concept effectively to robotics. For example, although differentiating the properties of two extremely thin foils is natural for most people when using their fingertips, it is an extremely difficult task for robots equipped with tactile sensors. Despite this fact, there are products on the market capable of conducting a similar task, such as an automatic page turning device and a bank note counter. However, the majority is non-versatile and limited to their specific task and function.

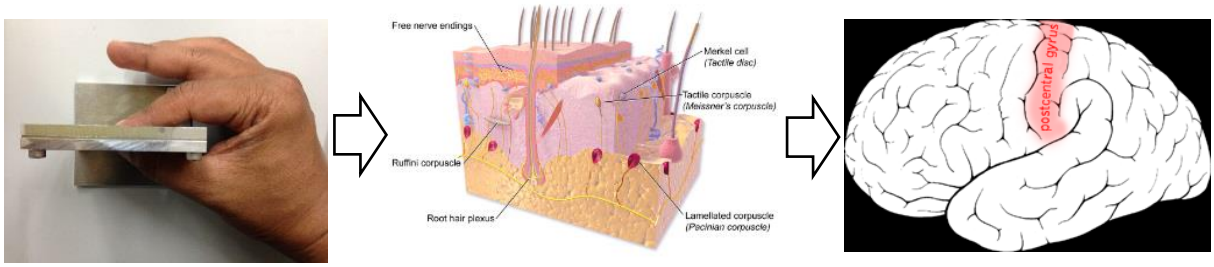

Fig. 16 Signal flow from stimulus to neural pulse and finally to the somatosensory cortex region of the brain for the perception of touch.

For this reason, the development of a dexterous mechanical hand capable of handling delicate functions is needed, especially for daily use. To create a device able to perform such critical tasks, the best option is to study the complexity of the human tactile mechanism, as shown in Fig. 16 for example. At first, contact is made between human tactile function (index finger and thumb) and metal foil (in this thesis, the stainless steel (SUS) or copper (Cu) foil). Next, the skin deforms and adapts to the object's shape. The mechanoreceptor senses and perceives change in their deformations, and transform the information into electrical signals (neural pulses). The stimulus is then carried via an extensive nerve network to the Central Nervous

System (specifically towards the somatosensory cortex region) for the next processing phase.

Through this study, we will be able to improve and optimize the performance of tactile sensors, especially in robotics. In this chapter, we shall discuss on the basic function of psychophysics, for the purpose of understanding human's tactile behavior.

3.2 Literature review

It is astonishing how the cutaneous function of human tactile sensation is capable of distinguishing ultra-thin foil thicknesses up to several 10 μms, yet is unable to be monitored by kinesthetic or joint sensory organs. This motivates us to further study this mechanism with a goal towards robotics application. Since tactile sensations play a major role in the thickness discrimination of ultra-thin foils, elucidating this mechanism is the aim of this psychophysics experiment.

Previous psychophysics studies by Miyaoka and Ohka (2001, 2002) have shown the existence of an undetected region when analyzing materials of 70 to 350 μm in thickness. For humans, the process of thickness discrimination is influenced by two major sensing systems: the cutaneous function (related to delicate contact or touch) and the kinesthetic function (influenced by muscle joint motion) (Jones and Lederman, 2006; Bossomaier, 2012). One hypothesis is that both systems are functioning simultaneously and the transition state occurs somewhere within this region. As mentioned previously, the activation of such critical skill could come from mechanoreceptors that are sensitive to constant pressure, constant velocity, or acceleration-type information, such as SA-I, SA-II, FA-I, and FA-II. It could be possible that plastic deformation also influence the judging process, especially when discriminating extremely thin materials (Miyaoka and Ohka, 2001). Until today, the application of psychophysics is still relevant in describing the relationship between a person's sensations versus psychological judgement; as supported by Gescheider (1997) and Read (2015).

In robotics, we can relate all of these ideas to the sensor fusion technique to enhance the performance of available sensors. We will monitor this phenomenon during the current psychophysics experiment using a group of extremely thin SUS and Cu foils. The evaluation process is more detailed with a higher thickness test ratio

(by focusing on a single thickness group with seven samples) as compared to previous experiments that conducted piecewise examination using four groups of material thicknesses, but with fewer samples (Miyaoka and Ohka, 2002).

Our objective is to study the behavior of the human tactile mechanism during the evaluation of extremely thin foils and to bridge the gap between the undetected regions, especially below 150-μm thickness. In order to do so, we will compare the Weber fraction between the current and previous psychophysics experiments. The number of thickness samples was increased to monitor the detection, especially between the cutaneous function and the undetected region.

Next, we shall review the basic psychophysics information and discuss the previous experiment results that are related to this research. As mentioned, psychophysics is defined as the study of the relationship between the physical properties of a stimulus and perception ability. It begins during the early 19th century, when E. H. Weber questioned the differences between stimulus and perception; and suggested that it could be possible to judge and measure human perception; even though the result may not equal actual physical measurement. G. T. Fechner analyzed this concept and proposed what is known as Weber's Law or the Weber fraction. In theory, the Weber fraction shows the ability of a subject to detect distortion of stimuli and discriminate stimuli thicknesses from the amount of distortion (Gescheider, 1997; Manning and Rosenstock, 1968; Stevens, 1975). The ratio between the change of stimulus intensity that is just noticeable difference ($\Delta\Phi$) and the actual value of stimulus Φ could be described using the constant value c, resulting in Eq. (1) below.

$$c = \frac{\Delta\ \Phi}{\Phi} \tag{1}$$

Fechner further expanded this law, resulting in Fechner's Law. The main difference is that Weber defines the psychophysics relation using a linear function, whereas Fechner's Law postulated the relation using a logarithmic function, which fits most psychophysics experimentation phenomena. This results in Eq. (2), where S and k represent the sensation magnitude and a constant value, respectively (Manning and Rosenstock, 1968).

$$S = k\ \log\ (\ \Phi) \tag{2}$$

In theory, the classical psychophysics method can be divided into three main categories: the Method of Limits, the Method of Adjustment, and the Method of Constant Stimuli. Each method can be used to measure the Absolute Threshold, RL (Reiz Limen), and the Difference Threshold, DL (Differenz Limen; also equal to $\Delta\Phi$). Either selection depends on the merits and weaknesses of each method. Among three experimental methods, we will be using the Method of Constant Stimuli and focusing on the DL output (where comparison and judgement shall be made by the test subjects between a standard stimulus and comparison stimulus). Although this method is considered one of the most accurate in psychophysics, it is also known as the most time consuming (Gescheider, 1997).

In measuring perception, basically we can divide it into three basic experimental protocols, which are magnitude estimation process, matching process and detection or discrimination process. During the magnitude estimation process, the test subject is required to visualize the perception in terms of figures or ranking. For example, to rate the perception of sound loudness, the magnitude is ranked by from 1 to 10 rate. One of the problem with this method is that the perception value may differ from one person with another. A way to control this is by introducing some limitation (for example by limiting it from minimum of 1 to maximum of 10 rate). As for the matching experiment type, the test subject is required to adjust one of two stimuli to match the other one as close as possible, for example to match the brightness of one lamp to match the other one. It is mostly applied using the Method of Limits, where the test subjects have control to matching the stimuli. Finally, in a detection type experiment, the test subject is required to detect the small difference in the stimuli. This is closely related to our experimentation, where we apply the Method of Constant Stimuli to measure the detection of thickness between two given sample.

Next, we discuss related psychophysics studies. The research done by John et al. (1989) in discriminating the thickness of thin copper plates shows that the test subjects were capable of discriminating thicknesses from t = 200 ~ 500 μm (within a 75-μm range). John et al. also discussed the influence of the gripping angle between the fingers, as there were no differences when discriminating between the foil's edge and the surface.

Miyaoka and Ohka (2011, 2012) performed similar experimentation, but with thinner SUS and Cu foils, proposing that humans are capable of discriminating until t

= 8 ~ 50-µm thickness (which normally cannot be detected by the angular sensory organs of the human finger). Their hypothesis is that evaluations of material of less than 70-µm thickness must be performed using the cutaneous function (of SA-I mechanoreceptor units) and, for thicknesses above 350 µm, the kinaesthetic function. There is an undetected region between 70- and 350-µm thicknesses that marks the transition state from one system to another, suggesting the inter-function state between both systems that we described in the earlier section.

Simulation work by Jusoh (2013, 2015) demonstrates the importance of finite element analysis towards indirect monitoring of human tactile behavior. We also highlighted the impact of angular load on the result and the need to maintain contact between human tactile function and the metal foils to improve the detection rate.

Finally, we shall discuss the influence of humidity and temperature on human performance. Based from Standard Ambient Temperature and Pressure (SATP), the average temperature setting for working laboratories should be around 25°C. Even though it may vary depending on local culture and climate, the comfort zone for average human should be around this range.

The basic performance can be divided into physical performance (working environment) and cognitive activities (creative mental task). Working performance increases with temperature up to 21 to 22°C and decreases with temperature above 23 to 24°C (Olli, 2006). Based on another study by Ehander (1990) learning task is optimum at 21°C whereas creative task (simple and choice reaction time) benefit from 27°C temperature state. Whereas high humidity lowers the concentration and increases sleepiness (Howarth, 1984).

As a conclusion, it is quite difficult to balance between the parameter of all the above studies, at the same time to control the humidity and temperature on actual environment. In relation to our psychophysics studies (tactile analysis with force decision method) which is also related to cognitive activities, the temperature needs to be between 21 to 27°C. As current humidity is around 80%, the basic hint is we need to ensure the humidity is around average level which is around 64%.

3.3 The Classical Psychophysics Method

In general, the classical psychophysics method can be divided into three; which is the Method of Limits, the Method of Adjustment, and the Method of Constant Stimuli.

We also mentioned regarding the two major thresholds in classical psychophysics, which is the absolute thresholds (RL) and difference thresholds (DL). The absolute threshold describes the intensity that an observer can barely detect, whereas the difference threshold refers to the minimum intensity by which a variable comparison stimulus must deviate from a constant standard stimulus in order to produce a noticeable perceptual difference (Ehrenstein, 1999) or in simple words, the minimum noticeable difference between two stimuli.

Basically, the experimental procedures for both RL and DL are totally different. In order to define experimentally the absolute threshold, we need to define the stimulus which can be noticed by 50% of the test subjects. To describe the DL, we need to have two stimuli to be presented to the test subjects. One shall be called the standard stimulus (which needs to be consistent throughout the whole experiment) while the other shall be called the comparison stimulus (which varied or changes during each steps). From the test subject's feedback, we able to obtain the probability function *p*, which shows how the subjects feels regarding the comparison stimulus compared to the standard stimulus (whether have greater or lesser feeling). Details regarding the classical method shall be explained accordingly below.

(i) The Method of Constant Stimuli

Compared to other methods, the Method of Consistent Stimuli is considered as the most reliable one, yet at the same time also known as the most time consumed. This is due to the high number of test result or trial required in order to come out with a good conclusion.

During the Method of Constant Stimuli, the threshold shall occur with a certain probability value, and the intensity must be defined statistically. In order to measure AT, the stimuli shall be presented to the test subject in random order, with each value repeated continuously. Feedbacks shall be taken from the test subject; for example, whether the stimulus is detectable or not, or whether one stimulus is much stronger than the other, etc. The responses shall be computed and the resulting graph can be represented using the psychometric function, for example as shown in Fig. 22 (described in the preceding section). The intensity of stimulus shall be plotted along the abscissa, while the percentage of perceived stimuli shall be plotted along the ordinate. In general, the absolute threshold (RL) shall be defined as the value in which the stimulus is detected 50% of probability by the test subjects.

As to measuring the difference threshold (DL), two sets of stimuli shall be presented to the test subjects, consist of the standard stimulus and the comparison stimulus. The test subject shall examine the pairs of stimuli and judge which stimuli produces a greater sensation. For analysis purpose, the standard stimulus needs to be maintained, while the comparison stimulus shall be changed during each trial. The positions or orders of the two stimuli also needs to be counter-balanced. Basically, this procedure is similar to previously mentioned RL procedure. The psychometric function shall be explained using two sets of difference threshold; represented by the upper threshold (DL_u) and lower threshold (DL_l) values. In general, the difference between the comparison stimulus at $p = 0.5 \sim 0.75$ shall be defined as the upper threshold, while the lower threshold is the range between $p = 0.25 \sim 0.5$ value.

ii) The Method of Limits

In this method, the stimulus of different magnitude shall be presented to the test subject in either an ascending or descending order. One simple example is during the new eye glass testing procedure, where the doctor shall change the intensity or magnification of the glass in sequence, until the patient can clearly view the description on the wall or on written paper. As in experiment, it begins by presenting a stimulus highly above or extremely below the threshold point towards the test subject. Next, the intensity of the stimulus shall be adjusted with a small increment or decrement until it reaches the threshold point. Feedback shall be taken from the test subject during each step, for example with a simple Yes-No feedback answer, to verify whether the stimulus can be detected or not. The experiment shall be terminated once the presence of the stimulus can be detected, or once the stimulus disappears (depending on the order of the sensation). In most cases, the ascending and descending series shall be alternated in order to obtain the average estimation value of the threshold.

In general, the Method of Limits are more popular and less time consuming compared to the Method of Constant Stimuli. The accuracy level can be considered as intermediate; sits between the most accurate one which is the Method of Constant Stimuli and the less accurate one (Method of Adjustment).

iii) The Method of Adjustment

Finally, we have the Method of Adjustment, which is the simplest and fastest

method compared to all. In general, it is almost similar with the Method of Limits. The main differences is that the test subjects is in charge of adjusting the intensity of the stimulus, whereas during the Method of Limits, this process was done by the tester and only feedback was taken from the test subject. One example is during the sound testing experiment; by adjusting the volume until it is clearly audible, or in reverse to adjust the volume until the minimum listenable volume. Another example is to match the standard stimuli by continuously adjusting the volume of the comparison stimuli. Due to the nature of this experiment, where the test subjects have full control to adjust the stimulus accordingly; this method provide the fastest tact time, with minimum number of trials.

3.4 Methodology of this study

Our main objective is to verify the range of tactile sensation between the undetected region (previously determined as within t = 70 ~ 350-µm thickness) in which the inter-function between the sensory mechanism of the cutaneous and kinaesthetic functions can occur. Our experiments were performed according to the Method of Constant Stimuli procedure described in the last section. Below, we highlight the improvements made to the psychophysics experiment:

- The main objective is to monitor performance during the lower range of thickness using a t = 20 ~ 150-µm range of SUS and Cu material.
- The material handling method has been standardized to reduce unnecessary finger movement through a specific gripping method. The test subject is required to maintain contact with the foil at all times. Gripping motion should follow the vertical versus angular loading method, which is similar to our simulation study (Fig. 17).
- The thickness discrimination process shall be performed by the index finger and thumb using both hands simultaneously. Each hand shall separately hold the comparison stimulus and standard stimulus material.

The main intention is to ensure that the psychophysics experimentation process matches closely with the previous finite element analysis simulation setting, especially during various loading angles. These key points shall be monitored closely

in order to observe the psychophysics behavior of the test subject during contact analysis. Details shall be discussed in the Results and Discussion section.

i) Experiment #1

The main purpose of the experimentation procedure is to measure the thickness difference thresholds using a pair of SUS or Cu foils. Six males aged in their twenties participated in this experiment as our test subjects, all with zero experience in psychophysics experiments, particularly in regard to the thickness differentiating process. Based on a simple interview, all test subjects were determined to be right handed.

Seven pairs of stainless steel foils (SUS 304) were used as stimuli with thicknesses of 20, 40, 60, 80, 100, 120, and 150 μm. Each foil was clamped between aluminum jigs with a 60-mm diameter exposed opening (Fig. 18). The temperature of the jig was controlled using two hot plates (AS ONE, EHP-250N), as shown in Fig. 19, each positioned beside the test subject's hand.

Fig. 17 Top view comparison between proper grip (OK) vs incorrect grip (NG).

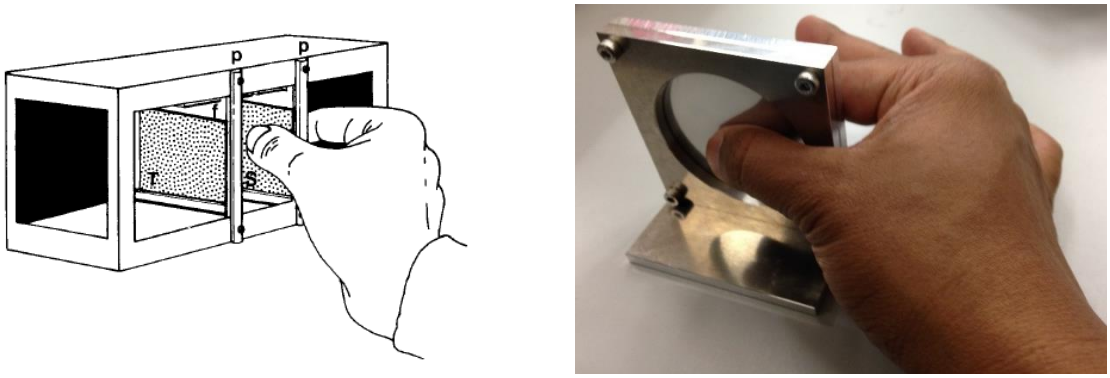

(a) (b)

Fig.18 Example on the experimental apparatus in evaluating material thickness by (a) John et. al. (1989) vs (b) current positioning jig for sheet.

First, each test subject was seated and required to wear an eye mask to prevent viewing any of the test materials. They were also required to wear earphones inputting white noise sounds to neutralize any external noise that could influence their judgement. Next, the tester randomly selected a pair of foils from each comparison stimulus and standard stimulus group, and placed the pair near the test subject's hands. After receiving a tap signal from the tester, the test subject gripped each foil simultaneously using the index fingers and thumbs of both hands. This was to determine which foil was perceived to be thicker using the two-alternative, forced-choice technique. The test subject was allowed to move their fingers with five times gripping motion only, maintaining contact with the metal foil throughout the whole process. Finally, each test subject answered which material was perceived to be thicker by raising the hand which perceived the thicker feeling.

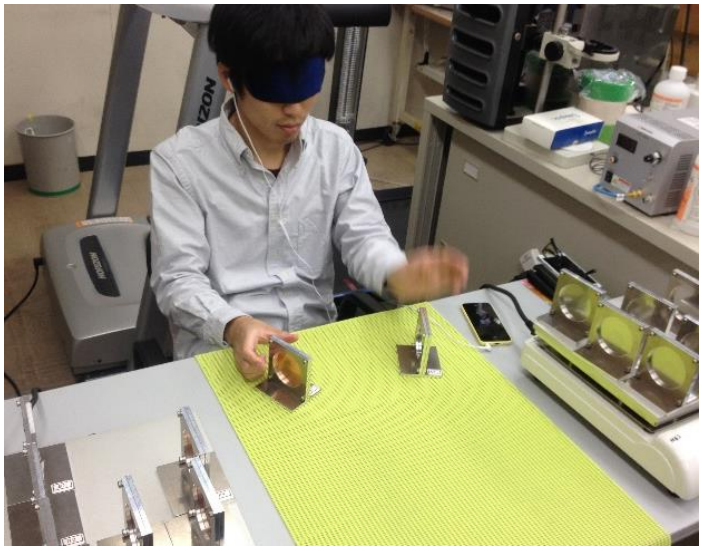

Fig. 19 Experimental setup.

(a) (b)

Fig. 20 Arrangements of test materials on hot plate (a) and humidity chamber used to preserve material sample (b).

The maximum time to give their feedback was 20 sec (including 15 sec of the gripping process) for each combination of stimulus. The inter-stimulus interval is important for the tester to record data and to exchange material for the next combination of stimulus. Basically, pair-wise combinations of seven distinct stimuli (plus self-combinations) produces 28 steps, with comparison between same thicknesses done twice. As it was necessary to counterbalance the right and left positions of stimuli, the total number of combinations doubles up to 56 steps. Overall, each subject performed around ten trials for each combination of stimuli, resulting in a total of 560 steps. The total simulation time per trial was about 30 minutes (including 10 minutes resting time during each interval). In order to maintain the decision-making quality, the maximum experiment time was kept below two hours, which limits the number of trials to a maximum of four per day.

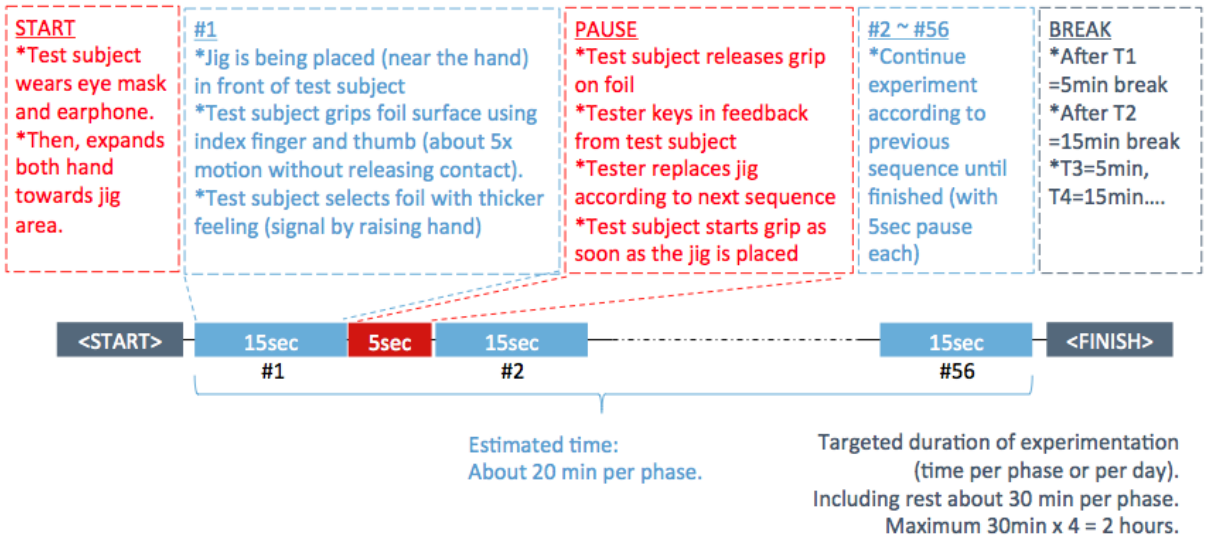

Fig. 21 Experiment flow.

ii) Experiment #2

The purpose of Experiment #2 is to measure the thickness difference thresholds using different type of material (with combination of SUS and Cu foils) and to propose an appropriate information processing mechanisms. We used the same test subject as experiment #1, again with zero experience of psychophysical experiments (on comparing different material type). As confirmed previously, all test subjects were right handed.

For stimuli, seven SUS foils (SUS 304) and seven Cu foils (fineness, 99.9%) shall

be used as stimuli using the same thickness properties (from 20 to 150-μm thickness). All of the foils shall be clamped inside the aluminum jig and the temperature of the jig shall be controlled with same setting as Experiment #1.

Similar as the previous procedure, the subject shall be seated in a chair while instructed to wear an eye mask and an earphone (with white noise played) to prevent from any external distraction. After the tester placed randomly selected foils (one SUS and one Cu foil) beside test subject's hand, the subject shall then proceed to grip each of the stimuli (foils) using the index finger and thumb of both hands simultaneously, and determines which foil was perceived to be thicker using the two-alternative, forced-choice technique by raising his hand. The total time between the gripping processes until feedback, including inter-stimulus interval is the same as the previous Experiment #1. The number of movement (until five times gripping motion) and contact should be maintained at all time.

The pair-wise combinations of seven distinct stimuli plus self- combinations shall produce 24. Compared to previous experiment, analysis on same thickness was done only once. As it was necessary to counterbalance the right and left positions of rings, the total number of combinations shall be around 48. Each subject shall perform ten trials for each combination of stimuli; producing a total of 480 trials for each subject. Each subject shall perform around ten trials for each combination of stimuli.

The temperature of the equipment and jig was also set according to previous setting. The same thing also applies towards the room temperature and humidity. The total simulation time also maintained around 30 minutes per trial (including 10 minutes resting time) with maximum of 4 trials per routine or per day.

In Experiments #1 and #2, the temperature of the hot plate needs to be kept within 35 ± 1 °C in order for the foil to be around 32 ± 4 °C (which is close to normal body temperature). Although the heat dispersion factor could probably increase or reduce the temperature of each foil depending on thickness, it will not influence the tactile decision if the temperature is kept within range. For the room temperature, it shall be maintained around 25°C. As for humidity, it shall be controlled within 60% range (Currently the average is about 50%, as the optimum indoor setting for either heating or cooling climate is also around this value).

3.5 The grip condition

Next is to define the suitable gripping force when handling the thin plate material. The gripping force was not specified during previous experimentations by John et al., and by Miyaoka and Ohka. As initial guidelines, the anthropometric data from FAA William J. Hughes Technical Center (1996) has been used to estimate normal gripping force when handling material between thumb and index finger; resulting in the value of 48 N for momentary and 28 N for sustained hold. Considering this value is too excessive compared to actual practice here, we have decided to reduce the load with an average of 1.0 N (for both index finger and thumb).

The loading value (1.0 N) is supported from the study by Serina et al (1997), which showed that the finger pulp produces most displacement when loading is less than 1.0 N. As the load exceed this value, the pulp starts stiffened rapidly. Further additional loading does not excite the mechanoreceptor especially towards fingertip's deformation and skin stretch (Phillips and Johnson, 1981; Westling and Johansson, 1987). From here, we could summarize that the performance of the fingertip during gripping process should be effective as long as the loading condition is kept below 1.0 N value. Other than that, Serina et al. also highlighted the influence of angle of loading towards pulp response. Details regarding contact analysis shall be briefed in chapter 4, using the 3D elastic model of the index finger and thumb.

The main reference for the current psychophysics experiment was based on the research of Miyaoka and Ohka (2001, 2002), especially when comparing the tactile behavior between different thicknesses. As stated previously, our objective is to verify the existence of two information processing systems in discriminating the thicknesses between the undetected regions. For this reason, we focused on a single group of materials with thicknesses between 20 to 150 μm. This is different compared to previous psychophysics experiment (of duplex theory), which used four different groups of material thickness.

3.6 Result and discussion

(i) Experiment #1

We analyzed the results of the psychophysics experiment presented by the psychometric function graph, as shown in Fig. 22. At first, the comparison result between SUS type materials (SUS vs. SUS). The ordinate represents the probability of the comparison stimulus to be judged as thicker than the standard stimulus and the abscissa represents the thickness of the comparison stimulus. Higher slope values demonstrate the ability of the test subject to differentiate between thicknesses better. Each line represents the probability trend of the base material or standard material.

For example, the data at the upper left corner (which represents the trend line for the SUS standard material of t = 20 μm) shows a probability of 0.7 for the t = 40-μm comparison material to be judged as thicker when compared to the 20-μm standard material. In general, value p = 0.5 marks the threshold point where the probability of judging both types of material thicknesses is similar (p.32). As long as the overall slope value is positive and not centered along this region, the ability to discriminate between materials is available.

The result could also be analyzed by converting the p values into z-score function (Gescheider, 1997) using selected data within the 95% confidence rate (Fig. 23). As a result, the positive increment of the slope shows the test subject's ability to appraise differences with an increase in z-score values over thickness. As described previously, continuous contact and the angular load could be factors that contribute towards the increase in detection rate between different thicknesses. Overall, the proportion of detections (whether expressed as p values or z-scores) increases as the thickness of the comparison stimuli increases. Again, this proves the ability of the tactile function (of the test subject) to discriminate the thickness from the stimuli.

Similar trend can be viewed from the p values of Cu vs. Cu comparison. Basically, the z-score function should also produce similar result. Compared to the SUS material, the probability of detection for Cu material is higher especially from t = 20 ~ 40-μm thickness. This was also experienced physically during experimentation; when using 20-μm Cu material as comparison or standard stimulus, the detection (of the 20-μm material) is almost 100% when compared with other thicknesses. The increment of p values and z-score function is also more rapid compared when using SUS material.

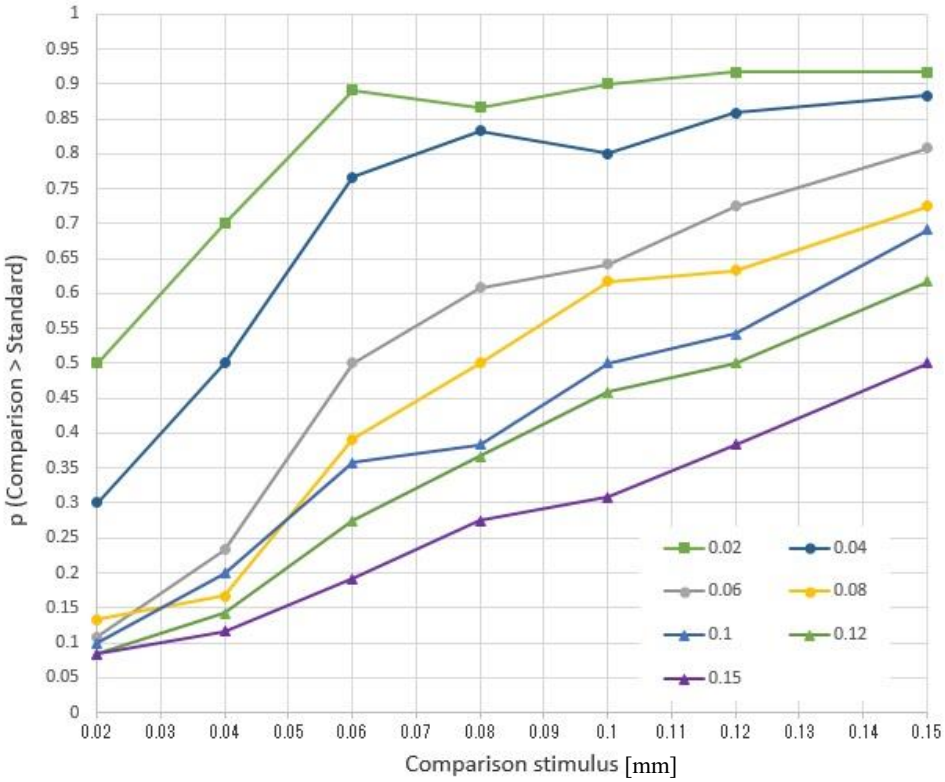

Fig. 22 Psychometric function of *p* values vs. thickness (SUS vs SUS).

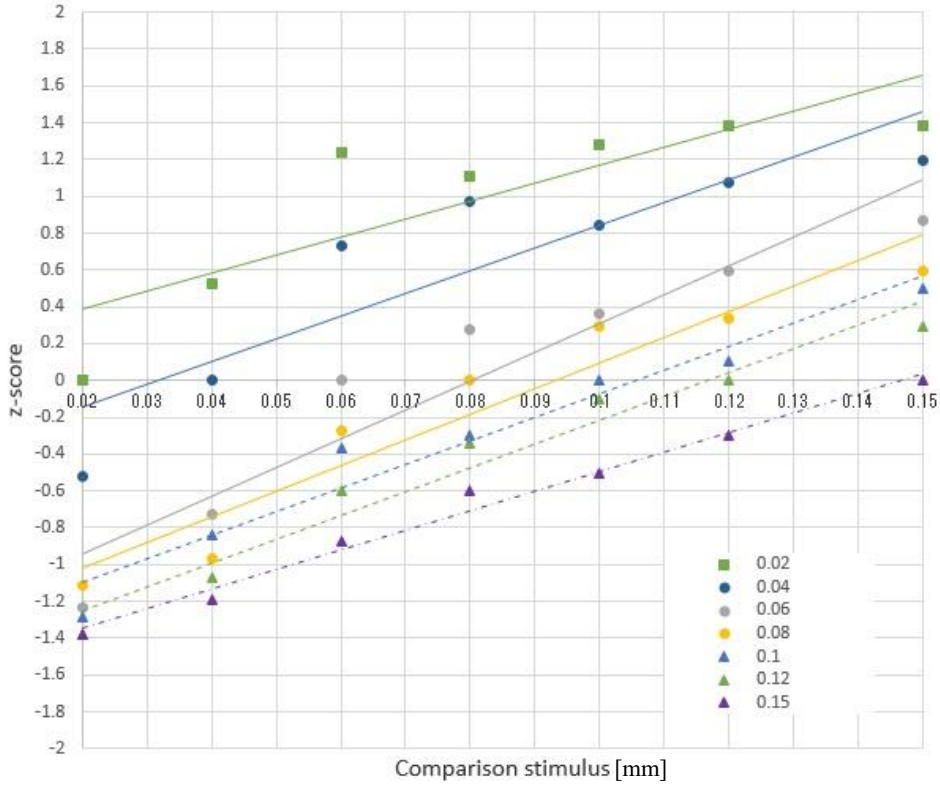

Fig. 23 Psychometric function of *z*-score vs. thickness (SUS vs. SUS).

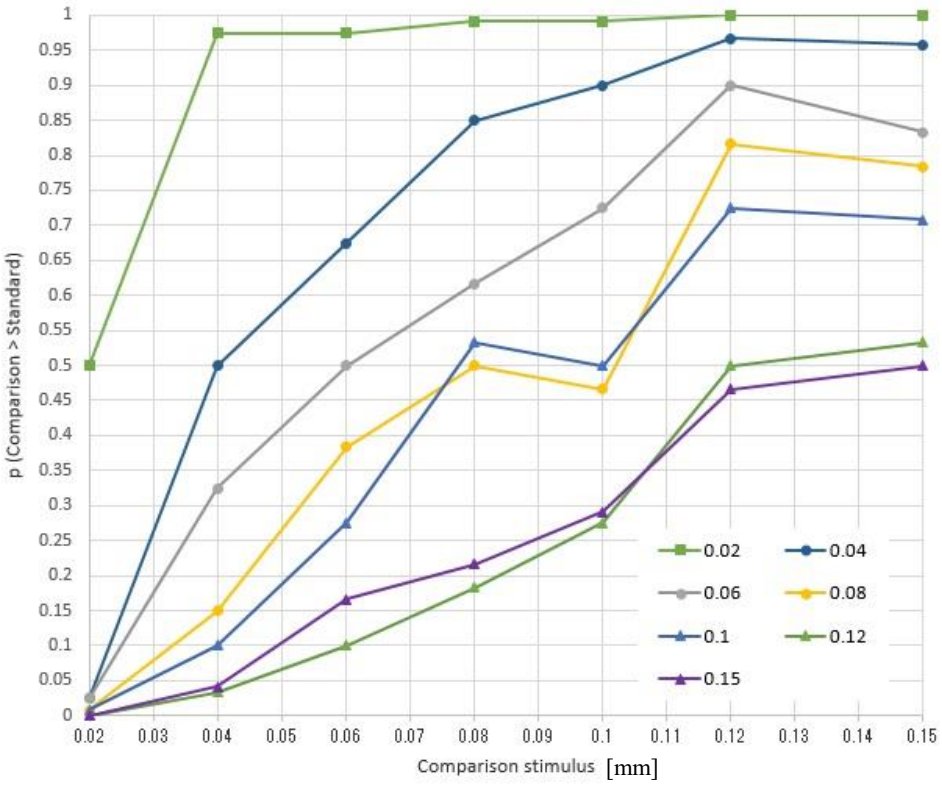

Fig. 24 Psychometric function of *p* values vs. thickness (Cu vs. Cu).

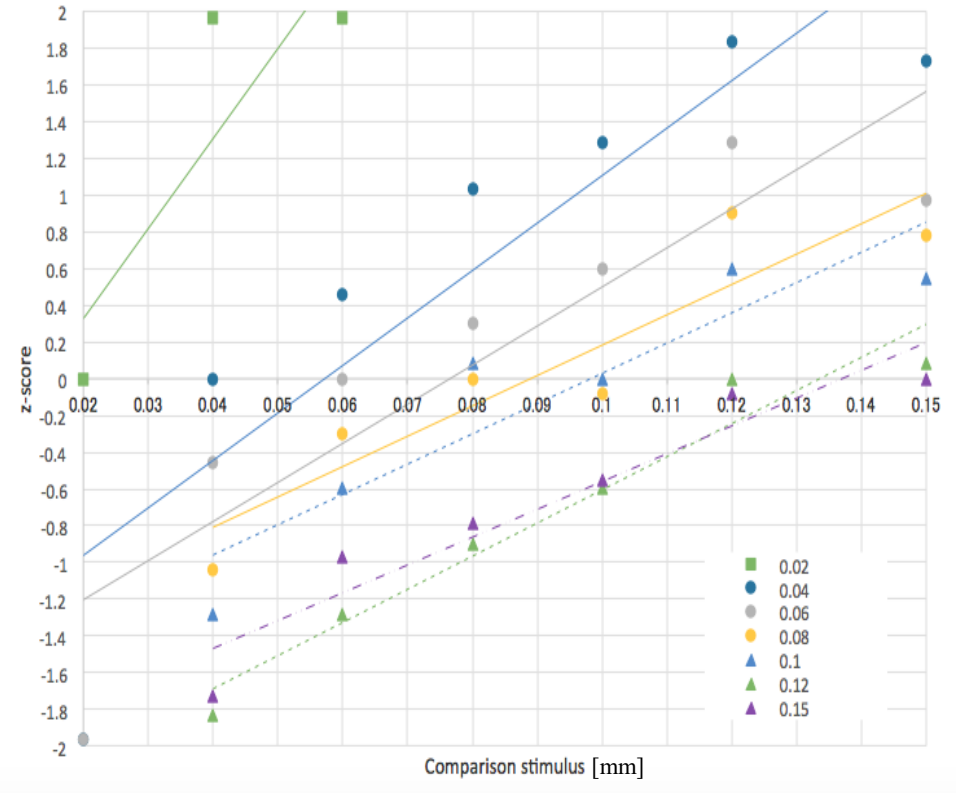

Fig. 25 Psychometric function of *z*-score vs. thickness (Cu vs. Cu).

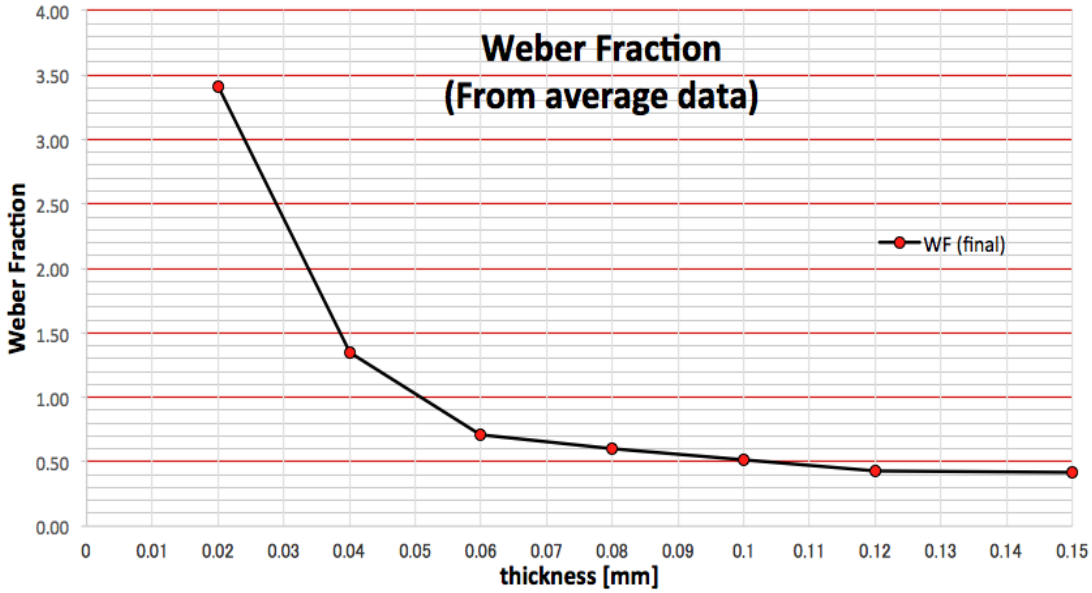

Fig. 26 Weber fractions vs. thickness (SUS vs. SUS).

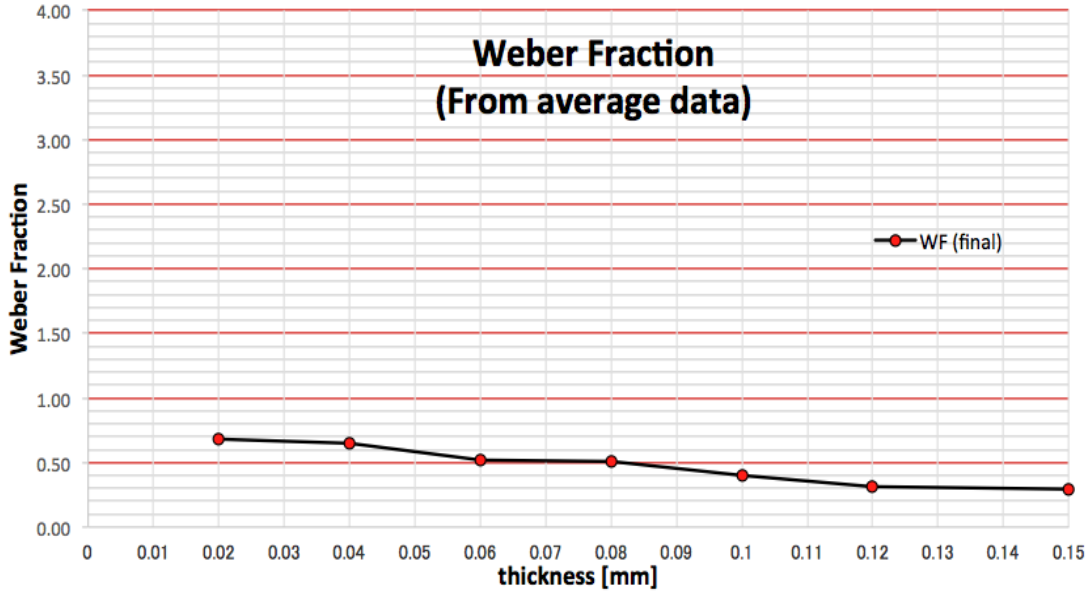

Fig. 27 Weber fractions vs. thickness (Cu vs. Cu).

Next is to brief regarding the Weber fraction result. In terms, the Weber fraction (p.29) shows the ability of a subject to detect distortion of stimuli, and discriminate between the thicknesses of stimuli from the amount of distortion. For SUS vs. SUS experiment (Fig. 26), the Weber fraction begins at the ratio of 3.4 when t = 20 μm and is further reduced when the thickness increases. As thickness increases, the slope is reduced until finally becoming consistent at around a 0.4 ratio for t = 120-μm thickness onwards.

However, the result for Cu vs. Cu is slightly different (Fig. 27). The reduction is more linear compared to SUS result. It starts with Weber fraction of 0.68 at 20-μm thickness, and ended around 0.28, with constant value from t = 120 ~ 150 μm thickness onwards. It is possible that the test subject could slightly detect the amount of differences between the thickness during this range. Finally in Fig. 28, the Weber fraction for SUS material is summarized with comparison to previous psychophysics results. A similar trend is observed from previous experimentation, with higher Weber fraction values especially during lower thickness.

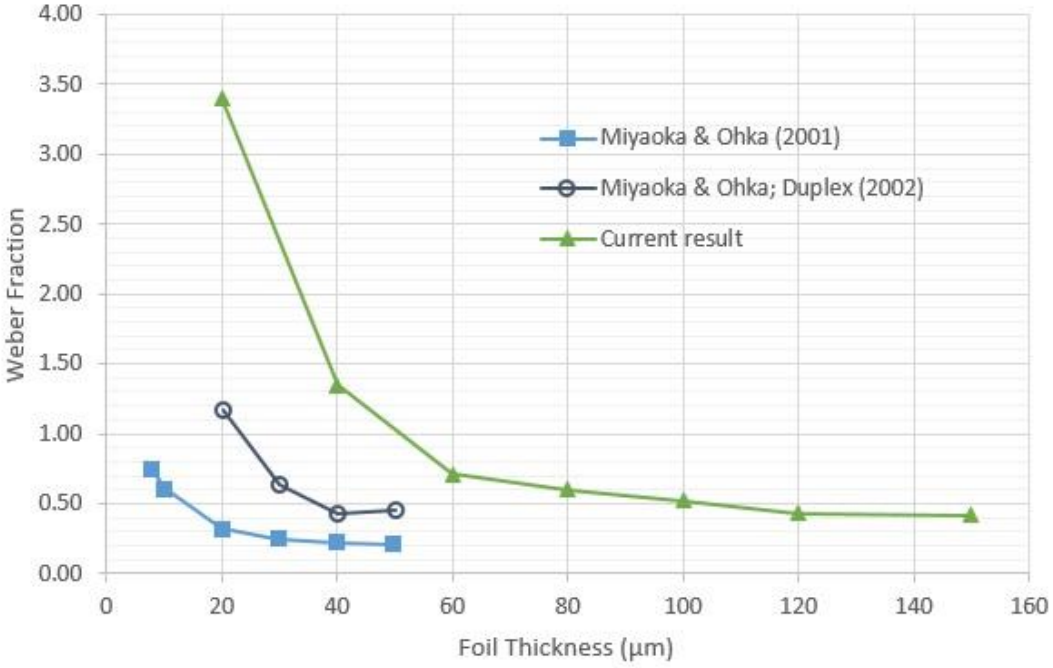

Fig. 28 Comparison between functions of Weber fraction.

From this experiment, the properties of the duplex theory could not be observed, as there was no increment of fraction values during the undetected region. Although some individual results were able to produce such progress, especially during t = 120 μm and onwards, the increment value was still minimal. Furthermore, the current Weber fraction is still high compared to our previous result. Such differences could occur due to the nature of this experiment, where we specifically instruct the test subject to analyze the thicknesses using both hands simultaneously along with other restrictions, whereas in the previous experiment the observation was done only with a single dominant hand.

Referring to the previous duplex theory by Miyaoka and Ohka (2002), the

undetectable region was defined as relatively wide at a range of 70- to 350-µm thickness, whereas currently the result shows that the undetectable region does not appear until 150-µm thickness. From the current result, we can conclude that the undetectable region exists between 150 and 350 µm of thickness.

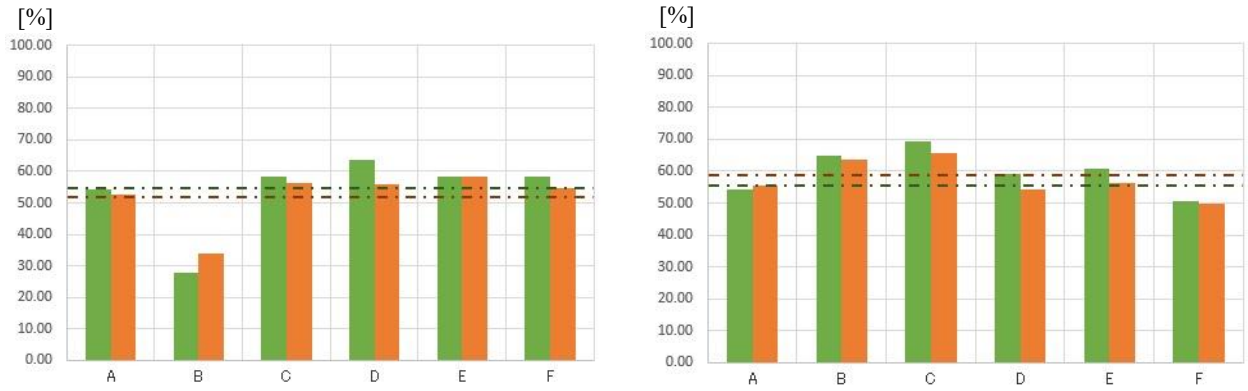

(a) (b)

Fig. 29 Tendency of six test subject (A~F) to select main hand while evaluating between same thickness (green color) & all thickness (orange color) using (a) SUS vs. SUS and (b) Cu vs. Cu materials.

Next, we shall review on the tendency of judgement using the main hand (Before the experiment, we already interviewed all user, and all confirmed as right handed user). The average result for all test subject is around 53.5% when judging the same thickness (For example, thickness of 20 µm vs. 20 µm) and 52% for overall thickness evaluation. This shows that the judgement of the test subject is almost balanced, and not influenced by the main hand factor.

As for Cu material, the tendency of judging using the right hand increased to 60% when judging the same thickness, and 57.5% for overall thickness evaluation. This shows that the judgement becomes more difficult, resulting in a biased decision making process towards the most commonly used hand (which is the right hand side). Also, with lesser spring function compared to SUS material, the material structure becomes easily compacted, thus reducing the accuracy of judgement. The time limit (to decide which material is perceived as thinner) also influence the result. This indirectly could force the user to decide or judge based from subconscious feeling rather than actual tactile sensation. This happens especially when comparing between material with a small thickness differences.

ii) Experiment #2

Figure 30 represents the psychometric functions obtained from SUS vs. Cu comparison. The fine line and dotted line represent experimental results, which adopt SUS and Cu as the standard material. For example, the probability function for copper (t = 20 μm) is very high, which shows that this material can be easily identified compared to others, and also proving that the ability to discriminate thickness was done based from material distortion information. Similar result could be seen from the z-score function as it was projected based from the psychometric function graph (Fig 30). Basically, the z-score function graph able to show positive increment of the material detection process. This can be viewed when using either SUS or Cu as standard material (refer Figs. 31 and 32).

Next, the tactile ratio shall be used instead of Weber fraction to summarize the discriminating rate, when dealing with two different types of material. Based from Miyaoka-Ohka (2001), which suggested that human judge the foil thickness based from the spring function, k. Supposed that the subject judges the thickness between two stimuli to be equal when their spring rate is equal, the tactile ratio can be determined using Eq. (11), which resulting in tactile ratio around 1.2 (refer details in Chapter 4).

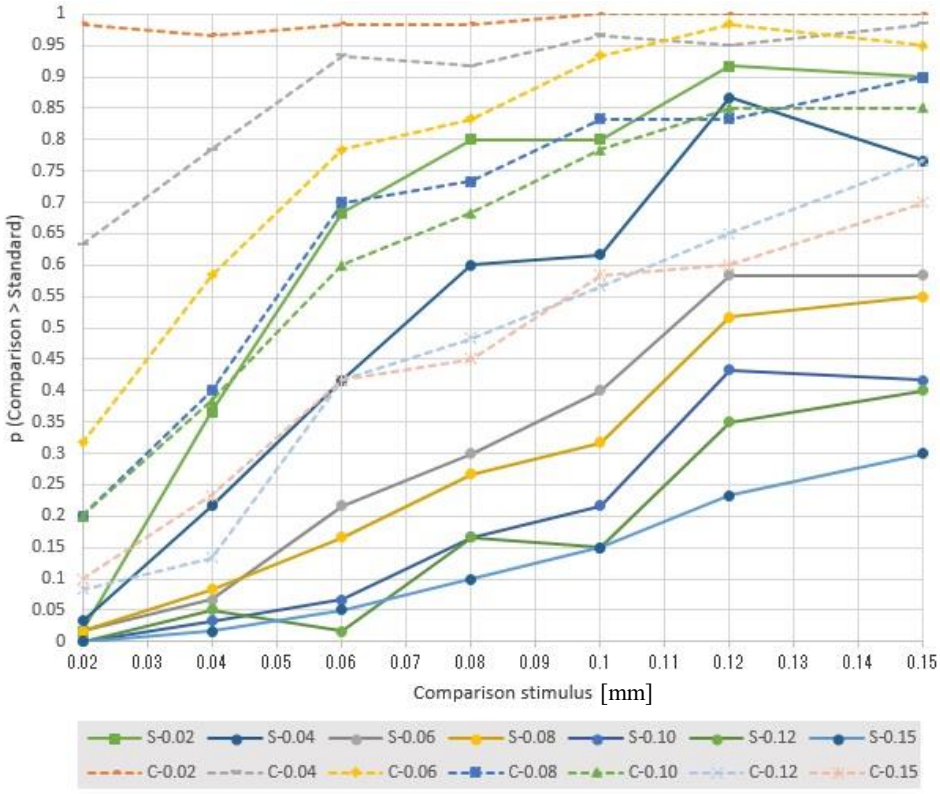

Fig. 30 Psychometric function of p values vs. thickness (SUS vs. Cu).

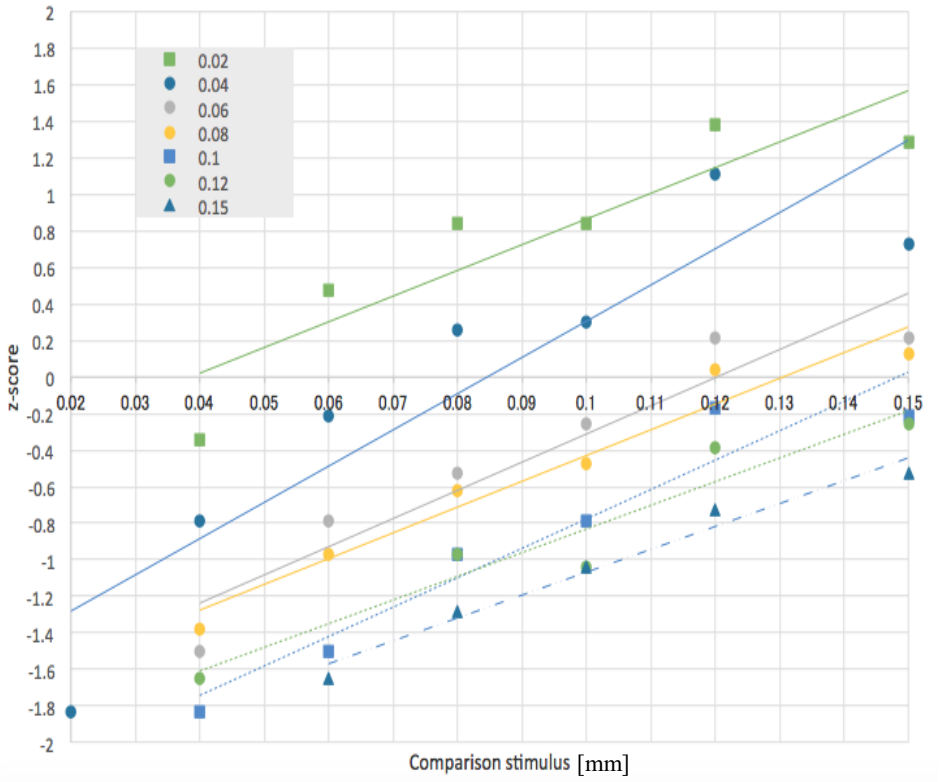

Fig. 31 Psychometric functions for SUS vs. Cu; with *z*-score functions plotted using SUS as standard stimulus.

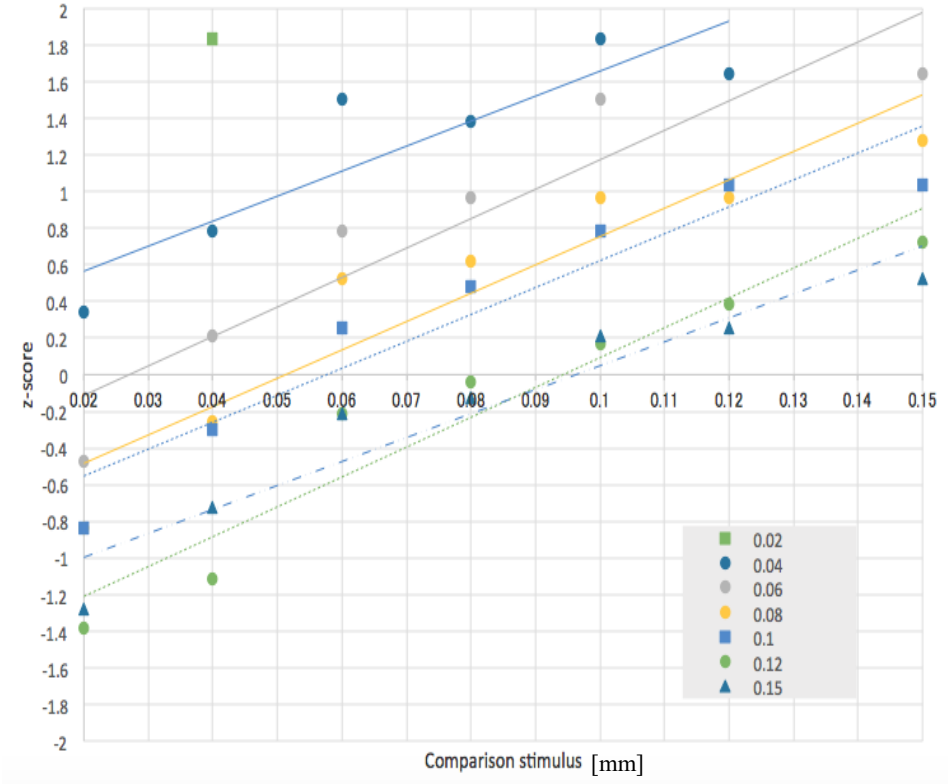

Fig. 32 Psychometric functions (SUS vs. Cu); with *z*-score functions plotted using Cu as standard stimulus.

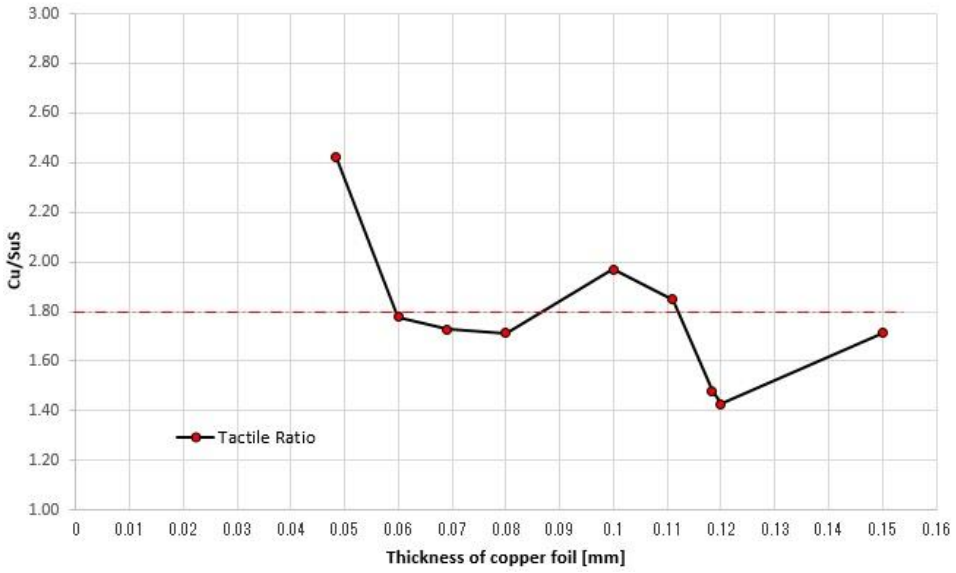

(a)

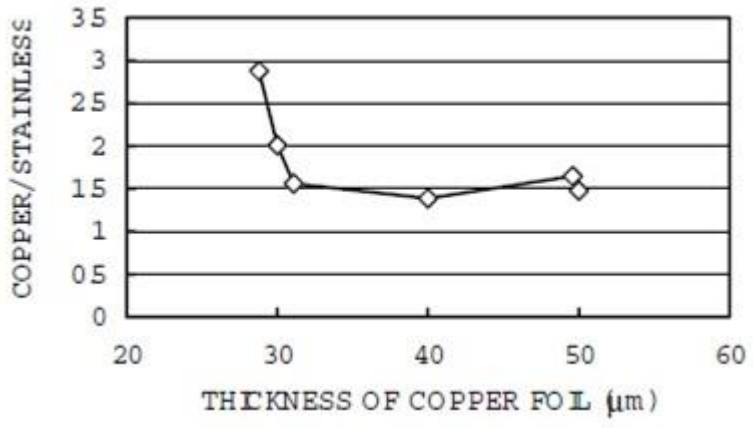

(b)

Fig. 33: Comparison between the ratio of thickness, of copper to stainless steel foils judged to be equal thickness. Result from (a) current experiment vs. (b) Miyaoka & Ohka (2001).

From Fig. 33, the ratio of thickness for Cu to SUS foils is represented at the ordinate, while the abscissa refers to the thickness of standard material (referring to SUS material). The data was extracted from the psychometric function of *p* values, considering the tactile feeling between both SUS and Cu materials having the same judgement. This is done by referring to the plotline which intersects with the 0.5 probability function.

As a result, from current experiment, the projection of the ratio of thickness is in the range of t = 50 ~ 150-μm thickness (Fig. 33 (a)). In general, we could monitor the continuation from previous psychophysics result for thickness above 50-μm thickness (Fig. 33 (b)). The result shows similar curve trend but with higher tactile ratio values (when t = 50-μm, ratio 1.5 is up to 2.4). Next, the average ratio also increased from 1.5 to 1.8. This suggests that by refining gripping method (by continuous contact and angle loading) between both fingers and foils, this could improve the tactile feeling towards comparing both materials.

As for the tendency of judgement using the right hand side, the average result is around 56 % when judging the same thickness and 53.8% for overall thickness evaluation (Fig. 34). As we are dealing with two different type of material, the judgement of the test subject is in intermediate range compared when using similar material type. Even by using the same thickness, the deflection is different, thus comparison process should be clear and understandable. This could be caused by the natural properties of Cu which is softer compared to the SUS material, which could enhance the detection of material distortion. Besides higher contact area between finger and distorted area, which is indirectly judged as a thin material.

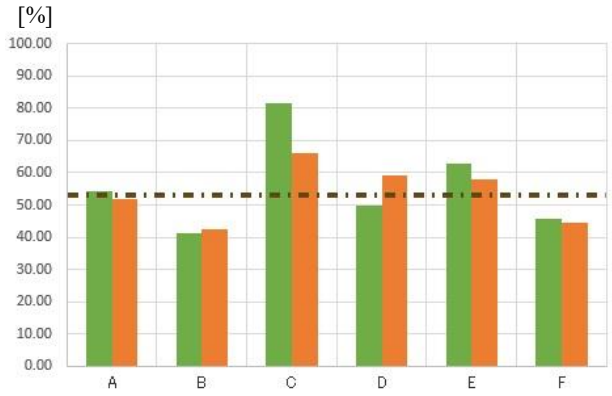

Fig. 34 Tendency of six test subject (A~F) to select main hand while evaluating between same thickness (green color) and all thickness (orange color) using SUS vs Cu materials.

3.7 Conclusion

Understanding human capability in performing critical tasks is a key to enhance sensor performance, especially in robotics. In this study, our objective is to analyze human tactile mechanism behavior in recognizing extremely thin foils using a psychophysics method. Seven pairs of stainless foils ranging in thickness from 20 ~

150 μm were used in the experiment. We applied the Method of Constant Stimuli to define the difference threshold. In order to increase the detection rate, contact between human tactile organs and the metal foils was maintained. As a result, we managed to achieve a similar trend to our previous experimentation. The Weber fraction c reduces as thickness increases and becomes constant with $c \approx 0.4$ from t = 120 μm onwards. We also validated the behavior of the undetected regions up to 150-μm thicknesses.

Unfortunately, we were unable to verify the contents on duplex theory. One of the reason is because the increment that should occur during $t > 70$ μm onwards is unnoticeable. Even though there are test subjects which able to produce such progress especially from t = 120 μm onwards, the increment is barely noticeable. Although duplex theory properties could not be observed, the achievement was quite significant considering the higher thickness test ratio.

In this psychophysics experiment, we employed a specific procedure to maintain contact between the human finger and SUS or Cu foils throughout the experiment. The test subjects were required to grip the material between the index finger and thumb without releasing contact with the foils in order to ensure that the only mechanism that activates during contact is the cutaneous stimuli (or mechanoreceptor), especially in detecting distortion. This also shows that the test subjects are capable of detecting the thickness of stimuli through this gripping method. The result should be improved compared to the previous psychophysical experiments where the combination of two index fingers was used as method for proving the duplex theory.

Miyaoka & Ohka (2001) shows that the test subjects were able to detect distortion of stimuli and discriminate between the thicknesses of stimuli from the amount of distortion. When the amount of distortion is small, the material thickness was defined as thick and vice versa. This is also seen during contact between human finger and soft object (Fujita and Ohmori, 2001). The mechanoreceptor responding to velocity or acceleration information could have been used in detecting such distortion (Johansson and Vallbo, 1979, 1984).

The previous hypothesis also discussed regarding the possibilities of intersection between two discriminating system process. From duplex theory (Miyaoka & Ohka, 2002), one of the conclusions is that the thickness discrimination was possible only when the stimuli is either extremely thin (from 20 ~ 70 μm thickness), or moving

towards thick region (from 350 ~ 1000 μm thickness). The discrimination of thickness was considered difficult by the test subjects when the thickness of the stimuli was between 70 ~ 350 μm, which marks the changing points from one discriminating system to another.

However, for the current experimentation, it's quite hard to judge the discriminating mechanism referring to the probability or z-score function only. Limitation could be from the nature of this experimentation. Basically, we need to set a time limit, so that the test subject could produce good judgement within standard time. Another reason is because, we need to restrict the quantity of material thickness which could be tested during each particular phase. As previously mentioned, the maximum time allowed for a single phase is below 30 min, in order to maintain the consistency of judgement. Higher number of thickness sample indirectly increases the number of material group. Even though the accuracy will increase, this also means more experimental time and work; as experienced during previous experimentation.

For the current simulation, even though majority of the effort is focused towards controlling the detection feeling through static load, it is quite impossible for the test subject to perform and response throughout the whole experiment without involving dynamic motion. As the thickness approaches 50~90 μm, the detection could have been made by another mechanoreceptor unit, such as the FA-II (Bolanowski et al., 1988).

In conclusion, we verified the ability of the human tactile function to detect an extremely thin object from the psychophysics result. Through specific control of the current experiment procedure, we managed to achieve a similar trend. Although the Weber fraction value differed compared to the previous experimental result, we managed to validate the behavior of the undetected regions up to 150-μm thickness. This is a great achievement considering the increased number of the thickness test ratio (between a minimum and maximum thickness range) in a single test group compared to the previous experiment. Further study on the behavior of the undetected regions, especially between the 150 ~ 350-μm thickness range, will be undertaken in the near future.

It is possible that for critical process, the decision making process could have been made subconsciously. As we mentioned previously, the human body is capable of the extraordinary either through trainings or experience. Exploring and understanding the unknown is the key for future advancement.

Chapter 4

FINITE ELEMENT ANALYSIS ON TACTILE MODEL

4.1 Introduction

The finite element (FE) is one of the method mostly used in solving physical problems related engineering analysis and design (Bathe, 1996). In order to clarify the tactile behaviour between different material and foil thickness, the FEA model of the index finger and thumb (both assumed to be an elastic body) has been generated and the contact stress analysis and displacement analysis shall be performed using Catia V5. From the simulation result, the related output such as the von Mises stress and displacement value shall then be extracted.

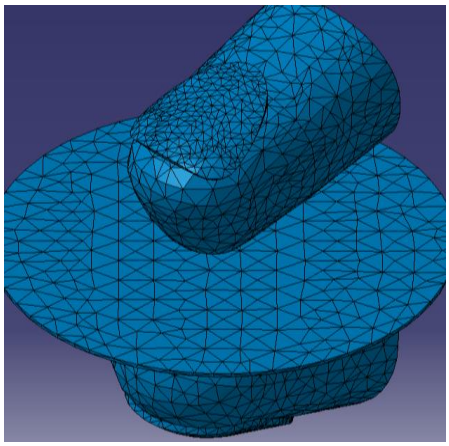

Fig. 35 Isometric view of the 3D model.

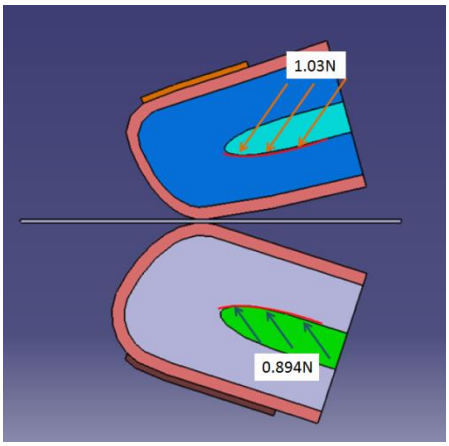

Fig. 36 Cross section view of the model (with load applied).

The skin of the finger model consists of the epidermal and the corium, while the bone and the nail shall be included inside the finger model (Refer Fig. 35). In order to simulate the previous psychophysical experiments by Miyaoka and Ohka (2001) effectively, the mechanical properties of copper and stainless steel foils with various thickness shall be tested accordingly. The contact analysis between metal foils and the

finger shall be performed, in order to obtain the distributed stress and displacement for each point (Refer Fig. 36). The cross section image of the overlapping area between index finger and thumb shall been generated from the simulation result in order to extract data from specified points.

4.2 Related theoretical contents

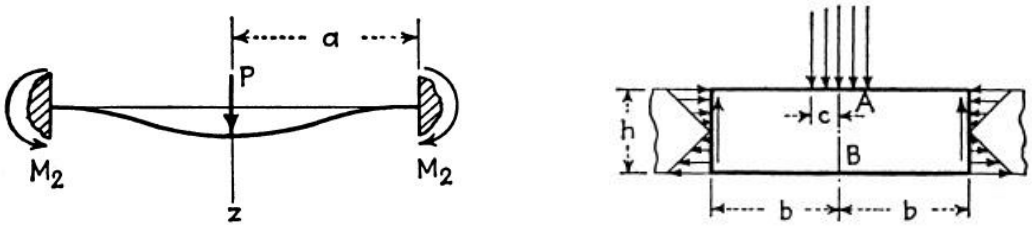

(a) (b)

Fig. 37 Free body diagram of (a) metal sheet with clamped edge and load (concentrated) at center and (b) central portion of the metal sheet extracted from overall model (Adapted from Timoshenko (1959).

The main reference come from the Theory of Plates & Shells by Timoshenko, article no 19 (pp. 67-72). One of the major purpose of this equation is to validate the differences between theoretical contents and simulation output. At first, we shall refer to the contents of circular plate with simple support state, while receiving concentrated loaded at center position. The deflection value could be explained using Eqns. (3) and (4) with description below:

P: Applied load [N]
r: Distance from center of metal sheet [mm]
a: Radius of metal sheet [mm]
d: Radius of finger or sphere [mm]
D: Flexure rigidity [$Pa \cdot m^3$] or [$N \cdot m$]
E: Young Modulus [Pa] *(Notes: Any usage of subscript S is referring to SUS, whereas C refers to Cu)*
t: Elastic thickness [mm] *(Notes: The initial h shall be used for mesh size)*
v: Poisson Ratio

Deflection at any point (with distance *r* from center) of a simply supported plate:

$$w = \frac{P}{16\pi D} \left[\frac{3+v}{1+v} (a^2 - r^2) + 2r^2 \log\frac{r}{a} \right] \quad (3)$$

Maximum deflection (at center) of a simply supported plate (when $r = 0$):

$$w_{max} = \frac{Pa^2\ (3+v)}{16\pi\ D\ (1+v)} \tag{4}$$

With the flexure rigidity of the plate referred using:

$$D = E\frac{t^3}{12}(1-\ v^2\ ) \tag{5}$$

From previous psychophysics experimentation, instead of using a simple support state as base, in actual the circular plate shall be clamped on the sides, producing uniformly distributed bending moment along the clamped edges (refer Fig 37(a)). For this reason, Eq. (6) and (7) instead shall be utilized in order to define the deformation that occur especially at critical position.

Deflection of clamped plate loaded at center can be formulated using:

$$w = \frac{Pr^2}{8\pi D}\log\frac{r}{a} + P\frac{(a^2-r^2)}{16\pi D} \tag{6}$$

As when $r \rightarrow 0$, defining the deflection that occurs at center position shall be:

$$w_{max} = \frac{Pa^2}{16\pi D} \tag{7}$$

As for the maximum stress, considering we are currently dealing with ductile material as base (which is copper and stainless steel), the maximum tensile stress that occur at centre of the lower surface can be described using the approximation formula below:

$$\sigma_{max} = \frac{P}{t^2}\ (1+v)[0.485\log\frac{a}{h}\ + 0.52] \tag{8}$$

The value *t, D, E* and *v* here are referring to the thickness, diameter, Young's modulus and Poisson's ratio, respectively. Also, the suffixes *s* and *c* here shall be referring to stainless steel and copper type of material, respectively. The basis of this

equation has been reduced to the problem of a symmetrical stress distribution in a circular cylinder as showed in Fig. 37(b); compared to the previous equation in displacement which focuses on the problem of stress distribution on the center of the plate. Further information on this can be referred from Timoshenko (1951 and 1959).

ii) The Hertzian stress function

By reviewing the concept of contact stress for elastic materials, when two elastic bodies are pressed to each other, a small contact surface shall be formed as a result of local deformation (Timoshenko, 1959). By considering the second body as a plane surface, Eq. (9) for radius of contact areas can be simplified to become Eq. (10). The distributed pressure, *P* can be defined as the contact pressure itself, shall be represented by Eq. (11).

$$a = 0.88 \sqrt[3]{Fd \ \frac{F(E_s + E_c)d_1 d_2}{2 \ E_s \ E_C \ (d_1 + d_2)}} \tag{9}$$

$$a = 0.88 \sqrt[3]{Fd \ \frac{(E_s + E_c)}{2 \ E_s \ E_c}} \tag{10}$$

$$P_{max} = 1.5 \frac{F}{\pi \ a^2} \tag{11}$$

By applying a load of F = 1.0 N towards the product, the calculation result shows that the radius of contact and also maximum pressure at contact area at both stainless steel and copper material is equal, which is around a = 1.2 mm and P_{max} = 126.86 kPa. As a result, due to the small value of force applied (F = 1.0N), indirectly this shall resulting in a very small differences between the value of contact surface and contact. Also, the range between the Modulus of Elasticity between both material is extremely high (E_s = 198 GPa, E_c = 110 GPa) compared to the skin properties (E_{skin} = 2 MPa), which resulting in similar output between both conditions.

As for our research, it is quite difficult to use this theoretical outcome in describing the physical differences between both material after contact. This is due to the differences, which is very small. However, at the latter stage of our simulation process,

the theoretical value of the contact surface has given a good hint towards defining the suitable range of analysis positioning for SA-I node points especially at the index finger.

iii) Spring function and ratio of thickness

$$k = \frac{16\pi E t^3}{3a^2(1+v^2)} \tag{12}$$

$$\frac{t_c}{t_s} = \sqrt[3]{\frac{E_s}{E_c}} \tag{13}$$

Based from previous psychophysics experimentation by Miyaoka and Ohka (2001), suggesting that Eq. (12) has been derived based from the differential equation for cylindrical bending of plates. (Timoshenko, 1959). This result suggests that human judges the thickness of foil based *k* value, which is the spring constant. This equation then shall be simplified into Eq. (13), which defines the discrimination rate of material thickness, by considering that the SA-I unit in judging the thickness of two stimuli to be equal when their spring constants are almost equal ($k_s \approx k_c$; where k_s and k_c are spring constants of stainless steel and copper, respectively). As for our research, this ratio shall be the basis in determining the differences between both of the material, especially while dealing with psychophysics application and experimentation results.

4.3 Initial simulation phase

i) Methodology

The main objective of this phase is to gain an overall perspective on the simulation result. The FE simulation has been conducted using Catia V5, using solid model with linear element with default mesh setting. The loading conditions has been described from Fig. 38 below, with slightly higher load from index finger section (1.03 N) compared to the thumb section (0.894 N). This is considering that the motion of index finger is more active compared to thumb during normal action. SUS and Cu material

with thickness from t = 25, 30, 40, 50, 60, 70, 75, 100, 200, 300, 400 and 500 µm has been tested accordingly, with minimum mesh quantity of 5,500 element. The properties for foil materials and finger components can be referred from Table 1. From the simulation result, a total of 14 evaluation points (from the node points) has been selected between the epidermis and dermis cross sectional view, which represents the position of SA-I mechanoreceptor unit (Refer Fig 39). The distribution of von Mises stress from both SUS and Cu data shall then be analyzed.

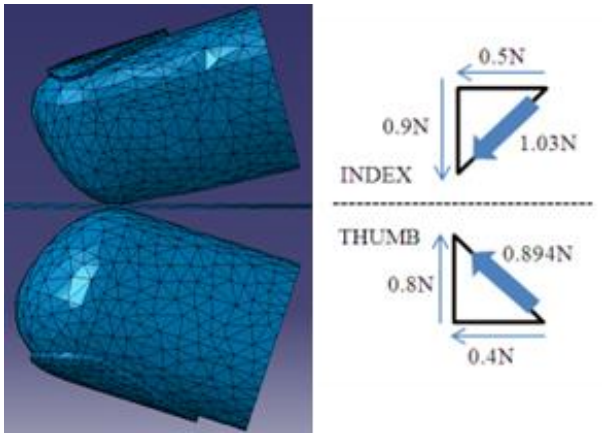

Fig. 38 Load distribution between index finger and thumb.

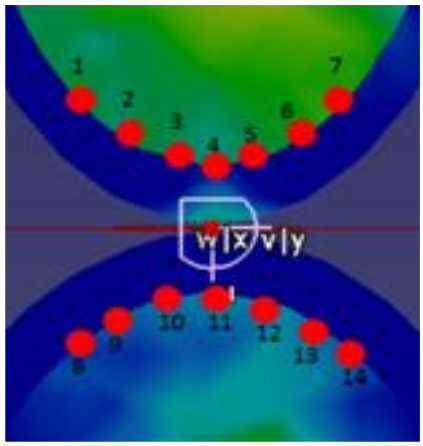

Fig. 39 Total of 14 evaluation points taken from index finger (upper side) and thumb section (bottom side).

Table 1 Properties for foil materials and finger components

<Properties>	<Material for foils>		<Finger component>			<Units>
	SuS	Cu	Epidermis & Dermis	Bone	Nail	
Density:	7860	8900	910	2710	1200	[kg/m^3]
Young's Modulus:	2.00E+11	1.10E+11	2.00E+06	1.70E+10	1.60E+08	[N/m^2]
Poisson Ratio:	0.266	0.33	0.49	0.37	0.38	
Tensile Stress (Yield):	2.50E+08	2.90E+08	---	9.50E+07	---	[N/m^2]
Thermal:	1.17E-05	1.65E-05	1.62E-04	2.36E-05	6.84E-05	[Kdeg]

ii) Result and discussion (Initial phase)

The von Mises stress based from 14 evaluation points have been summarised accordingly using 3-dimensional plot (Fig. 40), with vertical axis represents the von Mises stress and horizontal axis represents foil thickness and position of node points (either index finger or thumb). In general, we could observe the similarity of the result

except during low thickness state. Also, based from standard deviation analysis, more than 68% of the data has been verified to be distributed within the central deviation. This is related to skin's natural behaviour, where received force shall be absorbed and distributed accordingly. The distribution of the load begins from the contact area, and progressing outwards. Unfortunately, further analysis of the 3-dimensional plot from here is seen difficult.

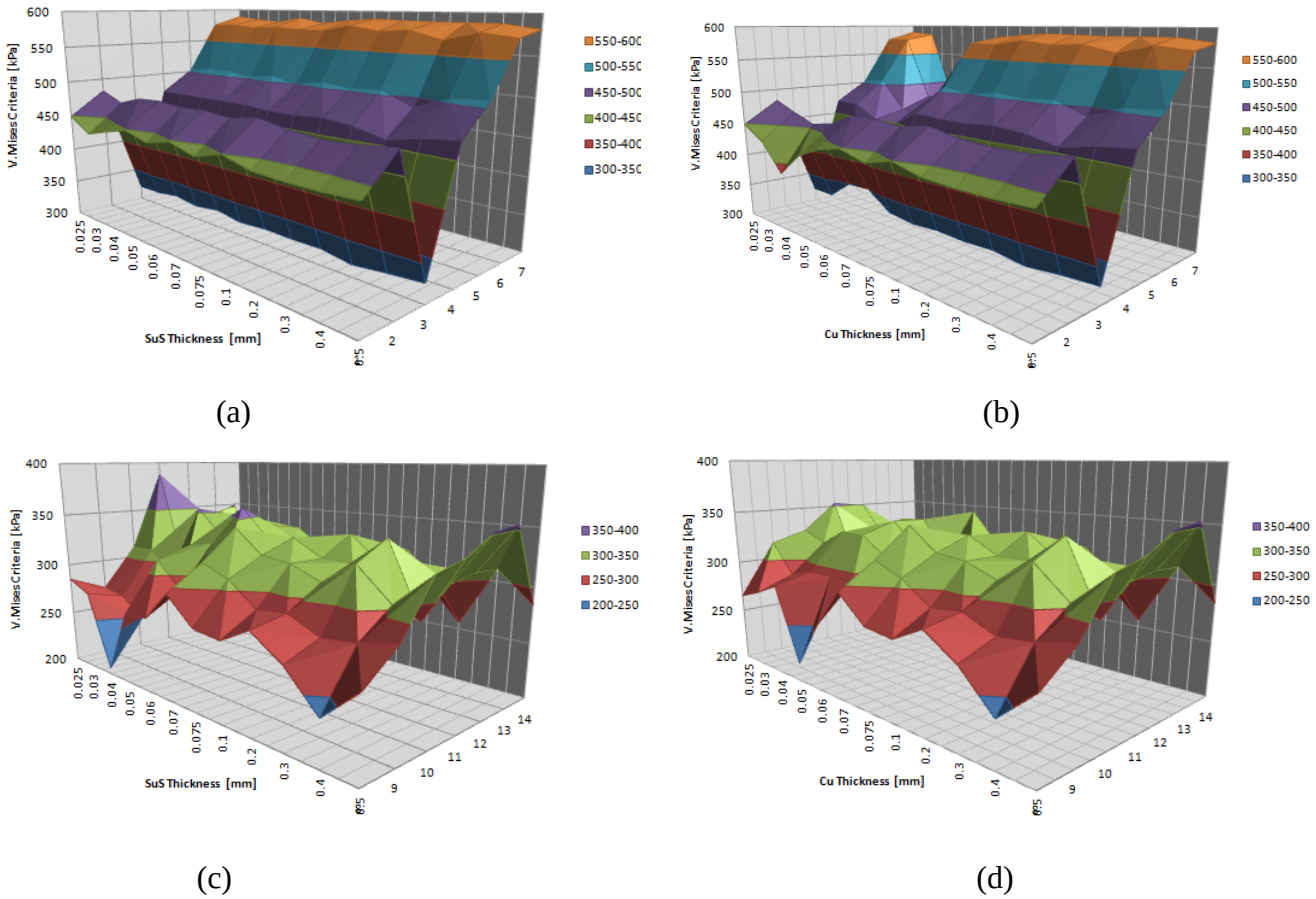

Fig. 40 Tactile response in multiple positions of index finger using (a) SUS and (b) Cu material. Also, on thumb using (c) SUS and (d) Cu material.

For further analysis, the von Mises stress have been summarised by considering the mean value of all evaluation point on each finger (refer Fig. 41). Similar result could be observed, where the differences between von Mises stress for material above 75 µm is very small. When $t < 75$ µm, the mean-von Mises stress for stainless steel is higher than copper material. As proposed from previous psychophysics result, the evaluation process of material thickness shall be performed by the mechanoreceptor based from the elasticity properties of the materials. Although the differences between the average

of overall data vs. extremely thin data is very small (which is less than 0.2%), our tactile function still capable in capturing such differences.

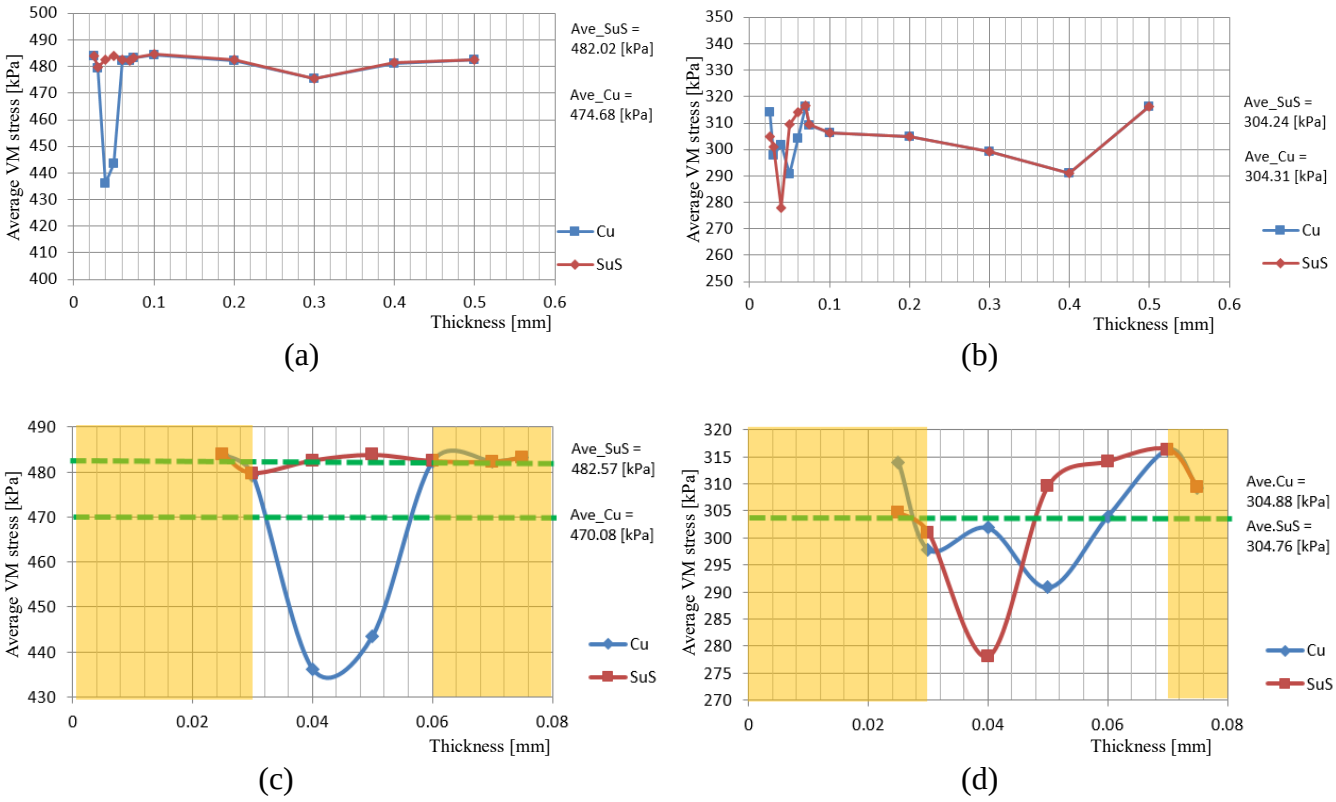

Fig. 41 Mean-von Mises stress for SUS and Cu material using overall data on ((a) index finger and (b) thumb) and extremely thin data on ((c) index finger and (d) thumb).

One of the hypotheses is that the index finger plays a main role in analysing the differences in properties of material. Basically, the index finger acts as the 'analyser' in order to monitor the differences of properties between materials. While the thumb basically act as the 'standard' in order to summarize overall data. This can be observed where the average of mean-von Mises stress for the thumb is minimum compared to index finger. Another reason is because normally the motion of index finger is more ‘aggressive’ compared to thumb during gripping process.

Next is to validate on the relation between thickness and stress criteria by referring to the average values of mean-von Mises stress for copper and stainless steel material (refer Fig. 40). Hypothesis from psychophysics experiment states that, the exact boundary of the undetected region is hard to discriminate between t = 75 ~ 350 µm (refer Fig. 1 in Chapter 1). From Miyaoka and Ohka (2001), the ratio between copper and stainless steel material is around $t_c/t_s \approx 1.2$. From this initial FEA result, we are able

to observe the activities of the mechanoreceptor in discriminating material with extremely thin thickness more clearly. When the thickness exceeds 75 μm, the average of mean-von Mises stress becomes more syncronised. One of the conclusion is that the SA-I mechanoreceptor (which is more sensitive in detecting light touch sensation) is involved during this process.

As a conclusion, for extremely thin material (t < 75 μm) , the von Mises stress for stainless steel is seen higher than copper (Fig. 41) and can be detected by the SA-I mechanoreceptor unit. As proposed from the previous psychophysics experimentation, there could be a chance that the differences in the modulus of elasticity for both material plays a role for the skin to evaluate the final value. Next, the ability to differentiate thickness reduces when the material exceeds 75 μm thickness. At the same time, the range estimated with mean-von Mises stress also reduces. This shows that the functionality of the mechanoreceptor (SA-I) reduces when material thickness increases. Previous psychophysical experimental results also show that the undetectable region exist during evaluation of thickness between 75 ~ 350 μm. From this initial FEA analysis, the transition state from one evaluation system (using SA-I mechanoreceptor function) to another system (for example the angular sensory organ, as proposed by John et. al (1989)) could be observed through monitoring of the mean-von Mises stress result. This shall be further investigated during the next preliminary stage.

4.4 Improvement on simulation process

i) Methodology

The main objective here is to increase the accuracy of the data. For this reason, we have decided to take some of these improvement steps such as:

- The finite element type of this simulation has been improved from linear to quadratic element using OCTREE tetrahedron element. One of the main reasons is to improve the aspect ratio of the model especially for sheet areas, at the same time to increase the convergence rate of the data.
- The element size has been reduced and simplified. From the default mesh, the size has been decreased to almost 50% compared to original. As a result, the

mesh of all parts has been revised to 1.0 mm (with sag 0.16) except for sheet, which is 1.5 mm size (with sag 0.24).

- Further reduction on the element size could be made accordingly in order to improve the convergence rate.
- The number of selected node points has been increased from 14 points (7 points for each finger) to 30 points (15 points for each finger) as shown in Figs. 42 and 43.
- We also introduced method to improve the node point's selection method by not only limiting it to the corner node points, but also on the mid node points (whichever is closest). This was possible due to the changes made from linear to quadratic element.
- Selection of material thickness has been revised from various range of thickness to a more standard interval or thickness between t = 50 ~ 500 µm (with 50 µm interval).

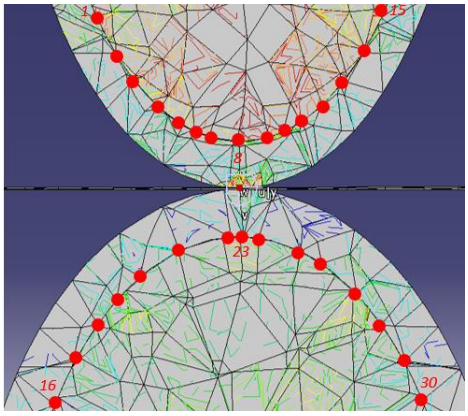

Fig. 42 Revision on number of evaluation points (for index finger and thumb).

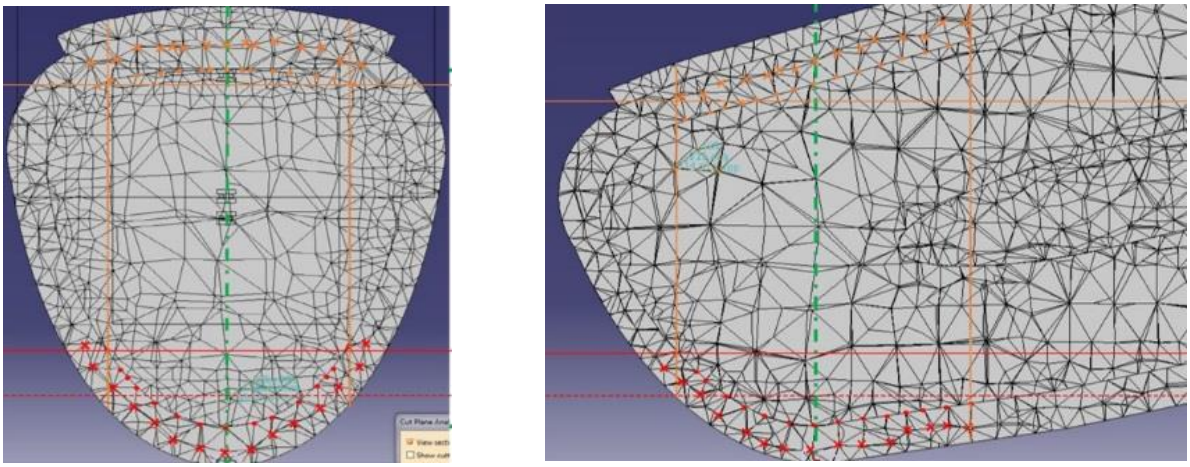

(a) (b)

Fig. 43 Cross section view of index finger from (a) front view and (b) side view.

- Additional points have been included between t = 100 μm region in order to monitor the threshold of the undetected region.
- We shall also monitor the deflection at foil surface (upper and lower surfaces) especially contact region areas. Theoretically, the ability to feel the increase of contact area could enhance our decisive factor towards a material.

Finally, the simulation result (especially the displacement value) shall be extracted and analyzed in order to evaluate the human mechanism in material thickness recognition.

ii) Discussion on improvement process

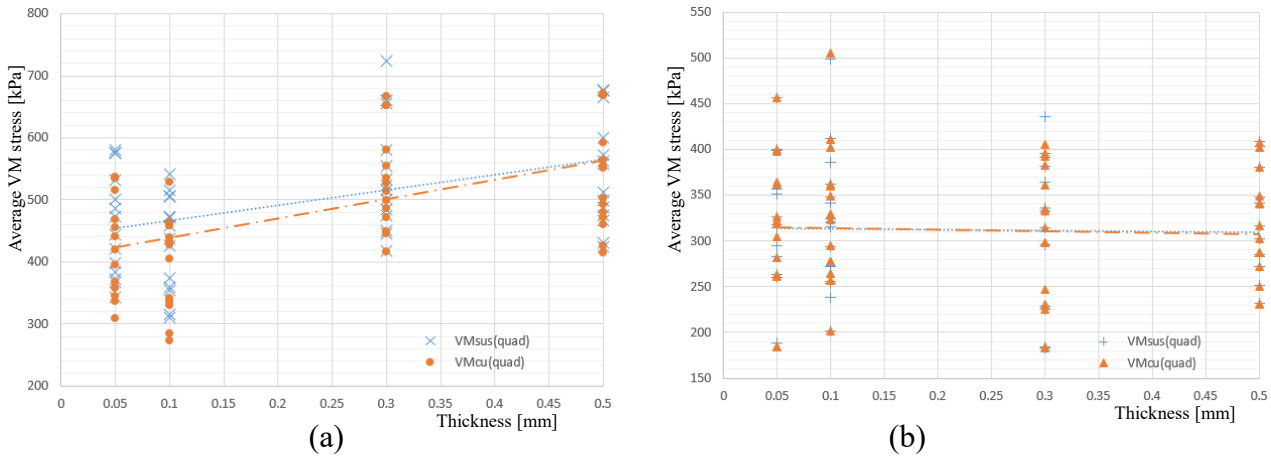

Fig. 44 Tactile response (Linearized data) of (a) index finger and (b) thumb.

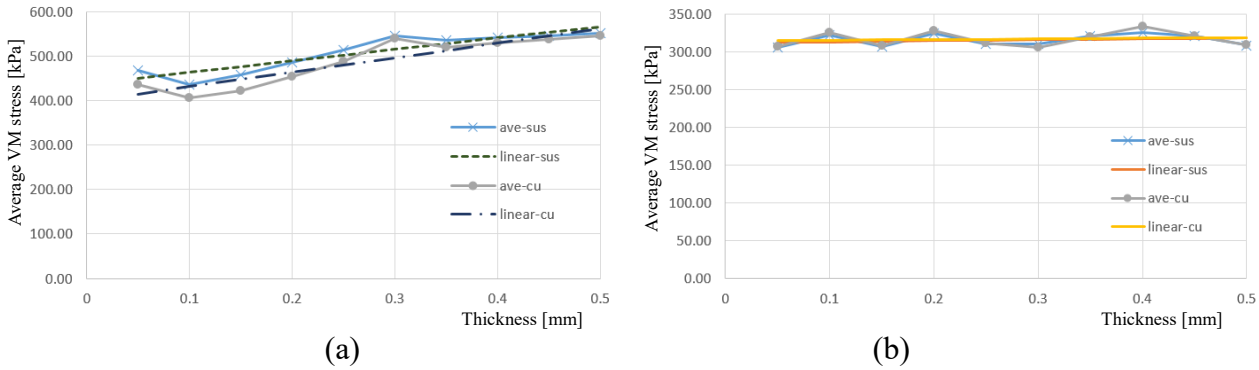

Fig. 45 Comparison of tactile response (average data vs. linearized data) between (a) index finger and (b) thumb.

From the simulation result, comparison has been made between the data for both fingers and foil surface. Figs. 44 ~ 46 refer to the latest outcome, after improvement from linear to quadratic element. At first, all of the data provides positive improvement, and is able to clearly state the differences between tactile response of

copper and stainless steel materials. Both results can be viewed either from the linearized data in Fig. 44 which is more-conservative or from the averaged data as shown in Fig. 45. The differences in tactile response on an index finger is also more obvious compared to the thumb section, which could support our previous hypothesis on the function of index finger as the 'analyser' and the thumb as the 'standard'.

In order to determine thickness perception, the tactile response result has been utilised in order to generate the tactile ratio between SUS and Cu materials. As a result, the trend line is almost similar compared with previous psychophysics experimentation result as shown in Fig. 46.

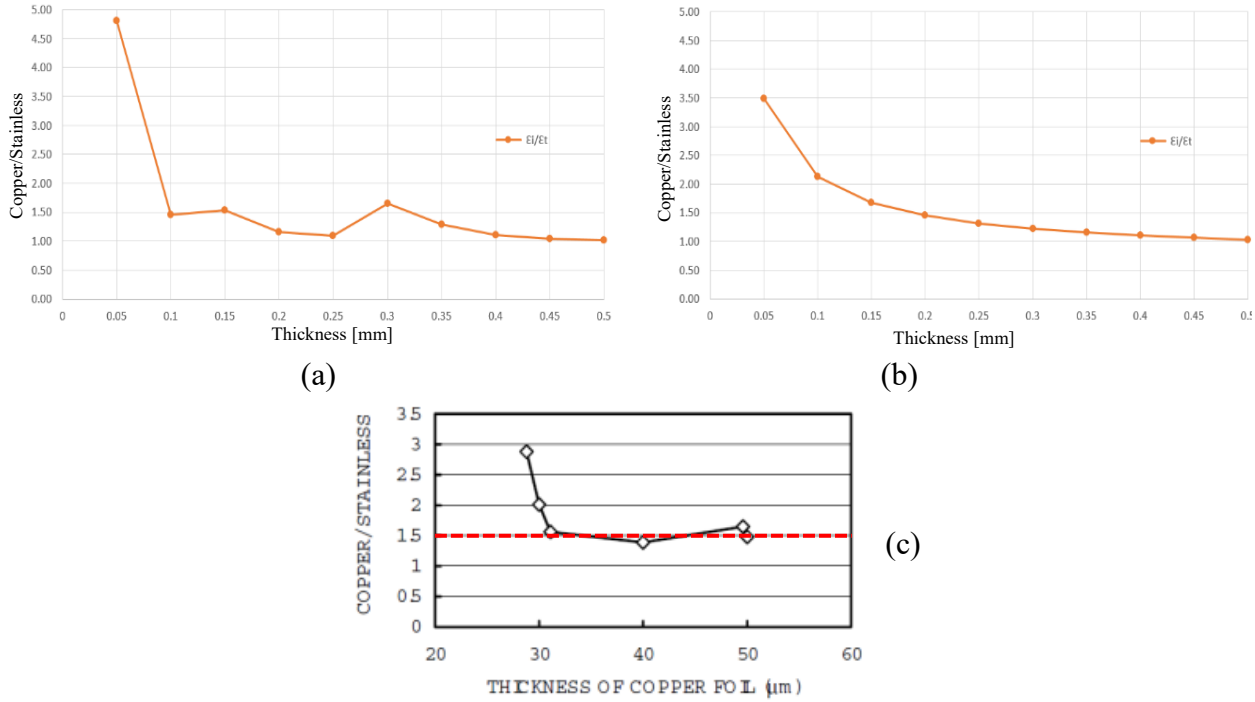

Fig.46 Comparison of tactile ratio using (a) average data and (b) linearized data vs (c) previous psychophysics result from Miyaoka & Ohka (2001).

Unfortunately, further improvement made towards converging of the data (by further reduction of quadratic element into almost 50% of the original size) provides an unexpected result. Although the process is capable of refining the output, the result is different. Referring to Fig. 47, based from the summarization on four major points (t = 0.05, 0.1, 0.3 and 0.5 mm) shows reduction on the differences of tactile response. At the same time, the von Mises stress value increased drastically compared to the initial state (before mesh refining). One of our hypothesis behind such failure could probably be caused by the lack of detail shapes such as the fingerprint ridges on the finger model.

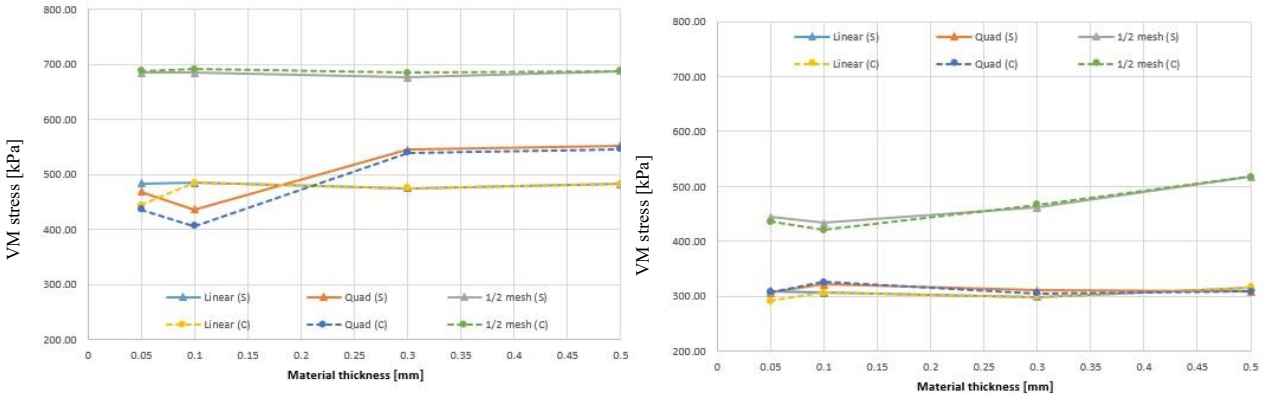

(a) (b)

Fig.47 Comparison of tactile response between linear element vs quadratic element vs half-mesh plus quadratic element data on (a) index finger and (b) thumb.

Due to this reason, the direction for preliminary analysis needs to be revised. Instead, we shall try to focus on the final idea, which is by referring to the displacement rate on the foil surface as the next focus. One of the reason for this action is because the displacement result should be more stable compared to the von Mises stress values in Fig. 48 (a). The research by Fujita and Ohmori (2001) which discussed regarding how human relates between the softness-feels in proportion to the increase in area of contact also supports such concept. Through the analysis of foil/plate deflection, relationship with tactile feeling could be made.

Referring to Fig. 48 (b), since the displacement is the inverse proportion to hardness, the parameter of t_c/t_s (which is the comparative ratio between copper and stainless steel) shall be calculated using u_c/u_s. From the initial state until t = 100 µm, the ratio of t_c/t_s takes almost a constant value of around 1.4 (except for the origin). However, between 100 µm ≤ t ≤ 175 µm, the ratio of t_c/t_s cannot be calculated due to the inability to compare with the base value. When the value of t exceeds 175 µm, the ratio of t_c/t_s takes the value within the range of a unit (Excluding t_c/t_s = 1.0; because human unable to discriminate between the thickness within this state). By comparing this with previous experimentation results, we can comprehend that these simulation results support the aforementioned hypotheses.

Next, when t > 350 µm, the simulation result shows that the displacement rate of copper and stainless steel is not overlapping. Within this region, the displacement rate is small enough (less than 0.2 µm) in a state where it is unrecognizable by the human tactile sensation. Whereas, based from previous psychophysics results, the human

subject is still capable in differentiating the thickness of both material, even though the simulation result shows otherwise. This suggests that there is a separate mechanism such as the angular sensory organs of the human finger in evaluating the above-mentioned differences.

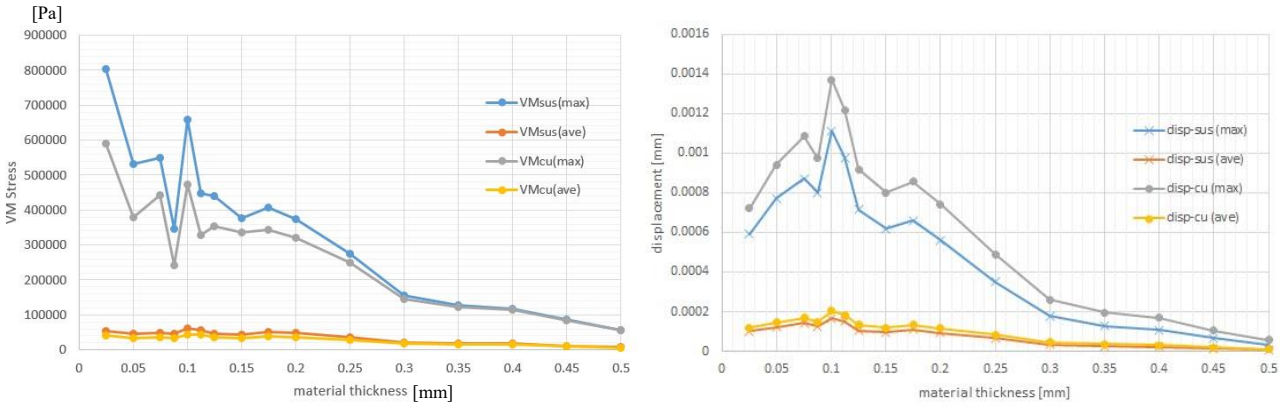

(a) (b)

Fig.48 Max and average value of (a) VM stress and (b) displacement at foil surface.

From calculated results, we have examined the displacement rate of the foil. As a result, the displacement rate for copper (which was monitored at the foil surface) is always higher compared to stainless steel. By comparing with previous psychophysics result, the simulation also proves similar traits; where human subjects discriminate thickness of foil according to material hardness when t < 100 μm, thickness is undetermined when 100 < t < 350 μm and evaluation is done via another system when t > 350 μm.

Based from the simulation result, we are able to monitor the basic behavior of the human tactile mechanism in defining the differences between two extremely thin foils. This simulation result also supports the initial hypothesis, in which the human mechanoreceptor unit plays the main role in defining the differences between both foils. By comparing this result with the previous psychophysical experimentations, we can monitor similar trend such as the inability to differentiate the material state when the material starts exceeding the 100-μm range. Also, referring to the overlapping condition during t > 350 μm, which proves on the transition state of human analysis from the proposed mechanoreceptor system towards another type of system such as the proposed gripping angle of finger.

Other additional idea was to improve the method in selecting points, by not only monitoring the areas between epidermis and dermis section, but also on other sections

such as between nail and epidermis. Also, we have planned to introduce additional cross sectional view from side (refer to Fig.43 (b)). Meaning that more data could be summarized.

Unfortunately, the above conclusion has been made through the analysis on the deflection at surface of sheet, as the result is much more stable compared to others. As mentioned previously, through the ability to detect the total of deflected areas, indirectly could possibly contribute in defining whether one material is harder or softer. And the direct contact between the surface of our finger and the sheet, could probably convey such information. However, this could only remain as one hypothesis, because our original objective was to monitor the changes in von Mises stress rate on mechanoreceptor position of contact fingers based from the studies by (Dandekar et. al. (1996) and Maeno et al. (1998).

At first, we shall discuss on some of the problems that occurred during this simulation stage. Referring to Fig. 47, the improvement that was done towards the simulation (by reducing mesh value) unfortunately has different impact towards the current simulation. The differences between average results of von Mises stress on finger section for both materials reduced drastically and almost unnoticeable compared to the previous simulation result whereas theoretically, smaller element size should have improved the quality of the output. For this reason, we need to re-define the method of our simulation during the next process.

Next, the method in defining the differences during contact, especially by using 3-dimensioning plot, could not solve the problem. One of the option is by choosing other solutions, such as the average value to summarize the outcome. Another concern is regarding the number of selected node points. Higher selection of node points indirectly could produce more error. As more node points selected, the further the position divert from actual contact point. Whereas the best option is to choose node positions which experiencing stress (such as the contact areas between finger surface and sheet metal). This shall be the main target during the next simulation phase.

4.5 Final simulation phase

i) Methodology

Since the main objective of this simulation is to identify the value of the von Mises stress inside the epidermis during contact, we need to re-evaluate the previous

working procedure (from initial until improvement stage) to achieve the most optimum element size for our simulation. And at the same time, to find the best solution for the problems that occurred previously. We conducted error analysis of our simulated result to validate the correctness of the element type.

The main focus for this analysis identifies the specific nodal points, which represent the contact areas and the location of the SA-I mechanoreceptor unit on the fingers. Similar as the previous results, the OCTREE tetrahedron element was applied with a revised element type from linear to quadratic to reduce the aspect ratio, especially on the foil part. The element size was further reduced and simplified to a 1.0-mm element size (except for sheets which uses 1.5-mm element size). Another additional change are, the applied load was also simplified and revised to 1.0 N for both fingers.

a) Optimal meshing

The main objective of this activity is to verify the significance of our simulation, especially in terms of the convergence rate. One of the simplest methods in FEA, is by reducing the element size until the smallest limit. Considering that a metal foil is the most critical part (due to the high aspect ratio), the verification process uses a simple model of a clamped circular foil with the concentrated load applied to the center. A simple example of this could be viewed through Fig. 49 which shows the physical improvement when element size has been reduced from 1.5 mm to 1.0 mm. It is important to remember that such changes should be compatible when applied towards the full model.

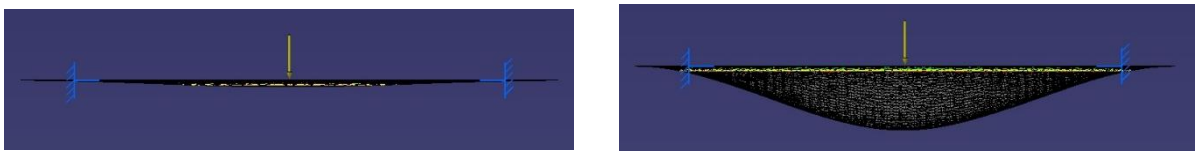

(a) (b)

Fig. 49 Improvement on deflection output when using (a) 1.5mm element size (with 0.24-mm sag) vs (b) 1.0-mm element size (with 0.16-mm sag).

The result based from error analysis performed towards the sheet model can be referred from Fig. 50 (a) ~ (d). Due to the complicated shape of the human finger, it is simpler to refer to this error analysis result for evaluating the actual model's behavior. The bending equation of the clamped circular plate obtained from the Theory of

Plates & Shells by Timoshenko (1960), which is the main reference in defining the maximum deflection (refer Eq. 7). Basically, we could see that the difference in displacement between SUS and Cu reduces as the material thickness increases (Fig. 50 (a)). Based from the error analysis in Fig. 50 (b), showing that the numerical error decreases as the thickness increases. Similar condition also occurred when referring to the maximum global error on sheet. We could also see that the error from simulation versus theoretical reduces as the material thickness increases. From FEA point of view, this happens due to the improvement of aspect ratio, which relates to the element size and material thickness. Replacing the linear element to quadratic also improves the analysis further by improving the convergence rate (with respect to element size reduction).

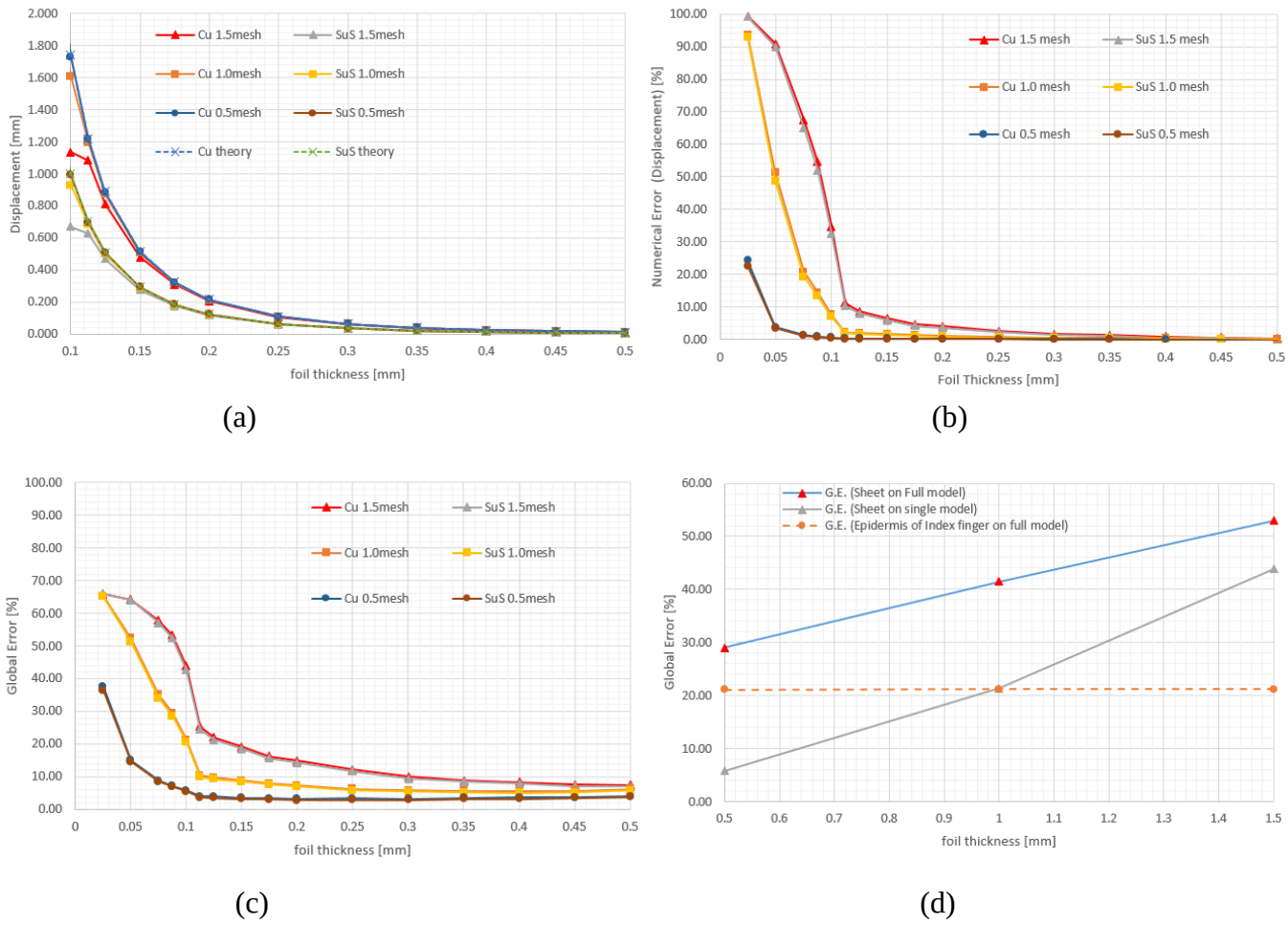

Fig. 50 Error analysis by referring to (a) max displacement using sheet model only (b) error of displacement (simulation vs theory) using sheet model only (c) max global error using sheet model only and (d) comparison of global error using full model vs sheet model only.

Unfortunately, the reduction of element size (on sheet metal) was unsuccessful when applied towards the full model. After trial, the minimum element size which is applicable towards the sheet metal (using full model) could only remain until element size h = 1.5 mm. This happens mostly due to hardware limitation. However, using the simulation result from single body of plates as reference, we could see that the numerical error increases abruptly under t = 125-μm and can be kept less than 10% with conditions where the thickness of the material is kept above t = 125 μm when we assume the element size h = 1.5 mm. We calculated cases of t > 0.2 mm with a 1.5 mm element size because the numerical error is within 4%. Since the case of t = 0 mm means direct touch between the index finger and the thumb, we focus on the calculation when the case is trusted. Between the initial thickness t = 0 until t = 200 μm, the evaluation is made using linear interpolation. Referring to Fig. 50 (d), we could see that the reduction of element size on sheet metal shall not be affecting the outcome on epidermis result. Also, through a separate simulation process, we have confirmed that further improvement on the element size of epidermis section only (from element size h = 1.0 mm, reduce to 0.75 mm) shall have minimum impact towards the deflection result on epidermis section.

In order to define the optimum setting for this simulation (by considering also the limitation of element size), we have verified that the optimum method in running this simulation is by using quadratic element, with element size h = 1.0 mm on all parts except for sheet metal, which still remains as h = 1.5 mm. One of the best options to improve the process is by referring to the simulation result of sheet model for the application towards overall model, considering that the physical deformation that occurs at sheet should be most critical compared to others.

As a conclusion, we have used this simulation result (on sheets) to link between the errors on overall simulation. Also from this analysis, we have confirmed that by using the above setting could support the simulation outcome (especially on the epidermis section) with numerical error less than 4%.

b) Measuring node points

Based from previous simulation, we realised that increasing the number of node points does not always produce the best outcome. By increasing the node points, (for example on the index finger) from 7 points to 15 points, the position of node points

reaches to almost centre position of finger. Whereas, the important thing is to monitor the result along the overlapping areas between finger and sheet. This could be one of the main reason why the error occurred (for example when tactile response value escalates).

Another problem experienced during previous simulation is on how to validate the outcome from the simulation. For example, defining the maximum displacement value from the analysis using a single sheet metal part is simple, for we can quickly determine that the location of maximum outcome always occur somewhere along the contact/load position, and can directly chooses the maximum result provided by the software. However, in case of contact analysis on a full model, the maximum displacement could be anywhere instead. Rather than using the overall maximum value (which was automatically provided), we need to specify the locations manually, extract all information and filter the data from specified position. This solution is more efficient, compared to our previous method (where the user needs to view and manually select each data).

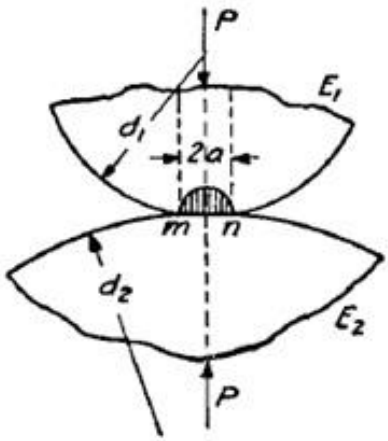

Fig. 51 Contact area based from Hertzian (Adapted from Timoshenko (1940)).

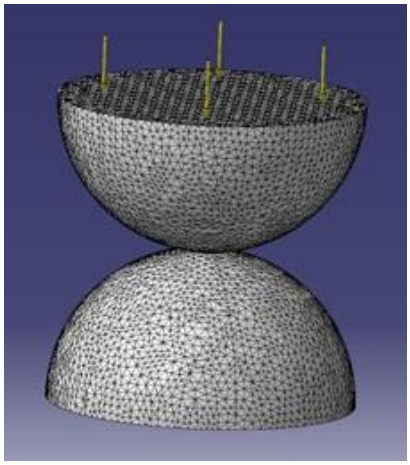

Fig. 52 Contact analysis using two semi-sphere.

Another problem with previous method is that the result could not capture the overall picture of the von Mises stress condition and also the deformation state when the data was extracted manually from cross section view. Also, the node points always changes when element size was revised (caused by the metal sheets which have variety of thickness). As for our simulation, the change in mesh does not occur on index finger and only effects the mesh of sheet and thumb section onwards. For this

reason, we have decided to focus on the contact point between the index finger and sheet, including other node points around it. Our previous simulation result also has proven that the detection rate at index finger is more noticeable compared to thumb.

Our next objective is to identify suitable locations for the nodal points for data extraction purposes. First, we focus on the contact points between the index finger and the foil as a base (for central nodal points) with the number of points around it to represent the behavior of mechanoreceptor activation during loading. Based on previous findings, the index finger is the main focus of this analysis. To define these contact areas, the Hertzian stress function is used as the main theoretical reference (refer Eqns. 9 ~ 10 and Fig. 51). By defining the diameters of each hemisphere as 19 mm to emulate a finger, we obtain a value of $2a$ = 2.96 mm as the horizontal diameter, which is caused by two hemispheres that contact the 1.0-N compression.

The second consideration is to analyze the horizontal dimension during contact between index finger and sheet. For this reason, the diameter for thumb has been revised to infinity; in order to expand the contact areas from curvature into flat surface. As a result, we obtain a value of $2a$ = 2.39 mm from the contact analysis between single hemispheres with the flat surfaces. Comparing this with the above contact result from two hemispheres (Fig. 52), shows that this calculation result is more reliable. Finally, after considering the tolerance factor and also element size, we have decided to use $2a$ = 2.0 mm as the parameter to represents the minimum contact diameter.

As Hertzian contact stress deals with linear state, there are possibilities that the actual contact area is bigger. For this reason, we have considered a second reference, which is the outer contact area (with diameter less than 5mm) in order to represents the outer contact position of the node points. Details regarding SA-I mechanoreceptor unit in Fig. 53 shall be used to support this.

Valbo and Johansson (1984) studied the properties of a human mechanoreceptor unit such as the size of receptive fields and the density of units. According to their report, the receptive fields of the SA-I mechanoreceptor unit consist of circular areas of around 2 ~ 5-mm diameter if a 400-μm threshold is assumed. We assumed that the numbers of mechanoreceptors within circular areas of $2a$ = 2 mm and 5 mm are $n \approx 9$ and 53 units, respectively. These values of unit numbers correspond well in our simulation. Considering the above analysis based on the mechanical contact problem and the physiology of tactile sensation, the FEA result will represent the SA-I

mechanoreceptor unit's activity. In our FEA, we assume that a circular area of $2a$ = 5 mm on the fingertip is a control area to evaluate the SA-I mechanoreceptor unit's activity in the next section because the largest diameter limit seems better for the tangential force for such cases as this simulation.

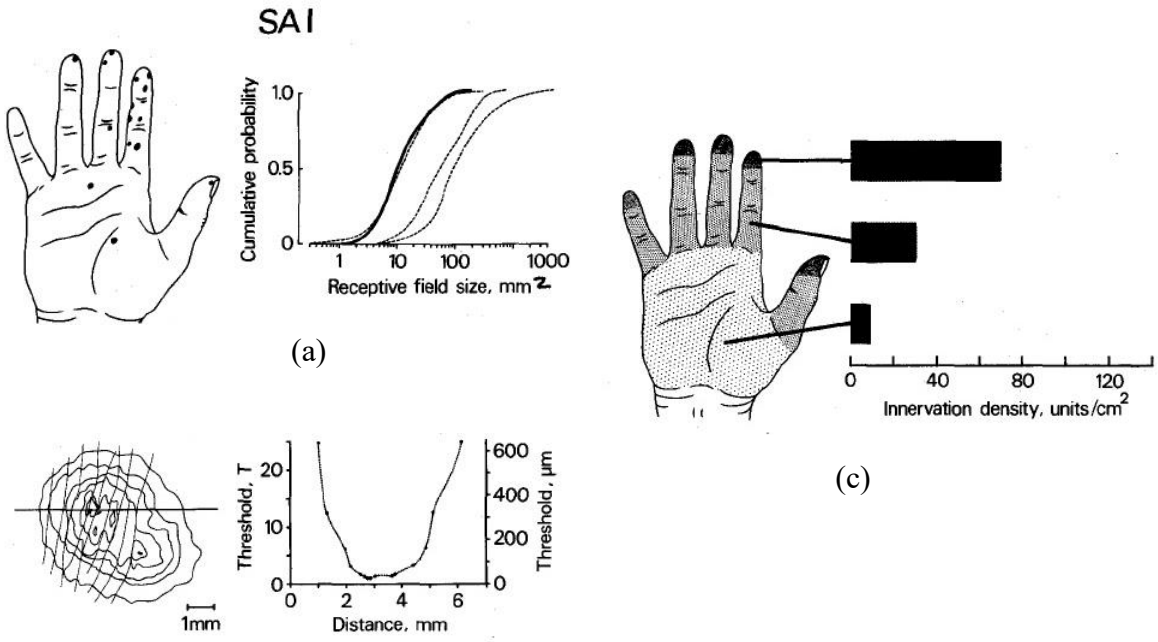

Fig. 53 Characteristics of SA-I mechanoreceptor unit. (a) Receptive field size. (b) Microstructure of receptive fields. (c) Average density of SA1I mechanoreceptor unit. (Adapted from Valbo and Johansson, 1984).

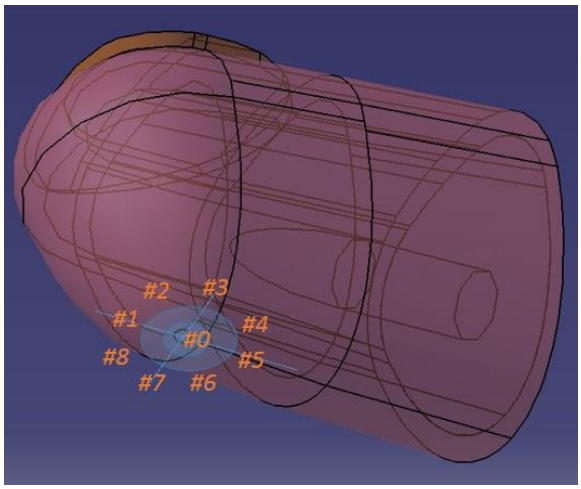

Fig. 54 New selected position/arrangement of node points.

For analysis purpose of the data, the positioning of selected node points shall be arranged in a symmetrical manner for a more balanced output (Fig. 54). Considering

the possibilities for future experimentation using 3-axis tactile sensor, the decision to use 2a = 5 mm as the final dimension for outer contact diameter is the best option.

c) Loading conditions

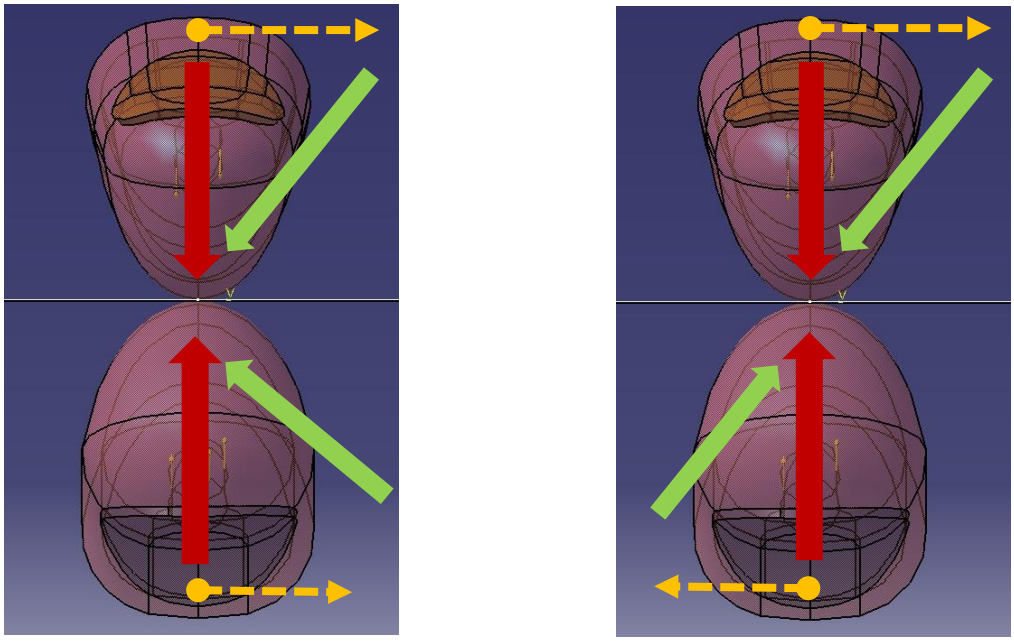

(a) (b)

Fig. 55 Loading condition referring to roll axis from Vertical (0°) direction to (a) pinch motion (15°, 30°, 45°) and (b) twitch motion (15°, 30°, 45°).

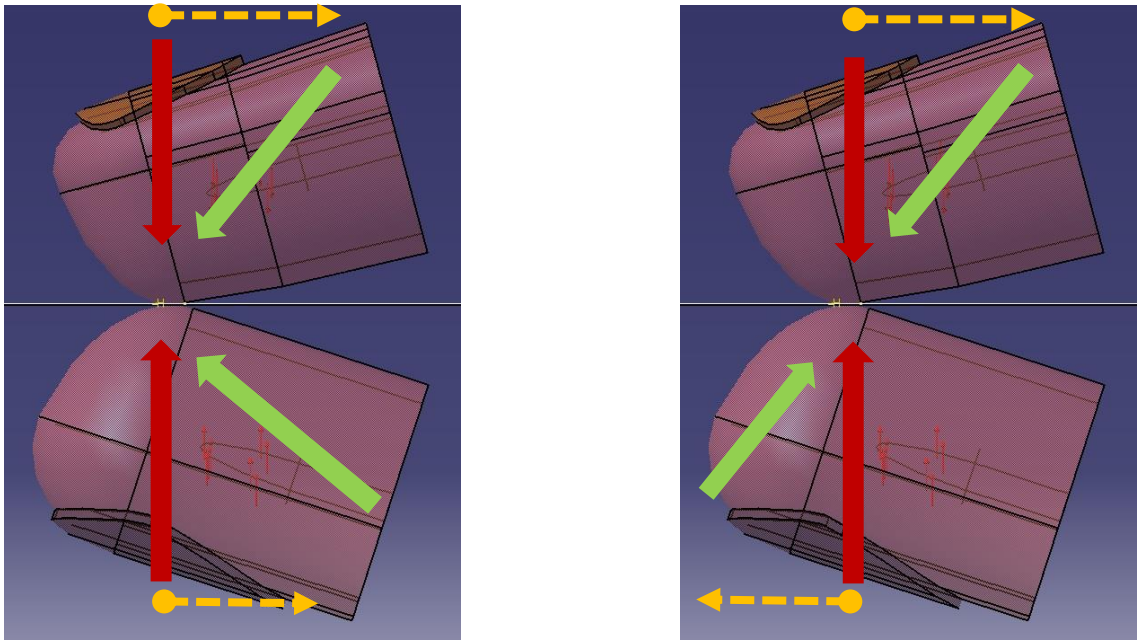

(a) (b)

Fig. 56 Loading condition referring to pitch axis from Vertical (0°) direction to (a) pinch motion (15°, 30°, 45°) and (b) twitch motion (15°, 30°, 45°).

As briefed previously, the main focus for this new analysis is to identify the performance from the 17 node points (Fig. 54), which represents the location of the SA-I mechanoreceptor unit and also contact region. Another change introduced (compared to the preliminary simulation method) is the loading angle shall be one of the control points. At first, the loading state has been standardized for both index finger and thumb (each shall be applying 1.0 N of load) to simplify the process. This is compared to the initial stage, where the load from index finger is slightly higher. The differences in result have been verified to be very minor.

We also studied the possible behavior of both the index finger and the thumb during the evaluation process of foil thickness by handling the foils. First, we divided the behavior into three basic conditions: the vertical loading state (datum), the angled load (pinch motion) state, and the angled load (twitch motion) state. Figs. 45 (a) ~ (b) represent the loading condition within the roll axis; Figs. 46 (a) ~ (b) represent the loading condition within the pitch axis. The roll axis only requires confirmation on the single phase due to a symmetrical shape, and the pitch axis requires confirmation of both the normal and opposite directions. The red arrows represent vertical load, green arrows show angle load, and yellow dotted arrows show change of motion direction. Yellow dotted arrows are reversed in cases of pitch axis (opposite).

During the first pilot numerical experiments, we did not verify the foil thickness through the von Mises stress that was caused by simple loadings. This assumes that humans do not discriminate the thickness through stimulations caused by simple loading but through stimulation differences caused by motion changes. In thickness discrimination, our hypothesis is that the ability to differentiate two extremely thin materials comes from the comparison process between the vertical loading state (which is the datum) versus the angled loading state (pinch or twitch motion).

Table 2: Description of loading conditions for angular loading

Loading type	Axis of load from Index finger	Axis of load from thumb
b) Pinch type	Roll axis +ve	Roll axis -ve
b) Twitch type	Roll axis +ve	Roll axis +ve
c) Pinch type	Pitch axis +ve	Pitch axis -ve
c) Pinch (Opp.)	Pitch axis +ve	Pitch axis +ve
c) Twitch type	Pitch axis -ve	Pitch axis +ve
c) Twitch (Opp.)	Pitch axis -ve	Pitch axis -ve

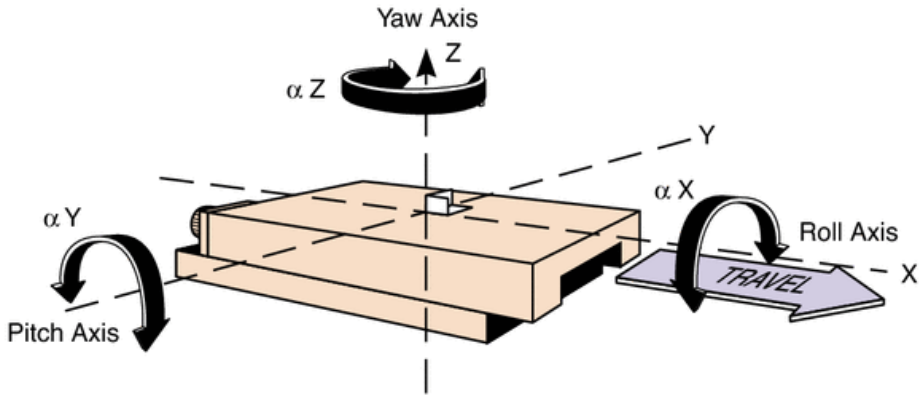

Fig. 57 Description of terms used in angular motion

ii) Result and discussion (Final phase)

In this section, we discuss the simulation result using the extracted von Mises stress data of the index finger that interacted with the thumb and the Cu and SUS foils from the selected nodal points. The arrangement of specific nodal points is shown in Fig. 54. Instead of using their averages, we discuss the maximum von Mises stress values of all the selected node points. Since using average data indirectly conceals the actual activity in some areas, the maximum value represents the most significant feature. The analysis of thickness is set to begins from t = 10 μm. Reason given, as when the thickness approaches 0, the von Mises stress value approaches infinite.

As a result, during analysis of the roll axis (pinch and twitch), the maximum von Mises stress occurs mostly at point #7. As for the analysis of the pitch axis (pinch and twitch), the maximum von Mises stress generally occurs at point #1, and for the pitch (opposite) and the twitch (opposite), it occurs more frequently at point #4. The average von Mises stress result from Fig. 58 onwards has been summarized according to this specific node points.

First, we examined all the simulation results and plotted them as a relationship between von Mises stress and foil thickness. In Fig. 50, almost all the curves decreased with an increase of thickness, where the SUS foil shows higher values than Cu foil in every case. Fig. 58 shows the comparison between the average von Mises stress for both copper and stainless steel material during each loading angle, from 0° to 45°.

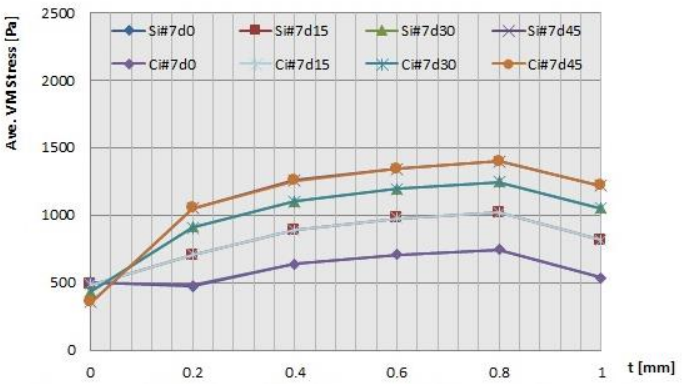

(a)

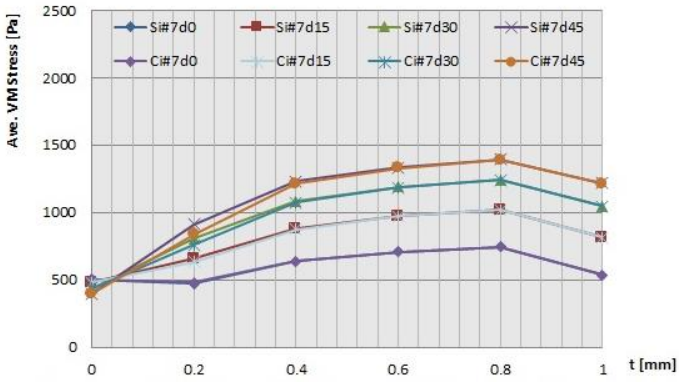

(b)

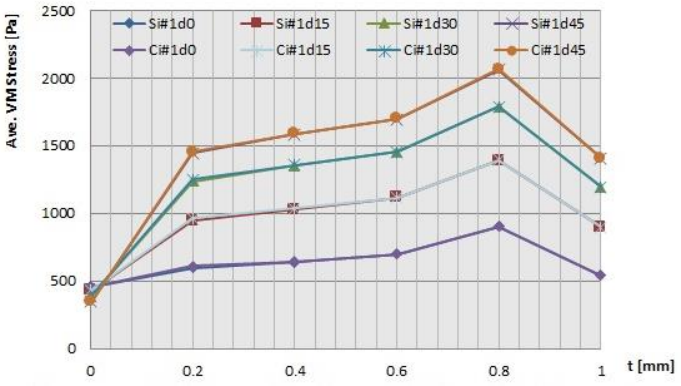

(b)

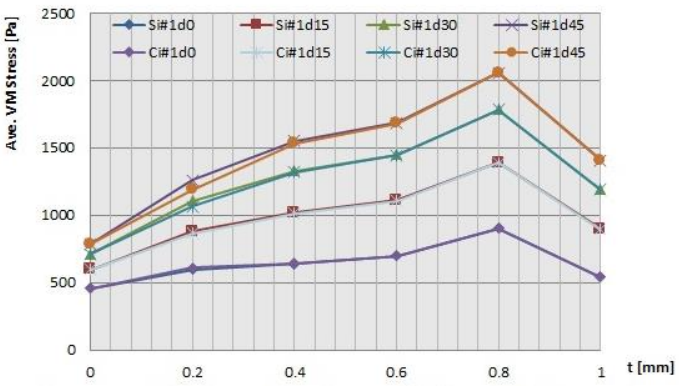

(d)

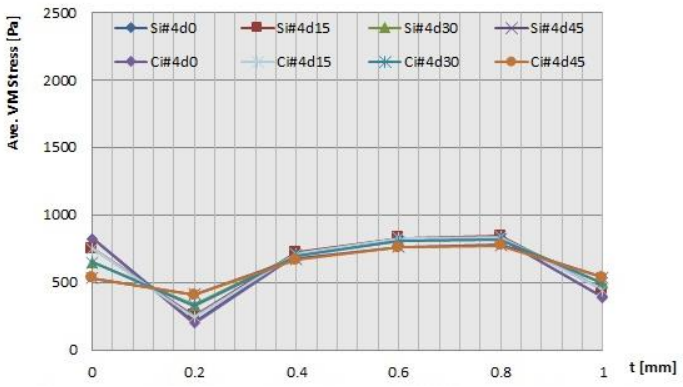

(e)

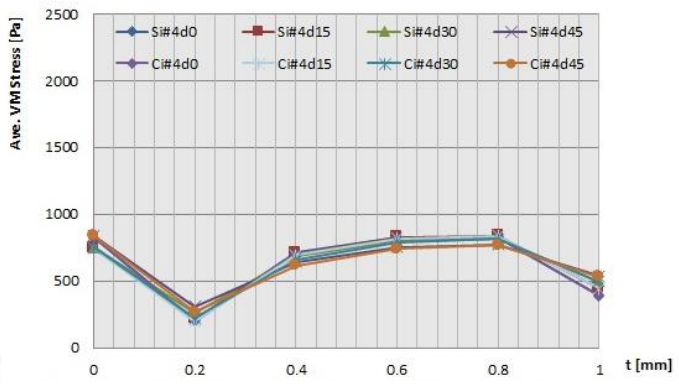

(f)

Fig 58 Comparison between average von Mises stress for Cu and SUS material; based on specific node points and loading state (a) pt.#7 roll axis with pinch method (b) pt.#7 roll axis with twitch method (c) pt.#1 pitch axis with pinch method (d) pt.#1 pitch axis with twitch method (e) pt.#4 pitch axis with pinch (opposite) method and (f) pt.#4 pitch axis with twitch (opposite) method.

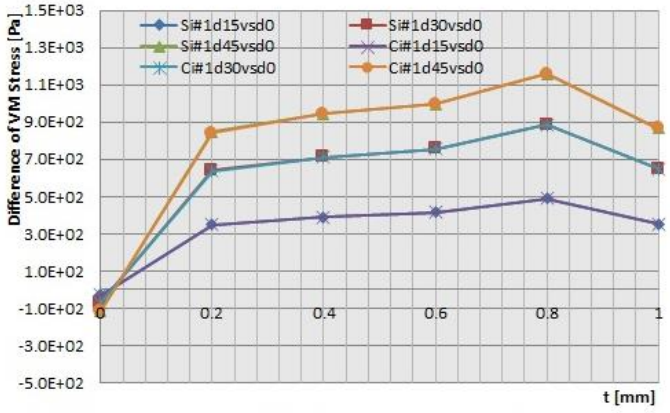

(a)

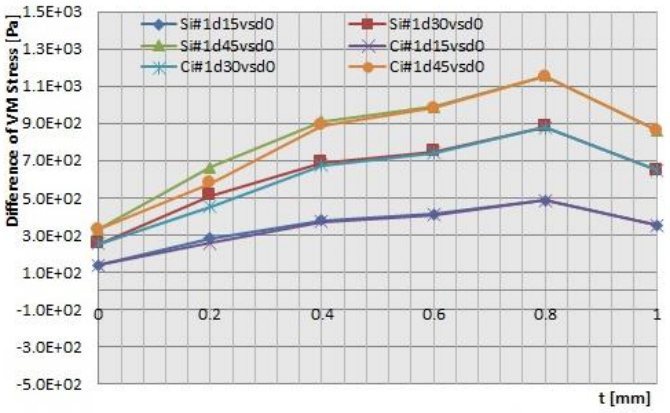

(b)

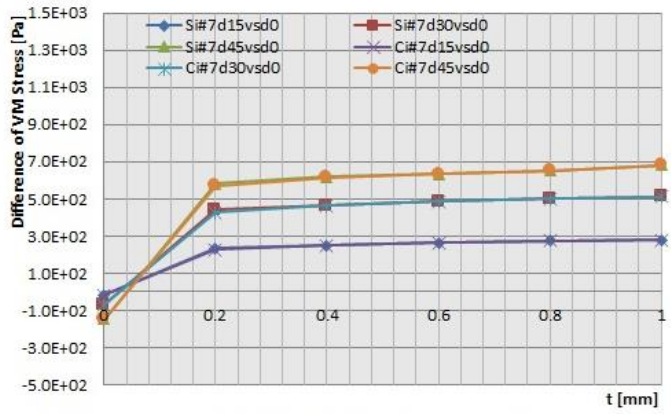

(b)

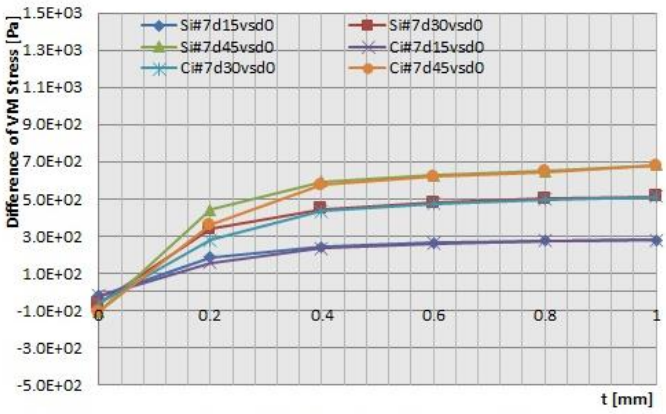

(d)

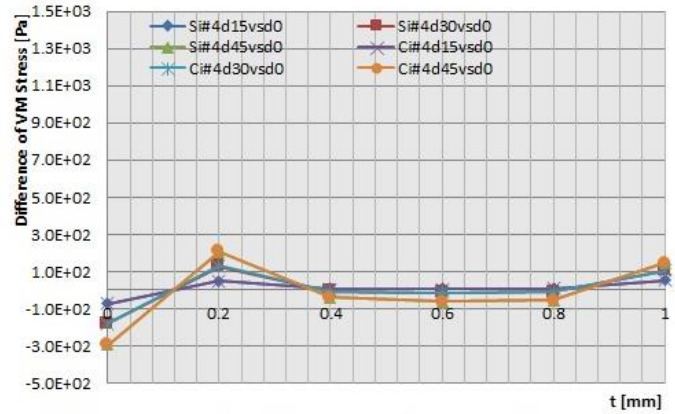

(e)

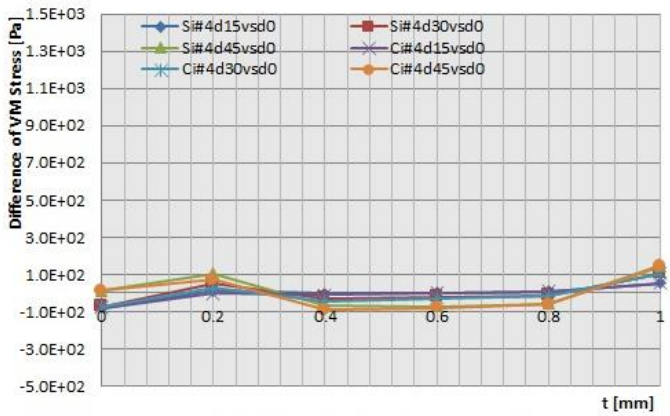

(f)

Fig 59 Comparison between difference of VM stress result of vertical load vs angle load; based on specific node points and loading state (a) pt.#7 roll axis with pinch method (b) pt.#7 roll axis with twitch method (c) pt.#1 pitch axis with pinch method (d) pt.#1 pitch axis with twitch method (e) pt.#4 pitch axis with pinch (opposite) method and (f) pt.#4 pitch axis with twitch (opposite) method.

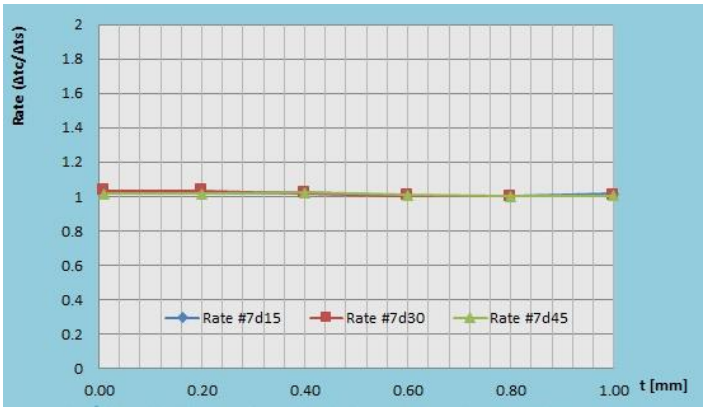

(a)

(b)

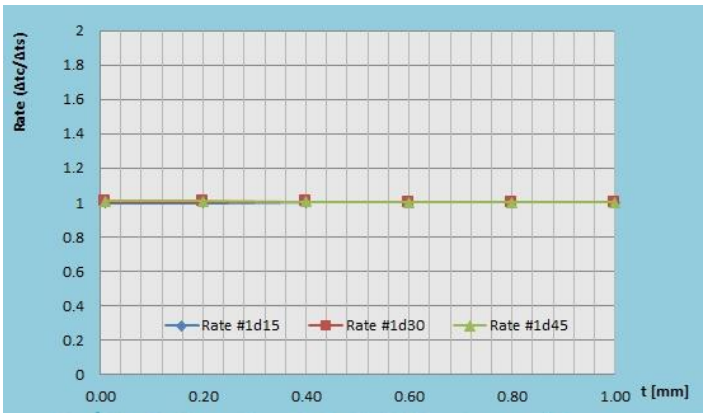

(b)

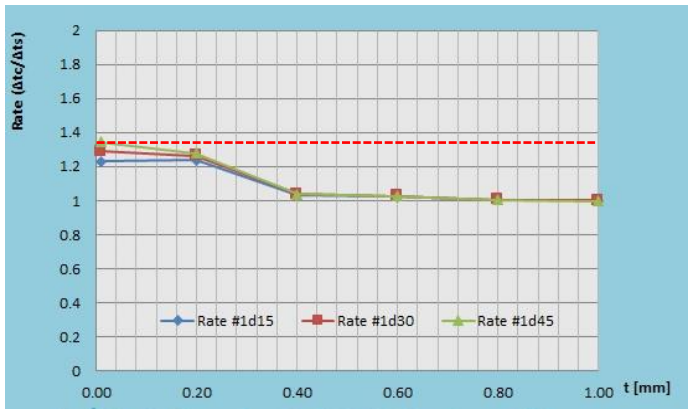

(d)

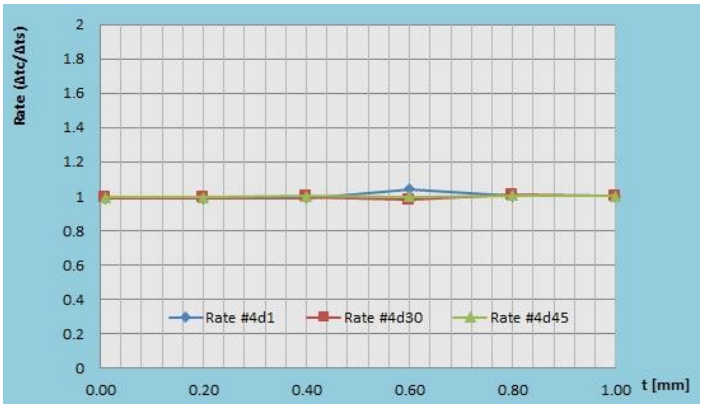

(e)

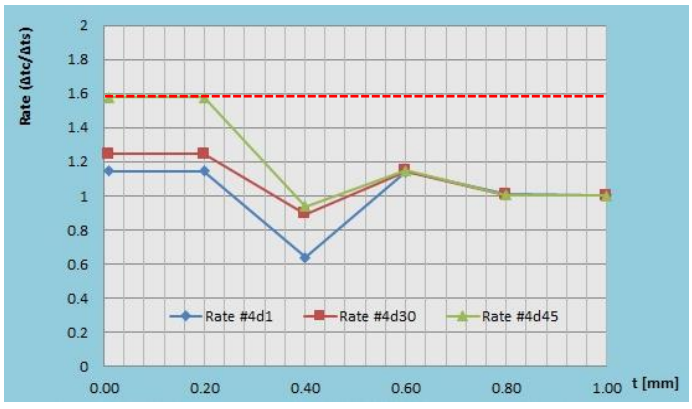

(f)

Fig 60 $\Delta t_c/\Delta t_s$ ratio (with reference to average von Mises stress of Cu and SUS) based on specific node points and loading state (a) pt.#7 roll axis with pinch method (b) pt.#7 roll axis with twitch method (c) pt.#1 pitch axis with pinch method (d) pt.#1 pitch axis with twitch method (e) pt.#4 pitch axis with pinch (opposite) method and (f) pt.#4 pitch axis with twitch (opposite) method.

Basically, we could monitor the differences between the von Mises stress more obvious during pinch method from zero thickness until 0.4 mm thickness. Similar result could also be monitored inside the t_c/t_s ratio graph in Fig. 60. The maximum tactile ratio is around 1.2, which occur during the pitch axis with twitch method. Overall, the result during twitch method is better compared to pinch method.

However, since this means that identical von Mises stress (SA-I mechanoreceptor unit activation) causes larger SUS foil thickness than the Cu foil, the single loading condition is not used to evaluate foil thickness. Consequently, we assumed that humans judge the foil thickness by the difference in the von Mises stress caused in the epidermis. This assumption is naturally accepted because in daily life we sometimes pinch sheets between two fingers and slide our fingers on them. Comparison between datum (defined using direct or vertical load in this research) with another condition must be available in order for us to differentiate between thicknesses.

Figure 59 shows the relationship between the differences of the von Mises stress on the vertical vs. angled load for both the SUS and Cu foils. The main objective is to validate the hypothesis, which is the ability to differentiate between thickness via tactile ratio is more obvious when the comparison is made between loads. These results show that the ability to differentiate between thicknesses by the difference of von Mises stress is more obvious when the comparison is made between twitch motion loads vs. direct load (datum). From majority of the results, the differences between both the Cu and SUS materials are more observable, especially during twitch motions.

Next, by referring to Fig. 60, the differences of the t_c/t_s ratio are also more noticeable depending on the difference of the loading motion. In the determination of t_c and t_s, we obtain graphs whose ordinate is the difference between the von Mises stresses of the angled load vs. the datum, the abscissa is the thickness, and t_c and t_s are estimated as the thickness that causes the same magnitude of the differences between the von Mises stresses in the graphs (Fig. 61). Especially in Fig. 60 (f), by comparing the ratios during a twitch motion of a 45° angle load with a datum, a maximum t_c/t_s = 1.6 ratio was achieved.

If we compare this with the ratios of previous psychophysics experimentations (Refer Fig. 46 (c)), which was around 1.5, the present result provides almost identical value. One of the hypothesis behind this higher comparison rate is because during this state, the loading direction shall be perpendicular with the nail surface and as the

angle increases, the tip of our fingernail shall apply more stress towards the skin, thus increases the detection rate on the material (Refer Fig. 62).

In a series of simulations, we compare the differences between the von Mises stresses generated in the skin under different loading states when the Cu and SUS foils are grasped. Since von Mises stress is equivalent to SED, we can estimate the tactile sensations from von Mises stress variations. On the other hand, we obtained the equivalent thickness of copper foil t_c to stainless steel foil t_s from a series of psychophysical experiments; ratio t_c/t_s was a constant value of around 1.5 in t_c = 30 ~ 50 μm.

In this simulation, ratio t_c/t_s is defined by the thickness that causes the same von Mises stress. However, since ratio t_c/t_s becomes larger than 1 through simple angled or vertical loading analysis, we use the difference of the von Mises stresses between angular and vertical loads (treated as a datum) to calculate it. On the basis of the simulated results, ratio t_c/t_s is evaluated to obtain optimal loading for the thickness of foils using t_s as the base and the projection value of t_c (Fig. 61).

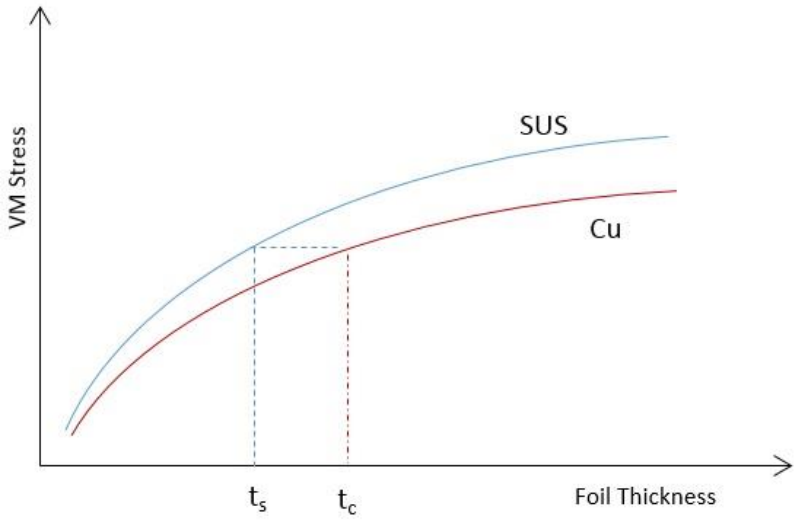

Fig. 61 Method in defining projection value of t_c for tactile ratio.

4.6 Conclusion

We conducted a series of simulations using CATIA V5 with a 3D elastic model of the index finger and thumb (consisting of the epidermis, dermis, bones, and nails) while grasping the Cu or SUS foil with final thicknesses between t = 200 ~ 1000 μm,

in order to elucidate the mechanism of foil thickness recognition. The main focus for this analysis identifies the specific nodal points, which represent the contact areas and the location of the SA-I mechanoreceptor unit on the fingers. An OCTREE tetrahedron element was applied with a revised element type from linear to quadratic to reduce the aspect ratio, especially on the foil part.

Compared to the psychophysics experiment, analysis for material thickness above 350 µm also has been made during this FEA simulation. One of the hypothesis is that, the detection could have been made from our joints (for example from FA-II or SA-II mechanoreceptor) during this region. This is because, from the thickness ratio, there was no major increment for thickness above 400 µm.

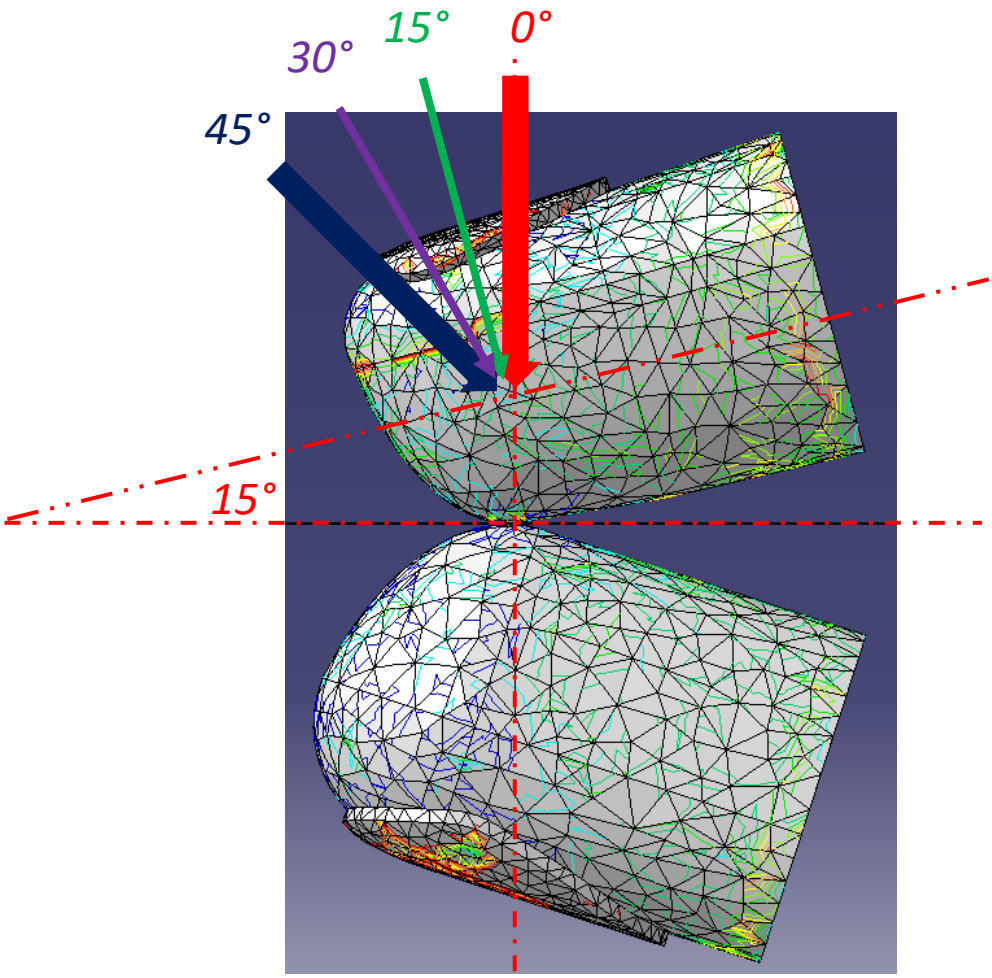

Fig. 62 Description on angle of load from pitch axis –ve.

As a result, we have achieved our main objective, which was to identify the von Mises stress value within the epidermis section. We managed to maintain the simulation's convergence rate by optimum use of the element size and to keep the numerical error below 4% during the simulation. Based on the simulation results, we monitored the basic behavior of the human tactile mechanism to define the differences between two extremely thin foils. This simulation result also supports our initial hypothesis in which SA-I mechanoreceptor units play the main role in defining the differences between the foils. Another hypothesis is that the existence of our finger nail, also contributes towards enhancing the detection rate between different material thicknesses. However, this hypothesis shall be confirmed during future experimentation.

In the future, we will expand the findings from the experimental procedures of robotic tactile sensing using a three-axis tactile sensor. With a robotic hand equipped with three-axis tactile sensors, we will evaluate the present loading manner to increase the precision of the foil thickness discrimination. We expect that continuing FEA to evaluate mechanoreceptor unit's activation will be embraced to deepen our understanding of the human tactile mechanism.

Chapter 5

THE THICKNESS DETECTION PROCESS VIA ROBOTS

5.1 Introduction

Due to the increase of aged population in Japan, at the same time worsen by the decreasing number of new birthrate year by year; the urge for a robot services to support these veteran aged group has increased drastically. Through the comprehensive strategy by the Ministry of Science, Technology and Innovation of Japan, it is expected that the services of these advanced robots can be expanded towards personal homes, medical fields and other sectors; especially in taking care of care of the elderly and disabled persons.

To achieve this target, the robots should be able to perform all the basic tasks, from providing meals to physical support (during movement to the toilet, in bed, etc.). At the same time, they should possess a high level of delicacy, especially in tactile sensation to conduct such task. For example, as a person ages, the posture and gait (posture) weakens. Especially, menopaused women may experience sudden reduction of mass or density of the bone due to calcium and mineral loss. In the worst cases, the bones become brittle and fragile; and may easily break if not handled carefully. For such cases, the delicate function of the robot is extremely important. This is an essential process, considering the amount of information required for handling objects, with various unknown parameters such as sizes, weight, hardness, surface texture and more. This is one of the reasons why the study of the delicate human detection process has been the focus in the tactile sensing field.–

In this chapter, we shall be evaluating the progress and development of tactile sensing research up to date, especially those related to thin sheet handling. In Ohka Lab, we are using the three-axis tactile sensor (Fig. 63), which is able to measure properties such as contact/touch, shape, force (normal and shear), slippage plus other physical attributes. Details regarding the three-axis tactile sensor can be referred from previous publications by Ohka et al. (2005~2014). Our aim is towards improving the performance of this sensor, using a more compatible material selection, by reducing

size and weight, by optimizing movement plus other ideas. In near future, we are planning to improve current research theme further using this tactile sensor as base. Most recent work is by Sugiman et al. (2015), which performs to count bill number through the evaluation of sheet thickness using 1,000-yen bills as medium. The 1,000-yen bill was used due to the amount of precision, stability in size plus other mechanical properties.

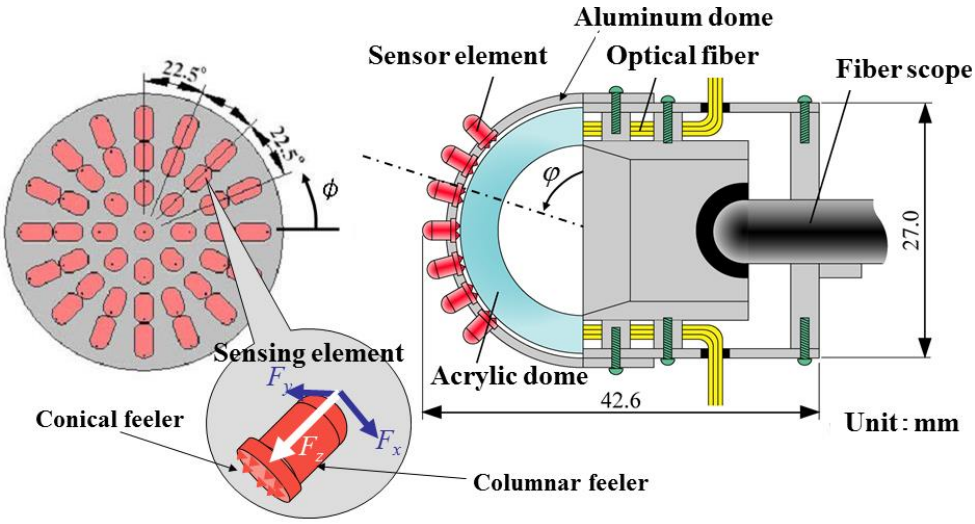

Fig. 63 Example of the columnar-and-conical-feeler type three-axis tactile sensor.

Since a robotic hand equipped with three-axis tactile sensors can detect not only grasped force caused by pinching motion but also slippage force by sliding fingers, it has been applied to various tasks such as cap twisting, exploring object shape and detecting hardness. This is one of the reason why the three-axis tactile sensor was chosen to conduct this experiment. Although such task is simple (when performed by human), it can be considered as one of the more difficult tasks when performed by robots. This is due to the flexibility and thinness of the 1,000-yen bill used.

5.2 Recent development of tactile sensing and robotic hands.

The development of tactile sensing already started from 1970's, and has matured well over the past 30 years' period (Harmon, 1982; Nicholls and Lee, 1989; Najarian et al, 2009; Dahiya et al., 2012). It was firstly introduced for the industrial use, and later on slowly spread out towards other applications and sectors. One example is the soft compliant actuation function, especially in rehabilitation process (Guizzo and Deyle, 2013). Other type of application is for stroke patient through neuro-rehabilitation

process. For example, the GENTLE/s method developed by Amirabdollahian et al. (2003), which is able to provide support by replicating therapy session through the combination of haptic and Virtual Reality (VR) technology. Whereas the ROAD robot system focuses on assisting patients with gait, balance and standing up problem (Carrera et al., 2011).

In definition, tactile sensor is a device capable of acquiring tactile information through physical contact. Some of the application of tactile sensor is in human-robotic interaction, biomedical, rehabilitation, prosthetic and more (Dahiya and Valle, 2013; Tawil, 2015). Recently, due to the demand of advanced robotic services in medical field, the objective is to increase the number of rehabilitation product especially ones related to human-robotic interaction (HRI). One of the example is to design robots or machines capable of interacting delicately with humans. Furthermore, effort for compliant actuation needs to improve other type of tactile sensing technologies.

There are three primary tactile topic areas for human and robot interaction (HRI), which are the interference contact (human contact that interferes with robot behavior execution), contribution contact (human contact that contributes to behavior execution) and developmental contact (human contact that enables behavior development or adaptation). Selection of sensor type is one of the important aspects, to enhance the rehabilitation process between robot and human subject (Argall and Billard, 2010).

In recent years, the developments of prosthetic parts and components have evolved rapidly. The design processes have improved, initially from external outlook, until recently focuses more towards detail functional of the product. Among the recent trend is the design of prosthetic parts capable of performing similar physical actions as normal human being. One example is the iBionic product, which produces mechanical prosthetic arms for handicapped person (Fig. 64). Through trainings, the patient able to control the motion of each individual fingers independently while performing daily actions. Another example is NAO robot, which is used as humanoid robots to interact with autistic patients during rehabilitation (Fig. 65). Through natural motion and gesture and of the NAO robot, physical interaction between the patient and robot could be encouraged.

The research and development of artificial skin also has become more sophisticated. In 2014, J. Kim and teams have tested the performance of a stretchable artificial skin (which able to sense pressure, temperature and humidity) on a prosthetic hand (Fig. 66). Also, the development of the Digital Tactile System (DiTact) by a group of researcher

lead by C. K. Tee in 2015, by combining artificial robotic hand with artificial mechanoreceptor capable of detecting very light touch by translating the pressure received by the sensor to digital signal which is directed to the neuron of test mouse (Fig. 67). Another example is the design of flexible and wearable liquid-based microfluidic tactile sensor by NUS in 2015 for biomechanics applications. All sharing the same objective, which is to support people with physical disability to be able to re-experience physical sensation using artificial skin as medium.

Fig. 64 The BeBionic prosthetic hand.

Fig. 65 Interaction between kids and NAO robot

Fig. 66 Artificial robotic hand with artificial mechanoreceptors. (Adapted from Tee et al 2015)

Fig. 67 Prosthetic hand and laminated electronic skin. (Adapted from Kim et al (2014)

5.3 The three-axis tactile sensor

i) Review on three-axis tactile sensor

In general, the three-axis tactile sensor can be divided into few categories such as the Micro Electric Mechanical System (MEMS) type, columnar and conical feeler type,

moving feeler type and many more. The development of the three-axis tactile sensor was initiated from the Advanced Robot Technology Research from 1983 ~ 1990; a national program promoted by the Ministry of International Trade and Industry (Japan). The Fuji Electric Corporation (Research and Development) took part in this project by producing two products, which is the 1-mm-three-axis and 3-mm-three-axis tactile sensor using Micro Electric Mechanical System (MEMS) technology. The single crystal silicon used in this design is has a good linearity feature, with static strength (almost) equivalent to stainless steel; even though fragile against impact force.

The optical waveguide tactile sensor was produced by the Agency of Industrial Science and Technology (of Japan), where the tactile information was obtained as image data through the phototransistor array (Tanie et al., 1986). This design concept was progressed to design our three-axis tactile sensor. Tanie's sensor is also known as the optical uni-axial tactile sensor. Earlier on, we have utilized the four-conical-feeler type for position sensor device (PSD) array, which possesses four isolated detection photodetectors in each element (Ohka et al., 2004). During the next development, it has been enhanced to eight-conical-feeler type for higher sensing precision. One of the advantages of our optical three-axis tactile sensor is that, it can obtain not only normal force distribution but also tangential force distribution. If assembled into robot arms, it is capable of detecting not only grasping force, but also slippage (Ohka et. al., 2004, 2008, 2009).

Ohka lab also produces the moving feeler type tactile sensor. Even though the columnar-and-conical-feeler type tactile sensor is superior for sensing curved surface and for isolating sensing element, the structure is still complicated. This was made possible through simplified hardware process (adapted from the optical uni-axial tactile sensor), where the three-axis force can be determined by the image data processing of the conical feeler's contact areas (Ohka et al., 2005).

ii) The principle of tactile sensing

Since the principle of our optical tactile sensor has been repeatedly explained in several conferences, journals and books (Ohka et al., 2005 ~ 2014), it is only briefly reviewed in this chapter. In the optical tactile sensor, light reflection and elastomer deformation are used as the basic principle. First, we assume a structure composed of a transparent board, a rubber sheet on it and small air gap between them; light is

introduced from the end of the board. Since total reflection is caused in the inside of the board, light is not observed from the back side of board. However, if an object is put on the sheet and force is applied to the object, contact between the board and rubber sheet back surface under the object is caused, and the contact is observed from the back side of the board as a bright area because the total reflection is projected on the contact surface.

It is comprised of a rubber sheet and a transparent acrylic plate illuminated along its edge by a light source. The light, which is directed into the plate, remains within it due to the total internal reflection that is generated. A rubber sheet featuring an array of conical feelers is placed on the plate to maintain array surface contact with the plate. If an object contacts the back of the rubber sheet, resulting in contact pressure, the feelers collapse, and at the points where they collapse, light is diffusely reflected out of the plate's reverse surface. The distribution of the contact pressure is calculated from the bright areas viewed from the reverse surface of the plate.

We have introduced several designs of the three-axis tactile sensor. Our sensors are divided into two groups: one of them is conical and columnar feeler type (Ohka et al., 2008, 2009, 2012) and another is the feeler movement type (Ohka et al., 2005). At present, the former is applied to a hand-arm-robot to achieve several tasks such as cap-twisting, object-passing and object-assembling. The former sensor uses a cylindrical rubber element with a hemisphere and conical projections on the point and bottom, respectively.

To explain three-axis force sensing, we introduce Fig. 68. If a force is applied to the parietal point, normal force is observed by bright spots caused on the contact between the conical tips and the acrylic dome. The normal force component is proportional to the brightness of the spots, while the tangential force component is observed by centroid movement of the bright spots. Since there is almost no interference between brightness and centroid movement, normal and tangential components are independently measured. Thus, normal and tangential forces are measured from an integrated brightness of the image data and the centroid movement of the bright area, which is expressed by U_x and U_y in local coordinates embedded on each sensing element. We assume that three components of applied force F_x , F_y, and F_z , are proportional to U_x , U_y and G. Since the image shall warp due to projection from a hemispherical surface, the warped image data shall be modified and analyzed using installed software in order to calculate U_x , U_y and G; and to obtain the 3-axis

force on the tip of the sensing element.

iii) Specifications of the ordinal optical three-axis tactile sensor.

Figure 69 shows the design of the ordinal optical three-axis tactile sensor, which can be reviewed from our previous article. Since we have recently introduced new designs, we call it the ordinal optical tactile sensor. It is composed of sensing elements, an acrylic dome, optical fibers, a fiber scope, a light source and a CCD camera. Light is directed from the light source through optical fibers to the acrylic dome; the side view attachment is mounted on the fiber scope end to observe the back surface of the acrylic dome.

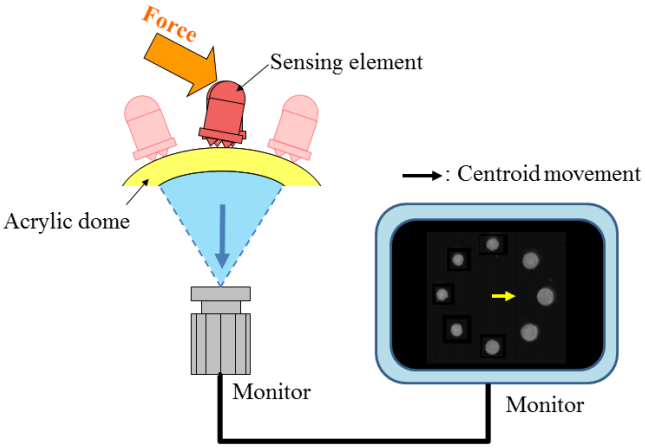

Fig. 68 Principle of the three-axis force.

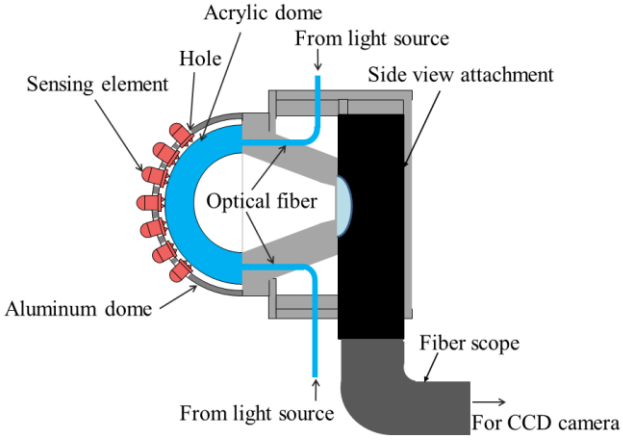

Fig. 69 Design of ordinal optical three-axis tactile sensor.

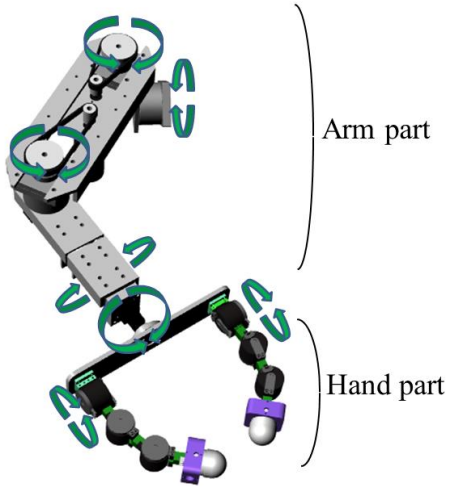

Fig. 70 Overall view of the hand-arm robot (with arrows indicating DOF).

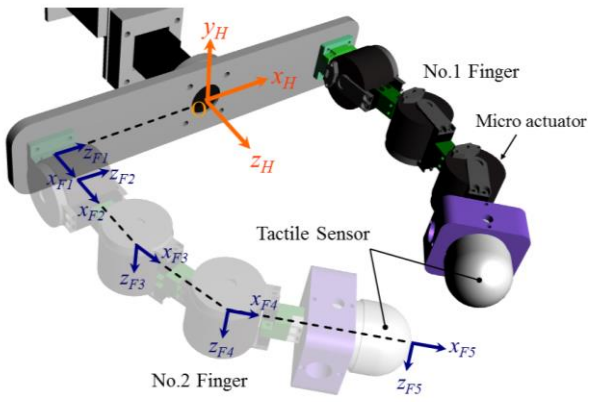

Fig. 71 Robot hand equipped with optical three-axis tactile sensors.

Although it has some disadvantages such as an invisible zone and unacceptable large force that we are trying to overcome through new sensor designs (Ohka et al., 2014), the ordinal optical three-axis tactile sensor (Ohka et al., 2018, 2009, 2012) is still used because the new designs still require several tests and improvement for application. In this study, we used the ordinal optical three-axis tactile sensor because the task of sheet handling does not require large force.

The specifications of this sensor are shown in Table 3. Maximum detectable normal and tangential force components are 2 N and 0.15 N, respectively; resolutions of these components are 10 μN and 35 μN, respectively. This sensor does not accept large force, whereas it has precise resolution of force components.

Table 3 Specifications of ordinal optical three-axis tactile sensor

Item	Value
Number of element	41
Detectable maximum force per element	
F_x; F_y	0.15 N
F_z	2 N
Acceptable maximum force per element	
F_x; F_y	2 N
F_z	3 N
Resolution	
F_x; F_y	10 μN
F_z	35 μN

iv) The robotic hand (Equipped with three-axis tactile sensors)

In our laboratory, an articulated hand-arm robot is developed to achieve the aforementioned intelligent tasks. In this study, we used the hand part of the robot as shown in Fig. 71. Each finger has three motors (Micro actuator, Yasukawa Co.) and an ordinal optical three-axis tactile sensor. The motor is composed of an AC servo motor,

a miniature harmonic drive and an encoder; since it generates 0.7 Nm torque, around 10 ~ 40-N force can be obtained as maximum force at the fingertip.

The hand is mounted on an articulated robotic arm: the hand-arm robot is shown in Fig. 70. Since the arm robot has only five degrees-of-freedom (DOF), the finger motors installed on the base are used for one wrist DOF. The schematic flowchart of finger motion control is shown in Fig. 72. The velocity vector of the fingertip is decided by normal force and its motion mode (pinching or sliding two fingers). In this paper, tactile data obtained from the tactile sensor mounted on Finger 2 are used for data sampling and the grasping force control.

We used three computers for finger control, arm control and tactile sensors. Tactile data and the hand-and-arm status are transmitted through a local area network.

5.4 Research methodology and result

i) Experimental procedure

Around 1 ~ 10 sheets of 1,000-yen bills was used to monitor the performance of the three-axis tactile sensor (Fig. 73 (a)). The 1,000-yen bill was chosen as sample instead of metal sheet due to the performance limit of the current three-axis tactile sensor to distinguish metal components. Even though the properties is not as good compared to metal, 1,000-yen bills and other typical money have strict standard especially in terms of quality, precision, dimension, mechanical properties and others. This is the main reason for choosing 1,000-yen sheet as sample. In order to distinguish the number of sheets, evaluation has been made by using direct pinch motion (normal load) and also by adding sliding motion (tangential load). The gripping force of the three-axis tactile sensor has been calibrated around 1.0 N range.

Using the above hand robot, this experiment was performed as follows. First, the robot pinches papers at the parietal point of each fingertip as shown in Fig. 71. At the start of this motion, each fingertip speed is set as 0.1 mm/s along x_H or $-x_H$ direction; when contact force at the point (at element #00 shown in Fig. 73 (b)) reaches 1.0 N, the grasping motion is stopped. For the pinching motion test, we obtained data for nine elements (from #00 to #08 shown in Fig. 73 (b)) to measure normal force distribution at the fingertip. We expected to observe difference in normal force distribution related to the number of pieces of paper.

For sliding two-finger motion, after the hand robot grasps papers with 1.0 N, Fingers 1 and 2 are linearly moved along y_H and $-y_H$ directions (the coordinate is shown in Fig. 71) with 0.5 mm/s, respectively. This sliding motion is terminated when slippage on the fingertip is observed; the slippage is defined as a time derivative of tangential force, of which magnitude becomes larger via vibration of slippage.

The ratio of element #00's normal force value to element #01 – #08s' mean normal value is obtained for evaluation of sheet number: the difference between maximum and minimum norm of tangential components of force vector at element #00 for sliding finger motion.

ii) Using direct pinch motion (Normal load)

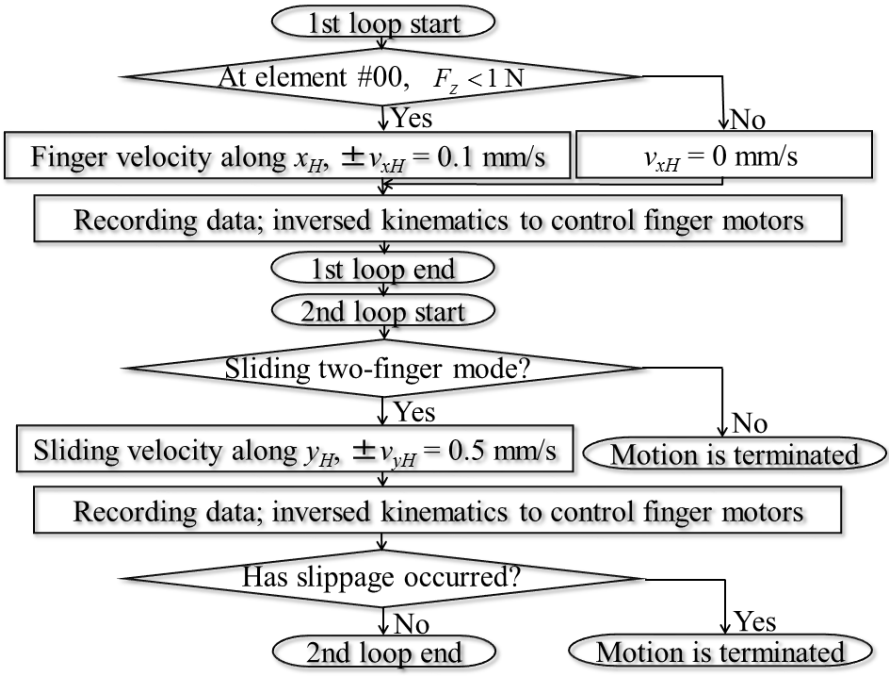

Fig. 72 Flowchart for grasping and sliding sheets.

When measuring the thickness of a thin sheet, we use a micrometer caliper to pinch them. First, we examine the simplest way to examine the number of pinched sheets as with a caliper. At this time, the joint data of the articulated finger do not seem suited for thin thickness meaurement because of the small playes being accumulated in the serial links of the finger. We assume that tactile data are efficient for this case. From the preceding psychophysical experiment, we introduced a hypothesis that "when judging thin sheet thickness, a human being judges the spring constant of the sheet instead of geometrical thickness". For robotics, we assume that the hypothesis is

applied to thin sheet thickness.

If we intend to obtain the spring constant without displacement value, we can estimate hardness from force distribution. When a thicker sheet is grasped, the difference between maximum and minimum normal forces becames smaller because the sheet is not so deformed, and thiner sheet vice versa. Based on this idea, we introduce a new parameter for emulation of the spring constant as shown in Eq. (14) below:

$$R_1 = \frac{(\text{Mean normal force of element \#1 } \sim \text{ \#8})}{(\text{Normal force of element \#0})} \times 100 \qquad (14)$$

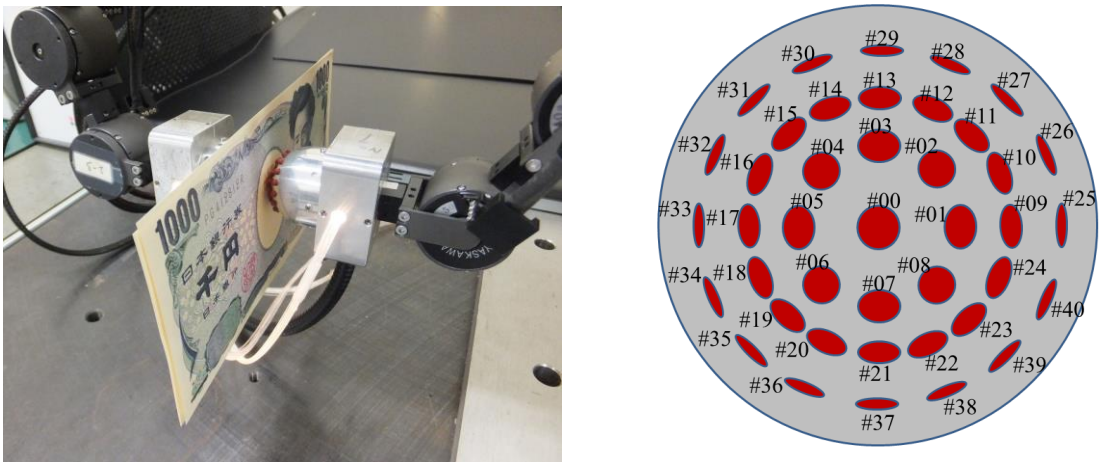

(a) (b)

Fig. 73 Hand robot grasping sheets (a) and configuration of sensing elements (b).

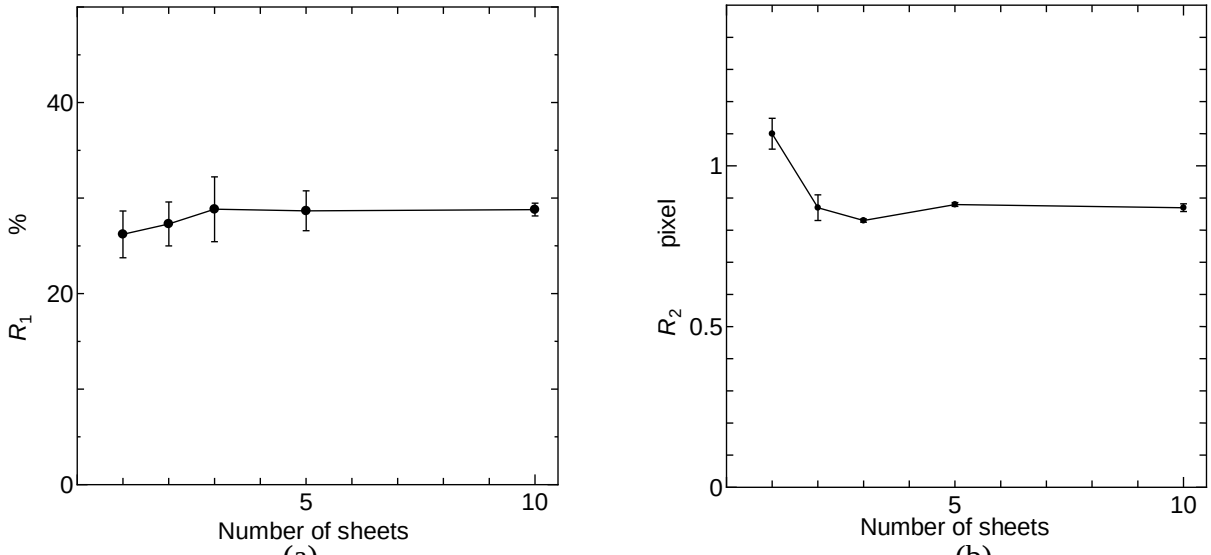

(a) (b)

Fig. 74 Experiment result for (a) direct pinch motion and (b) sliding motion (Error bar: SD).

Fig. 74 (a) shows the results from 1~ 10-sheet grasping. As a result, an increase of sheet number also increases the R_1 value. The value of R_1 slightly increases from 1 to 3 sheets, then it is saturated, while standard deviation is very large. Although the sheet number seems to be counted through pinching motion in the range from 1 to 3 sheets, the discrimination of number is not so easy because of small difference in R_1.

iii) Using sliding motion (Tangential load)

We introduced two parameters for pinching motion and sliding motion: one of the parameters is for evaluation of sheet pliability; the other is for evaluation of slippage between two sheets. Experimental results show that sheet number discrimination is difficult for pinching motion causing normal force. However, it is possible through sliding fingers causing tangential force.

Compared to pinching motion, sliding two fingers seems to be effective because we have experience handling two sheets separation through a similar manner. To evaluate the effect of this motion, we introduce another parameter for easiness of sliding as shown in Eq. (15) below:

$$R_2 = \mathrm{Max}\left(\sqrt{F_x(t)^2 + F_y(t)^2}\ \right) - \mathrm{Min}\left(\sqrt{F_x(t)^2 + F_y(t)^2}\ \right) \qquad (15)$$

where F_x (t) and F_y (t) are time functions of x- and y-directional force vector components at element #00.

Figure 74 (b) shows the difference in parameter R_2 obtained from 1 ~ 10 sheets (unit of R_2 is pixel). As a result, the R_2 value is 1.10 for 1 sheet, while it decreases to 0.87 for 2 sheets and keeps a constant value of around 0.83 after that; standard deviation is small enough at a glance. Thus, the result of 1 sheet is completely different from other cases. This is because slippage between sheets is occurring in the case of more than 2 sheets, while stational friction force is generated in the case of 1 sheet. Therefore, the difference between 1 sheet and others can be evaluated through sliding two fingers; the criteria of R_2 becomes effective for evaluation of the difference. Furthermore, since the robot has at least repeatibility of 0.1 mm, thickness of over 2 sheets seems to be measured by pinch distance of the two fingers through revolution angles obtained from joint encoders. In the future, if we use the

combination of tactile and joint angle information, the robot will comprehend sheet number as human beings can.

5.5 Conclusion

As a result, we found that it was difficult for the robotic hand to distinguish between the numbers of sheets using only normal load. By including tangential load, the differences was more observable especially between low numbers of sheets. The result shows the relation between *R*-values versus number of sheets. The *R*-value refers to the easiness of sliding through comparison between maximum and minimum value of tangential load. It can be defined as difference between maximum and minimum tangential load magnitudes $|F_t|$, when the robot hand slides fingers after grasps sheets.

Although different set of material was used in this experiment (compared to current psychophysics experiment and FEA simulation which uses SUS and Cu foil as medium), the main objective is to show the possability in relating thickness evaluation processes between human vs. tactile sensor. Surprisingly, the efficiency of the human tactile sensation is more sensitive when evaluating extremely thin material. This supports our hypothesis where the cutaneous function plays a role towards enhancing detection and feeling of the grasped sheets.

In future work, we will incorporate a hybrid control mechanism of positioning and force to the hand robot to accomplish turning and counting pages. Furthermore, the developed technology will be applied to handling another material such as aluminum foil and various cables.

Chapter 6

OVERALL SUMMARY

6.1 Overview

At the beginning of this thesis, we have explained regarding the excellent capability of human body in performing simple yet delicate task, especially those related to tactile function. We have covered the general and future trends in tactile sensing studies related to robotic field. We also mentioned regarding available research progresses from such an invasive type as microneurography to non-invasive type. Basically, our direction is more towards non-invasive type by using psychophysics and FEA method. Also, in Chapter 1, this research objective and general methodology have been covered. Finally, the significance of studying the human tactile sensor has been highlighted towards the development of better tactile sensor design.

Next, in Chapter 2, we have covered on the human tactile system, which consists of tactile sensing, the sense of touch, psychophysics behavior of human, and others. In general, the human tactile sense plays an important role in our daily life. Each physical action triggers the activation of such mechanism whether we notice this or not. A major focus in the tactile sensing field is the study of the delicate human detection process.

As for this research, it is more specific towards the function of SA-I mechanoreceptor function. One of the objectives is to analyze human tactile mechanism behavior in recognizing extremely thin foils through psychophysics experimentation and FEA method. Through the study of the distinctive ability of human tactile function on membrane thickness, we will be able to improve and optimize the performance of current tactile sensors. It is also valuable for future application and development of a new robotic sensor or other human-machine interface, especially for the one used in robotics.

In Chapter 3, we have briefed regarding psychophysics experimentation process. Comparison with previous experiment by Miyaoka and Ohka (2001, 2002) also has been made. From here, the hypotheses are that the evaluation for material with less than 70 μm thicknesses shall be made using the SA-I (Slowly Adaptive Type I)

mechanoreceptor unit that exist inside the structured layer of the human skin. As for material with thickness more than 350 μm, the evaluation shall be made by another system such as the angular sensory organ. Also, there exist an undetected region between mechanoreceptor unit's evaluation versus other system. One hypothesis is that both the cutaneous and kinesthetic system was functioning simultaneously during this period, and the transition state also occurs within this region. As in discriminating extremely thin materials, it could be possible that plastic deformation may also influence the result.

In Chapter 4, we have focused on the application of FEA in order to verify the performance during gripping process. We have briefed and discussed regarding each level of design process involved throughout the analysis. The FEA analysis has been conducted using the 3D model of index finger, thumb and also various sheet metal as base. We managed to maintain the convergence rate of the simulation by optimum use of element size and being able to keep the numerical error below 4% during the simulation. By selecting node points within contact area, we able to provide the best outcome compared to other tested method or options. In general, the objective which is to monitor the performance of the von Mises stress value inside the epidermis section has been achieved.

In a series of simulations, we compare the differences between the von Mises stresses generated in the skin under different loading states when the Cu and SUS foils are grasped. The simulation result was extracted from selected nodal points from the index finger, which interacted with the thumb and the Cu and SUS foils. As explained previously, since von Mises stress is equivalent to SED, we can estimate the tactile sensations from von Mises stress variations.

We also studied the possible behavior of both the index finger and the thumb during the evaluation process of foil thickness by handling the foils. In thickness discrimination, our hypothesis is that the ability to differentiate two extremely thin materials comes from the comparison process between the vertical loading state (which is the datum) versus the angled loading state (pinch or twitch motion).

In Chapter 5, we have discussed regarding the history and latest trends in tactile sensing and robotic research. Among the example is towards rehabilitation process, through the design of prosthetic parts and more. We also discussed regarding the demands of advanced robot services towards supporting the ederly aged group especially in Japan. Next, we have reviewed regarding the history, principles and

functions of the three-axis tactile sensor in Ohka Lab. We also briefed on the application of this sensor towards discriminating the thickness of extremely thin sheets.

6.2 Summary

During the psychophysics experiment, the method of constant stimuli (using difference threshold concept) has been applied, by evaluating between standard and comparison stimulus (refer Chapter 3). From this experiment, we able to verify the influence of gripping angle towards increasing the detection rate between different material type and different thicknesses. As a result, the psychometric function increases as the thickness of comparison stimuli increases. This shows the ability of the tactile function (of test subject) to discriminate the thickness of the stimuli, increases as the thickness of comparison stimulus material increases. Overall, the proportion of detections (whether expressed as *p*-values or *z*-scores) increases as the thickness of the comparison stimuli increases. Again, this proves the ability of the tactile function (of the test subject) to discriminate the thickness from the stimuli.

Further evaluation of the result shows that the Weber fraction *c* (= threshold/thickness) reduces as thickness of stainless steel foils increases (Weber fraction is used as medium to measure and explain the intensity of stimuli). Next, from t = 120 μm onwards, the Weber fraction becomes constant. From the hypothesis, this proves that the test subject is able to distinguish the properties of extremely thin foils through the sensitive cutaneous function. The ability to detect deformation as the thickness is effective. This is due to the limitation of our finger to induce deformation on the material, until a certain limit where only the kinesthetic function is available to define the differences. Overall, the Weber fraction is high during low thickness and further reduced to constant value as the thickness increases. This shows that the test subject is able to detect the thickness of stimuli through normal vs. angled load motion. Unfortunately, the duplex theory could not be observed in this experiment.

During experiment, we employed a specific procedure to maintain contact between the human finger and SUS foils throughout the experiment. The test subject was required to grip the material between the index finger and thumb without releasing contact with the foils in order to ensure that the only mechanism that activates during

contact is the cutaneous stimuli (or mechanoreceptor), especially in detecting distortion. This also shows that the test subject is capable of detecting the thickness of stimuli better through this gripping method.

Next, referring to the FEA simulation result in Chapter 4, the plotline decreased with an increase of thickness; where the SUS foil shows higher von Mises stress than the Cu foil during each case (refer Figs. 48 ~ 50). As a result, the differences between the von Mises stress is more obvious during pinch method, especially between 0 ~ 0.4-mm thickness. Similar result could be monitored from the t_c/t_s ratio (Refer p.64 for description) or tactile ratio vs thickness graph. The maximum tactile ratio value is around 1.2, which happens during the pitch axis with twitch method. Overall, the result during twitch method was better compared to pinch method.

One of the hypothesis for the high comparison rate is because during this state, the loading direction shall be perpendicular with the nail surface and as the angle increases, the tip of our fingernail shall apply more stress towards the skin, thus increases the detection rate on the material. From this result, we could see that the twitch method provides the maximum tactile ratio compared to all. Referring to the actual mechanism of human finger, we should notice that the ergonomics position of both index finger and thumb while holding sheets of paper is not as ‘symmetrical’ as we imagined. Looking closely, the position of our thumb is slightly twisting with around 45 ~ 90° rotation angle. And during the gripping process, the best mechanism which perfectly describes this gripping behavior is the twitch method as we proposed. Another factor which contributes towards this result is the availability of our finger nail, as we have described earlier.

Overall, we able to verify the significance in comparing between load direction in order to optimize the performance and increase the detection rate. Also, the importance of selecting specific nodal points, which represent the contact areas and the location of the SA-I mechanoreceptor unit on the fingers. Validation of the hypothesis, which is the ability to differentiate between thickness via tactile ratio is more obvious when the comparison is made between loads, has been achieved. The results show that the ability to differentiate between thicknesses by the difference of von Mises stress is more obvious when the comparison is made between twitch motion loads vs. direct load (datum). As briefed in Chapter 4, the differences between both the Cu and SUS materials are more observable, especially during twitch motions.

Finally, during the experiment using the three-axis tactile sensor, around 1 ~ 10

sheets of 1,000-yen bills has been used for thickness discrimination. Compared to the psychophysics and FEA simulation, the 1,000-yen bill was chosen as sample instead of metal sheet due to the performance limit of the current three-axis tactile sensor to distinguish metal components. The experiment was performed under two conditions, which is under direct pinch motion (Normal Load) and sliding motion (Tangential Load). As a result, it was difficult for the tactile sensor to discriminate thickness during normal load. During tangential load, the discrimination result was more observable especially between low numbers of sheets. In future, through the combination of tactile and joint angle information from the robotic hand, the ability to discriminate between sheet numbers is expected to improve drastically.

In this thesis, we able to highlight the influence of tangential load towards distinguishing between thicknesses. This is different from contemporary human thinking. We solely believe that to increase detection feel, focusing the load on perpendicular or normal direction is sufficient, whereas the current experimental result shows otherwise. Such phenomena occured when dealing with the delicate and complicated human tactile function.

In terms of application, this finding could be applied to improve the design, functionality and performance of available sensor such as our current three-axis tactile sensor. Also, it could be considered to optimise the performance of prosthetic parts such as BeBionics, for tactile sensors of surgical devices such as the DaVinci system, for tactile sensors performing palpation inspection method or other robotic devices). The basic idea is to improve the feedback system and to provide a more delicate response between patient and user.

In conclusion, we verified the ability of the human tactile function to detect an extremely thin object from the psychophysics result. Through specific control of the current experiment procedure, we managed to achieve a similar trend. During the psychophysics experiment, even though the Weber fraction value was different compared to the previous result by Miyaoka and Ohka (2001, 2002), we managed to validate the behavior during the undetected regions up to 150-μm thicknesses. This is a great achievement considering the increased number of the thickness test ratio (between a minimum and maximum thickness range) in a single test group compared to the previous experiment. Further study on the behavior of the undetected regions, especially between the 150 ~ 350-μm thickness range, shall be undertaken in the near future.

As for the FEA simulation result, we have achieved our main objective, which is to identify the von Mises stress value within the epidermis section. We manage to maintain the simulation's convergence rate by optimum use of the element size, and keeping the numerical error below 4% during the simulation. Based on the simulation results, we able to monitor the basic behavior of the human tactile mechanism in defining the differences between two extremely thin foils.

This simulation result also supports our initial hypothesis in which SA-I mechanoreceptor units play the main role in defining the differences between the foils. Another hypothesis is that the existence of our finger nail, also contributes towards enhancing the detection rate between different material thicknesses. This hypothesis shall be verified in future experiment. As described earlier, one of the reason in choosing psychophysics and FEA as the main method is that it is very difficult to monitor and measure stress value directly beneath our fingers. Looking at the three-axis tactile sensor as an option, in near future, we able to evaluate the performance of this device during contact, which hopefully behaves and functioning similar to the mechanoreceptor in a human tactile system.

References

Abraira, V.E. and Ginty, D.D. (2013). The sensory neurons of touch. *Neuron*, 79(4), pp. 618-639.

Amirabdollahian, F., Topping, M., Loureiro, R., Driessen, B. and Harwin, W. (2003). Upper limb robot mediated stroke therapy—GENTLE/s approach. *Autonomous Robots*, 15(1), pp. 35-51.

Beyerstein, B. L. (1999). Whence cometh the myth that we only use ten percent of our brains. *Mind Myths: Exploring Popular Assumptions about the Mind and Brain*. New York, NY: J. Wiley & Sons, 314-335.

Biobook (2015). Retrieved on September 27, 2016 from https://adapaproject.org/bbk_temp/tiki-index.php?page=Leaf%3A+How+do+neurons+transmit+electrical+signals+long+distances%3F.

Blausen.com staff. "Blausen gallery 2014". *Wikiversity Journal of Medicine*. DOI:10.15347/wjm/2014.010. ISSN 20018762.

Bolanowski, S. J. Jr., Gescheider, G. A., Verrillo, R. T. and Checkosky, C. M. (1988). Four channels mediate the mechanical aspects of touch. *Journal of the Acoustical Society of America*, 84, 1680-1694.

Bossomaier, T. R. (2012). *Introduction to the Senses: From Biology to Computer Science*. Cambridge University Press.

Boyd, R. (2008). Do people only use 10 percent of their brains? *Scientific American*.

Cabinet Office, Government of Japan, *Comprehensive Strategy on Science, Technology and Innovation* (2013). Retrieved from http://www8.cao.go.jp/cstp/english/doc/20130607cao_sti_strategy_provisional.pdf.

Campbell, N. A., Reece, J. B., Urry, L. A., Cain, M. L., Wasserman, S. A., Minorsky, P. V. and Jackson, R. B. (2008). *Biology*, Eighth Ed. Pearson Benjamin Cummings, San Francisco.

Carrera, I., Moreno, H.A., Saltarén, R., Pérez, C., Puglisi, L. and Garcia, C. (2011). ROAD: domestic assistant and rehabilitation robot. *Medical & Biological Engineering & Computing*, 49(10), pp. 1201-1211.

Dahiya, R. S., Metta, G., Valle, M., and Sandini, G. (2010). Tactile sensing from humans to humanoids. *Robotics*, IEEE Transactions on, 26(1): 1–20.

Dahiya, R. S., & Valle, M. (2012). *Robotic tactile sensing: Technologies and system*. Springer Science & Business Media.

Dandekar, K., Balasundar, I. R., and Srinivasan, M A. (2003). 3-D finite-element models of human and monkey fingertips to investigate the mechanics of tactile sense. *Journal of Biomechanical Engineering* 125, no. 5: 682-691.

Darian‐Smith, I. (1984). The Sense of Touch: Performance and peripheral neural processes. *Comprehensive Physiology*.

Harmon, L. D. (1982). Automated tactile sensing. *The International Journal of Robotics Research*, 1(2): 3–32.

Ehrenstein, W.H. and Ehrenstein, A. (1999). Psychophysical methods. *In modern techniques in neuroscience research*, Springer Berlin Heidelberg, pp. 1211-1241.

Enander, A. E. and Hygge, S. (1990). Thermal stress and human performance. *Scandinavian Journal of Work, Environment & Health*, 44-50.

Fechner, G. T. (1860). Elemente der Psychophysik (2 vols.). Leipzig: Breitkopf und Härtel (reprint 1964. Amsterdam: Bonset).

Fecht, S. (2014, December 10). Stretchy artificial skin lets prosthetic hand sense heat, humidity, and pressure. *Popular Science*. Retrieved on September 21, 2016 from http://www.popsci.com/artificial-skin-can-distinguish-between-wet-and-dry-diapers.

Fujita, K. and Ohmori, H. (2001, October). A new softness display interface by dynamic fingertip contact area control. In 5th World *Multiconference on Systemics, Cybernetics and Informatics*, pp. 78-82.

Gardner, E.P., Martin, J.H. and Jessell, T.M. (2000). The bodily senses. *Principles of neural science*, 4, pp. 430-450.

Gerling, G. J. and Thomas, G. W. (2008). Fingerprint lines may not directly affect SA-I mechanoreceptor response. *Somatosensory & Motor Research* 25, no. 1: 61-76.

Gerling, G. J., Rivest, I. I., Lesniak, D. R., Scanlon, J. R., & Wan, L. (2014). Validating a population model of tactile mechanotransduction of Slowly Adapting Type I afferents at levels of skin mechanics, single-unit response and psychophysics. *IEEE Transactions on haptics*, 7(2), 216-228.

Gescheider G. A. (1997), *Psychophysics the Fundamentals*, Third ed., Lawrence Erlbaum Associates.

Goodwin, A. W., Macefield, V. G., & Bisley, J. W. (1997). Encoding of object curvature by tactile afferents from human fingers. *Journal of neurophysiology*, 78(6), 2881-2888.

Guizzo, E. and Deyle, T. (2013). *Robotics Trends for 2012*. IEEE Spectrum. Retrieved on December 16, 2013 from http://spectrum.ieee.org/automaton/robotics/robotics-hardware/robotics-trends-for-2012.

Ho, V. and Srinivasan, M. A. (1997). *Human haptic discrimination of thickness*.

Hoon, T. S., Guan, B. H. and Nasariya, S. (2008). Complete Reference: *Matriculation Biology 1*, Kuala Lumpur: Oriental Academic Publication, ISBN 978-983-3127-702.

Howarth, E., and Hoffman, M. S. (1984). A multidimensional approach to the relationship between mood and weather. *British Journal of Psychology*, 75(1), 15-23.

Johannes, Z. (2010). *Sensation, Perception and Action. An Evolutionary Perspective*. Palgrave Macmillian.

Johansson R. S. and Vallbo Å. B. (1979), Tactile sensibility in the human hand: Relative and absolute densities of four types of mechanoreceptive units in glabrous skin, *J. Physiol*., Vol. 286, 283-300.

Johansson R. S. and Vallbo Å. B. (1983), Tactile sensory coding in the glabrous skin of the human hand, *Trends Neurosci*, 6, 27–31.

Johansson, R.S. and Flanagan, J.R. (2009). Coding and use of tactile signals from the fingertips in object manipulation tasks. *Nature Reviews Neuroscience*, 10(5), pp. 345-359.

John, K. T., Goodwin, A. W., and Darian-Smith, I. (1989). Tactile discrimination of thickness. *Experimental Brain Research*, 78(1), 62-68.

Johnson, K.O. and Phillips, J. R. (1981). Tactile spatial resolution. I. Two-point discrimination, gap detection, grating resolution, and letter recognition. *Journal of Neurophysiology* 46, no. 6: 1177-1192.

Johnson, K.O. (2001). The roles and functions of cutaneous mechanoreceptors. *Current opinion in neurobiology*, 11(4), pp. 455-461.

Jusoh, M.A.M., Ohka, M., and Miyaoka, T. (2016). Comparison of tactile discriminations to verify the undetectable region of SUS foil thickness. *Jurnal Teknologi (Science and Engineering)*.

Jusoh, M.A.M., Ohka, M., and Miyaoka, T. (2015). Finite element analysis of human tactile sensing to differentiate thin foils through comparison between vertical & angled loads. *Procedia Computer Science 76*: 40-46.

Jusoh, M.A.M., Ohka, M., Wang, Y.C. and Miyaoka, T. (2014). Understanding of human tactile mechanism in comparing material properties through the analysis of displacement on foil surface. In *Micro-NanoMechatronics and Human Science (MHS)*, 2014 International Symposium on, pp. 1-2.

Jusoh, M.A.M., Ohka, M., and Wang, Y.C. (2013). Finite element analysis on the mechanism of human tactile sensation in comparing different material properties and thickness. *In Applied Mechanics and Materials*, vol. 393, pp. 617-622.

Kandel, E. R., Schwartz, J. H., & Jessell, T. M. (Eds.). (2000). *Principles of Neural Science* (Fifth Edition, pp. 500). New York: McGraw-Hill.

Kim, J., Lee, M., Shim, H.J., Ghaffari, R., Cho, H.R., Son, D., Jung, Y.H., Soh, M., Choi, C., Jung, S. and Chu, K. (2014). Stretchable silicon nanoribbon electronics for skin prosthesis. *Nature communications*, 5.

LaMotte, R. H., & Srinivasan, M. A. (1987). Tactile discrimination of shape: responses of slowly adapting mechanoreceptor afferents to a step stroked across the monkey fingerpad. *The Journal of neuroscience*, 7(6), 1655-1671.

LaMotte, R. H., & Srinivasan, M. A. (1987). Tactile discrimination of shape: responses of rapidly adapting mechanoreceptive afferents to a step stroked across the monkey fingerpad. *The Journal of neuroscience*, 7(6), 1672-1681.

Lesniak, D. R., and Gerling, G. J. (2009). Predicting SA-I mechanoreceptor spike times with a skin-neuron model. *Mathematical biosciences* 220, no. 1: 15-23.

Maeno, T., Kobayashi, K. and Yamazaki, N. (1998). Relationship between the structure of human finger tissue and the location of tactile receptors. *JSME Int J*, Ser C 41: 94 –100

Manning, S. A. and Rosenstock, E. H. (1968). *Classical Psychophysics and Scaling*, McGraw-Hill Book Company.

Miyaoka, T. and Ohka, M. (2001). Tactile information processing mechanism to discriminate foil thickness. *Proceedings of the Seventeenth Annual Meeting of the International Society for Psychophysics*, Vol. 17.

Miyaoka, T. and Ohka, M. (2002). The duplex theory of thickness discriminations by touch. *JSME Annual Meeting 2002(1)*, pp. 231-232.

Moss-Salentijn, L. (1992). The Human Tactile System. *Advanced Tactile Sensing for Robotics and Automated System*, 5, 123-150.

Najarian, S., Dargahi, J., Mehrizi, A. A. (2009). *Artificial Tactile Sensing in Biomedical Engineering*. McGraw Hill Professional, ISBN: 0071601511.

National University of Singapore. (2015, September 23). Highly flexible and wearable tactile sensor for robotics, electronics and healthcare applications. *ScienceDaily*. Retrieved on December 19, 2015 from www.sciencedaily.com/releases/2015/09/150923083530.htm.

Nicholls, H. R. and Lee, M. H. (1989). A survey of robot tactile sensing technology. *The International Journal of Robotics Research*, 8(3): 3–30.

Nicholls, H. R. (1992). Advanced Tactile Sensing for Robotics. University College of Wales Aberystwth, *World Scientific Series in Robotics and Automation*, Vol. 5, pp. 123-150.

Ohka, M., Mitsuya, Y., Higashioka, I. and Kabeshita, H. (2005). An experimental optical three-axis tactile sensor for micro-robots, *Robotica*, Vol. 23-4, pp. 457-465.

Ohka, M., Kobayashi, H., Takata, J. and Mitsuya, Y. (2006). Sensing precision of an optical three-axis tactile sensor for a robotic finger. *The 15th IEEE International*

Symposium on Robot and Human Interactive Communication (ROMAN 2006), pp. 214-219.

Ohka, M., Kobayashi, H., Takata, J. and Mitsuya, Y. (2008). An experimental optical three-axis tactile sensor featured with hemispherical surface, *Journal of Advanced Mechanical Design, Systems, and Manufacturing*, Vol 2(5), pp. 860-873.

Ohka, M. (2009). *Robotic Tactile Sensors*, Wiley Encyclopedia of Computer Science and Engineering (Editor: B. W. Wah), Vol 4, pp. 2454-2461.

Ohka, M., Takata, J., Kobayashi, H., Suzuki, H., Morisawa, N. and Yussof, H. (2009). Object exploration and manipulation using a robotic finger equipped with an optical three-axis tactile sensor, *Robotica*, Vol 27-5, pp. 763-770.

Ohka, M., Abdullah, S. C., Wada, J. and Yussof, H. B. (2012). Two-hand-arm manipulation based on tri-axial tactile data, *International Journal of Social Robotics*, Vol 4-1, pp. 97-105.

Ohka, M., Yussof, H. and Abdullah, S. C. (2012). Three-axis tactile sensor, *Introduction to Modern Robotics II*, (Edited by D. Chugo and S. Yokota), Concept Press Ltd., pp. 113-126.

Ohka, M., Tsunogai, A., Kayaba, T., Abdullah, S. C. and Yussof, H. (2014). Advanced design of columnar-conical feeler-type optical three-axis tactile sensor, *Procedia Computer Science*, 42, pp. 17-24.

Ohka, M., Yamamoto, Y., Yussof, H. and Abdullah, S. C. (2014). All-in-type optical three-axis tactile sensor, 2014 *IEEE International Symposium on Robotics and Manufacturing Automation*, pp. 79-84.

Ossola, A. (2015, October 16). Prosthetic limbs could have artificial skin that really feels. *Popular Science*. Retrieved on September 21, 2016 from http://www.popsci.com/better-artificial-skin-for-mind-operated-prosthetics.

Penfield, W. and Rasmussen, T. (1950). *The cerebral cortex of man; a clinical study of localization of function.*

Poole, H. H. (1989). *Fundamentals of Robotics Engineering*. Poole Associates, Van Nostrand Reinhold, New York, pp. 110-116.

Read, J.C.A. (2015). The place of human psychophysics in modern neuroscience. *Neuroscience*, 296, pp. 116-129.

Seppanen, O., Fisk, W. J., and Lei, Q. H. (2006). *Effect of temperature on task performance in office environment.* Lawrence Berkeley National Laboratory.

Serina, E.R., Mote, C.D. and Rempel, D. (1997). Force response of the fingertip pulp to repeated compression—effects of loading rate, loading angle and anthropometry. *Journal of biomechanics*, 30(10), pp. 1035-1040.

Srinivasan, M. A. and Dandekar, K. (1996). An Investigation of the mechanics of tactile sense using two dimensional models of the primate fingertip. *J. Biomech Eng* 118: 48 – 55.

Silvera-Tawil, D., Rye, D., & Velonaki, M. (2015). Artificial skin and tactile sensing for socially interactive robots: A review. *Robotics and Autonomous Systems*, 63, 230-243.

Smith, K. N. (2015, October 15). Artificial Skin for Prosthetic Limbs Can Sense a Grain of Salt. *Discover Magazine*. Retrieved on September 21, 2016 from http://blogs.discovermagazine.com/d-brief/2015/10/15/prosthetics-artificial-skin-touch-sensation/#.V-J_-5h97IU.

Srinivasan, M. A., & Dandekar, K. (1996). An investigation of the mechanics of tactile sense using two-dimensional models of the primate fingertip. *Journal of biomechanical engineering*, 118(1), 48-55.

Srinivasan, M. A., & Lamotte, R. H. (1987). Tactile discrimination of shape:

responses of slowly and rapidly adapting mechanoreceptive afferents to a step indented into the monkey fingerpad. *The Journal of neuroscience*, 7(6), 1682-1697.

Sripati, A. P., Bensmaia, S. J. and Johnson, K. O. (2006). A continuum mechanical model of mechanoreceptive afferent responses to indented spatial patterns. *Journal of Neurophysiology* 95, no. 6: 3852-3864.

Steepergroup (2015) The world's most lifelike bionic hand. Retrieved on September 21, 2016 from http://bebionic.com/

Stevens, S. S. (1961). To Honour Fechner and Repeal His Law. *Science*, New Series, Vol. 133, No. 3446, pp. 80-86.

Stevens, S. S. (1975). *Psychophysics: Introduction to Its Perceptual, Neural and Social Prospects*, John Wiley & Sons, Inc.

Sugiman, K., Jusoh, M. A. M., Ohka, M., Yussof, H., Abdullah, S. C (2015). Thin flexible sheet handling using robotic hand equipped with three-axis tactile sensors. *Procedia Computer Science.*

Summers, I., and Irwin, R. (2005). Tactile discrimination of paper. *Proceedings of the HAPTEX 5*.

Tanie, K., Komoriya, K., Kaneko, M., Tachi, S. and Fujikawa, A. (1984). A high resolution tactile sensor, Proc. of 4th *Int. Conf. on Robot Vision and Sensor Control*, pp. 251-256.

Tee, B. C. K., Chortos, A., Berndt, A., Nguyen, A. K., Tom, A., McGuire, A., Lin, Z.C., Tien, K., Bae, W.G., Wang, H. and Mei, P. (2015). A skin-inspired organic digital mechanoreceptor. *Science*, 350(6258), 313-316.

Timoshenko, S. P. (1940). *Strength of Materials (Part 2) Advanced Theory and Problems*. 2nd Ed. D.Van Nos-trand Company, pp. 339-360.

Timoshenko, S. P. and Krieger, S. W. (1959). *Theory of Plates and Shells*. 2nd Ed. McGraw-Hill.

Vallbo A. B. and Johansson R. S. (1984). Properties of cutaneous mechanoreceptors in the human hand related to touch sensation *Hum. Neurobiol.* **3**, 3–14.

Westling, G. and Johansson, R.S. (1987). Responses in glabrous skin mechanoreceptors during precision grip in humans. *Experimental Brain Research*, 66(1), pp. 128-140.

Wu, J. Z., Welcome, D. E., and Dong, R. G. (2006). Three-dimensional finite element simulations of the mechanical response of the fingertip to static and dynamic compressions. *Computer methods in Biomechanics and Biomedical Engineering*, 9(1), 55-63.

Yussof, H. (2013) Robot-Autism Project. Retrieved on September 21, 2016 from https://hanafiahyussof.wordpress.com/research-2/robot-autism-project/

Zanker, J., (2010). *Sensation, Perception and Action. An Evolutionary Perspective*, Palgrave Macmillian.

Zimmerman, M. and Snow, B. (2012). Retrieved on September 26, 2016 from http://2012books.lardbucket.org/.